

2012

Biofiltration for Treatment of Gases Contaminated by Beta-caryophyllene

Weili Hu

Louisiana State University and Agricultural and Mechanical College, whu3@tigers.lsu.edu

Follow this and additional works at: https://digitalcommons.lsu.edu/gradschool_theses



Part of the [Civil and Environmental Engineering Commons](#)

Recommended Citation

Hu, Weili, "Biofiltration for Treatment of Gases Contaminated by Beta-caryophyllene" (2012). *LSU Master's Theses*. 740.
https://digitalcommons.lsu.edu/gradschool_theses/740

This Thesis is brought to you for free and open access by the Graduate School at LSU Digital Commons. It has been accepted for inclusion in LSU Master's Theses by an authorized graduate school editor of LSU Digital Commons. For more information, please contact gradetd@lsu.edu.

**BIOFILTRATION FOR TREATMENT OF GASES CONTAMINATED BY
BETA-CARYOPHYLLENE**

A Thesis

**Submitted to the Graduate Faculty of the
Louisiana State University
Agricultural and Mechanical College
in partial fulfillment of the
requirements for the degree of
Master of Science in Civil Engineering**

in

The Department of Civil and Environmental Engineering

by

**Weili Hu
B.S., Huazhong Agricultural University, 2007
May, 2012**

ACKNOWLEDGMENTS

I would like to gratefully acknowledge the input and assistance provided by my advisor Dr. William M. Moe. I would like to thank Dr. John H. Pardue and Dr. Donald Dean Adrian for serving on my thesis committee. Also, I would like to thank numerous people in the laboratory who provided valuable assistance; in particular, Jie Chen, and Jacob Dillehay. Finally, I would like to thank my family, relatives, and friends who helped and supported me to finish.

TABLE OF CONTENTS

ACKNOWLEDGMENTS	ii
LIST OF TABLES	v
LIST OF FIGURES	vi
ABSTRACT.....	ix
CHAPTER 1 INTRODUCTION	1
CHAPTER 2 LITERATURE REVIEW	4
2.1 Overview of Wood Drying and Processing	4
2.1.1 Kiln Drying of Lumber	4
2.1.2 Drying Strands in Oriented Strand Board Manufacture.....	7
2.1.3 Production of OSB and Plywood	8
2.2 Terpenes Emission from Wood Industry	10
2.2.1 Emission of Terpenes from Wood Industry	10
2.2.2 Emission of Monoterpenes from Wood Industry.....	11
2.2.3 Emission of Sesquiterpenes from Wood Industry	12
2.3 Biofiltration of Terpenes from Wood Drying and Processing.....	13
2.3.1 Pollutant Loading Rates of Biofilters Treating Gas Phase Terpenes.....	14
2.3.2 Temperature Effects on Biofilter Operation	16
2.3.3 Impact of β -Caryophyllene to Environment.	16
2.3.4 Biodegradation of β -Caryophyllene and Other Terpenes	18
CHAPTER 3 MATERIALS AND METHODS FOR BIOREACTOR EXPERIMENTS	20
3.1 Introduction	20
3.2 Materials and Methods.....	20
3.2.1 Chemicals.....	20
3.2.2 Experimental Apparatus.....	20
3.2.3 Bioreactor Start-up and Operation	21
3.2.4 β -Caryophyllene Biodegradation Test	23
3.3 Analytical Procedures	25
3.4 Results.....	26
3.4.1 Temperature	26
3.4.2. pH.....	27
3.4.3. Total Suspended Solids (TSS)	28
3.4.4 Serum Bottle Tests	30
3.5 Discussion and Conclusions	34
CHAPTER 4 BIOFILTER OPERATION AND PERFORMANCE	35
4.1 Introduction	35
4.2 Materials and Methods.....	35
4.2.1 Experimental Apparatus.....	35

4.2.2 Abiotic Adsorption Capacity Test.....	37
4.2.3 Biofilter Inoculation and Start-up	37
4.2.4 Biofilter Operation	38
4.2.5 Analytical Procedures	39
4.3 Results.....	39
4.3.1 Abiotic Adsorption Test.....	39
4.3.2 Inoculation, Startup, and Summary of Overall Performance.....	41
4.3.3 Biofilter Performance during Period 1 Operation.....	44
4.3.4 Biofilter Performance during Period 2 Operation.....	48
4.3.5 Biofilter Performance during Period 3A Operation	51
4.3.6 Biofilter Performance during Period 3B Operation	55
4.3.7 Biofilter Performance during Period 4 Operation.....	58
4.3.8 Biofilter Performance during Period 5A Operation	62
4.3.9 Biofilter Performance during Period 5B Operation	65
4.3.10 pH, Headloss and Temperature.....	68
4.4 Discussion and Conclusions	69
 CHAPTER 5 BIOFILTER PERFORMANCE UNDER SHUT DOWN/RE-START OPERATIONS.....	72
5.1 Introduction.....	72
5.2 Materials and Methods.....	72
5.3 Results.....	73
5.4 Discussion and Conclusions	76
 CHAPTER 6 OVERALL CONCLUSIONS AND RECOMMENDATIONS FOR FUTURE WORK	77
6.1 Overall Conclusions and Discussions	77
6.2 Recommendations for Future Research	78
 REFERENCES CITED.....	79
 APPENDIX A: STRUCTURE OF β -CARYOPHYLLENE	86
 APPENDIX B: CALCULATIONS RELATED TO The β -CARYOPHYLLENE BIODEGRADATION TEST	87
 VITA	89

LIST OF TABLES

Table 2.1	Previous studies of off-gases treatment from wood drying and processing.	15
Table 2.2	Physical/chemical properties of β -caryophyllene	17
Table 3.1	Summary of the serum bottle tests. Each treatment was conducted in duplicate. ..	24
Table 4.1	Summary of biofilter operating conditions	38
Table 4.2	Summary of the biofilter loading conditions during each Period.	41

LIST OF FIGURES

Figure 3.1	Schematic diagram of the gas-sparged bioreactors used for cultivating β -caryophyllene degrading microbial populations.	21
Figure 3.2	Serum bottles used for β -caryophyllene biodegradation test.	23
Figure 3.3	Temperature measured in the aqueous phases of the sparged-gas bioreactors.	26
Figure 3.4	Temperature measured on the lid of the sparged-gas-bioreactors.	27
Figure 3.5	pH measured in the aqueous phases of the two sparged-gas bioreactors.	28
Figure 3.6	TSS concentrations measured in the aqueous phase of the low and high temperature sparged-gas bioreactors.	29
Figure 3.7	Low temperature bioreactor (left) and high temperature bioreactor (right) on day 22 (top) and 34 (bottom) following startup.	30
Figure 3.8	CO ₂ concentrations measured in serum bottles inoculated with biomass from the lid (left) and aqueous-phase (right) of the low temperature sparged gas bioreactor....	31
Figure 3.9	CO ₂ concentrations measured in serum bottles inoculated with biomass from the lid (left) and aqueous-phase (right) of the high temperature sparged gas bioreactor...	32
Figure 3.10	CO ₂ produced by β -caryophyllene for low temperature aqueous phase bottles (left) and high temperature aqueous phase bottles (right).	33
Figure 3.11	Image of a polyurethane foam cube from a serum bottle inoculated with biomass from the lid of the high temperature sparged gas bioreactor and supplied with no β -caryophyllene (left) and high purity β -caryophyllene (right) at the end of the incubation.....	34
Figure 4.1	Schematic diagrams of the laboratory-scale biofilter apparatus. 1) laboratory air supply, 2) activated carbon filter, 3) pressure regulator, 4) electronic mass flow controller, 5) humidification chambers in series, 6) syringe pump, 7) liquid drain, 8) glass column assembled in sections, 9) foam packing medium, 10) septum-filled monitoring ports, and 11) effluent.	36
Figure 4.2	The effluent concentration of the adsorption test for a Period of 8 days (left) and the effluent concentration of adsorption test for the last 24 hours(right).	40
Figure 4.3	(A) Influent and effluent pollutant concentrations; (B) Influent gas flow rate (C) Influent loading rate and overall elimination capacity; (D) pH of leachate collected at the bottom of the biofilter (E) Headloss across the packed bed; (F) Gas temperature exiting the biofilter.	42

Figure 4.4	Experimentally measured influent and effluent gas-phase pollutant concentrations during Period 1.....	45
Figure 4.5	Loading rates and removal efficiency for Period 1.....	45
Figure 4.6	Elimination capacities for Period 1.....	46
Figure 4.7	VOC concentration profiles measured on days 4, 15, 18, and 36.....	47
Figure 4.8	Influent and effluent concentrations from high purity β -caryophyllene experiment at the end of Period 1.	48
Figure 4.9	Influent and effluent concentration of Period 2.	49
Figure 4.10	Loading rates and removal efficiency for Period 2.....	49
Figure 4.11	Elimination capacities for Period 2.....	50
Figure 4.12	VOC concentration profiles measured two days after the nutrient addition on days 43, 50, 57 (top) and two days before nutrient addition on day 46, 53, 60 (bottom) during Period 2.....	51
Figure 4.13	Influent and effluent concentration of Period 3A. Arrows denote the days when nutrients were added.	52
Figure 4.14	Effluent concentrations as a function of time since nutrient addition in Period 3A with data plotted separately for each week (top); Effluent concentration as a function of time since nutrient addition with data plotted as average of all four full weeks of operation during Period 3A (bottom).	53
Figure 4.15	Loading rates and removal efficiency (top) and elimination capacities (bottom) for Period 3A.	54
Figure 4.16	Experimentally measured influent and effluent gas-phase pollutant concentrations during Period 3B.....	55
Figure 4.17	Loading rate and removal efficiency (top) and elimination capacities (bottom) of Period 3B.	57
Figure 4.18	Influent and effluent concentrations measured during high purity β -caryophyllene test in Period 3B.....	58
Figure 4.19	VOC concentration profiles measured on days 78 (Period 3A) and 92 and 106 (Period 3B) following addition of three different nutrition solution concentrations (one, three, and six times the baseline nutrient concentrations, respectively).....	58

Figure 4.20	Influent and effluent concentration of Period 4. Arrows denote the days when nutrients were added.	59
Figure 4.21	Loading rate and removal efficiency (top) and elimination capacities (bottom) of Period 4.	60
Figure 4.22	VOC concentration profiles measured on days 144, 148, 162, and 165 during Period 4.	61
Figure 4.23	Influent and effluent concentration of Period 5A. Arrows denote the days when nutrients were added.	62
Figure 4.24	Effluent concentration of the first day after the start of Period 5A.	63
Figure 4.25	Loading rate and removal efficiency (top) and elimination capacities (bottom) of Period 5A.	64
Figure 4.26	VOC concentration profiles measured two days after nutrient addition day (days 176, and 183), and five days after nutrient addition day (days 193 and 200) during Period 5A.	65
Figure 4.27	Influent and effluent concentration of Period 5B. Arrows denote the days when nutrients were added.	66
Figure 4.28	Loading rate and removal efficiency (top) and elimination capacities (bottom) of Period 5B.	67
Figure 4.29	VOC concentration profiles measured two days after nutrient day on days 214, 221, 225, and 232 during Period 5B.	68
Figure 4.30	pH of the drainage (D), headloss across the bed (E), and effluent gas temperature (F).....	69
Figure 5.1	The effluent concentration for the first 12 hours following resumption of β -caryophyllene following the 14-day interval of no pollutant loading.	73
Figure 5.2	Experimentally measured mean daily influent and effluent gas-phase pollutant concentrations after restart (top) and raw effluent concentration data for this Period (bottom).	74
Figure 5.3	Loading rates and removal efficiency (top) and elimination capacities (bottom) for five days after restart.....	75

ABSTRACT

Fixed-film biological treatment processes, commonly referred to as biofilters, have been applied to successfully treat a wide variety of volatile organic compounds (VOCs) present in air emitted by a wide variety of industrial operations. The ability of biofilters to treat some classes of VOCs, however, has not been well established. In particular, the performance of biofilters treating sesquiterpenes has not been widely studied. In the research described herein, a laboratory-scale biofilter was operated to treat a synthetic waste gas stream containing β -caryophyllene, a sesquiterpene emitted by conifer trees and industrial wood processing operations.

An enrichment culture developed in an initial experiment conducted in a sparged gas reactor was used to seed a laboratory-scale biofilter that was subsequently operated under mesophilic conditions for more than 262 days. During the first 244 days of continuous operation, there were seven distinct periods of biofilter operation, designated as Periods 1, 2, 3A, 3B, 4, 5A, and 5B. Period 1 was the initial period of biofilter operation following startup, and Periods 2 to 5 involved progressively higher gas flow rates and pollutant loading rates. To assess the impact of nutrient supply on biofilter performance, the concentrations of nutrients supplied to the biofilter changed at various time intervals. An additional experiment was conducted to evaluate the capacity of the system to recover following a 14-day interval of no β -caryophyllene supply.

Collectively, data presented herein demonstrated that β -caryophyllene can be successfully treated using biofilters. This expands the classes of compounds successfully treated in biofilters to include sesquiterpenes. Data reported herein also demonstrate that local nutrient limitations can cause diminished treatment performance, a phenomenon observed in previous studies involving other pollutants. The biofilter was capable of relatively rapid recovery following resumption of pollutant loading following a 14-day starvation interval.

CHAPTER 1 INTRODUCTION

Biofiltration has been successfully applied as a comparatively low cost and environmentally friendly means of removing and destroying a wide variety of volatile organic compounds (VOCs) and hazardous air pollutants (HAPs) over the past several decades. While there have been many successful applications, much remains to be determined regarding the applicability of this technology and its performance in treating some of the VOCs emitted by the wood products industry, a major industrial sector in the U.S. VOCs are released during lumber drying as well as processes associated with manufacture of wood-derived products (e.g., pressing wood chips with binding agents at high temperatures during the manufacture of oriented strand board).

Among the naturally occurring compounds emitted by live trees and during the industrial processing of wood are terpenes, compounds having the general formula $(C_5H_8)_n$. Among these, perhaps the most generally recognizable are the monoterpenes [$n=2$, $(C_5H_8)_2$] α - and β -pinene, the compounds primarily responsible for the recognizable scent of pine trees. Sesquiterpenes [$n=3$, $(C_5H_8)_3$] are also produced by live trees and are emitted by high temperature wood processing operations. In mixed southern pines of the United States, β -caryophyllene appears to be the dominant sesquiterpene (Stromvall and Petersson, 2000). β -caryophyllene is of potential concern as an air pollutant because it is highly reactive with hydroxyl radicals, ozone, or nitrate radicals, forming fine particulate matter (Sillman, 1999).

In the research described in this thesis, experiments were conducted in a laboratory-scale biofilter to assess the ability of biological processes to effectively treat a synthetic waste gas stream containing β -caryophyllene. Experiments evaluated treatment performance under a

variety of pollutant loading conditions and nutrient supply rates.

The first task in the effort to evaluate biofiltration of β -caryophyllene was to develop an enrichment culture able to biodegrade this target contaminant. Laboratory studies employed a sparged-gas reactor to enrich for β -caryophyllene-degrading microorganisms. Total suspended solids (TSS), pH and temperature were monitored over time until the cultures were enriched with microbes able to degrade β -caryophyllene. The enrichment cultures was then used as a seed culture in subsequent biofilter experiments.

Following inoculation, there were seven distinct Periods of operation in the laboratory-scale biofilter. These periods were arbitrarily designated as Periods 1, 2, 3A, 3B, 4, 5A, and 5B. Period 1 encompassed the initial period of operation, and Periods 2 to 5 involved progressively higher gas flow rates and pollutant loading rates. To assess the impact of nutrient supply on biofilter performance, the concentrations of nutrients supplied to the biofilter changed at various time intervals.

After the biofilter received a nutrient addition, the biofilter was temporarily shut down for a period of 14 days. No β -caryophyllene was supplied to the biofilter, but a small gas flow rate to prevent anaerobic conditions. Upon restart, the system was returned to previous operation the same as before shut down and performance was monitored to assess the capacity of the system to recover.

The organization of this thesis is as follows. Chapter 2 of this thesis contains a literature review summarizing previous research and providing the rationale for the research described herein. Chapter 3 contains a description of the materials and methods used in the bioreactor experiments. Chapter 4 contains biofilter performance under long term continuous operations at a variety of gas flow rates and pollutant loading rates. Chapter 5 contains a description of

biofilter performance under temporarily shut down/restart conditions. Chapter 6 contains overall conclusions of this study and discussions. Chapter 7 contains a listing of the references cited throughout.

CHAPTER 2 LITERATURE REVIEW

2.1 Overview of Wood Drying and Processing

Trees can be divided into two general categories: softwood and hardwood. Softwoods consist of needle-leaved species such as pine, spruce and fir, and are generally used by the building industry for use in house framing and other general construction purposes. Hardwoods consist primarily of broad-leaved species such as oak, hickory, ash, maple and poplar, and are generally used for more specialized purposes, such as cabinets, furniture, doors and window casings. The actual hardness of the wood in either category is highly variable. The basic processes utilized to manufacture lumber in either category are essentially the same; however, specific processing details are sufficiently different that lumber mills generally specialize in only one of the two categories. A general description of timber processing operations and how they results in VOC emissions are described in the following sub-sections.

2.1.1 Kiln Drying of Lumber

When live trees are harvested, their wood is generally extremely wet, with water content often exceeding dry wood content, by weight. After transport to a sawmill for processing, logs are loaded onto a deck and then sawn into lumber. After being sawn, the boards' ends may be trimmed to obtain uniform lengths prior to being sorted and stacked for drying. The moisture content of green (fresh) wood generally ranges from 30 to 200% on a dry weight basis, depending upon tree species and type of wood (i.e., sapwood vs. heartwood). Generally, lumber must be dried to the range of 8 to 19% moisture content to ensure stability for indoor applications and prevent rotting. In commercial operations, lumber drying is achieved through the use of kilns. A lumber kiln consists of one or more chambers designed to provide and control

the environmental conditions of heat, humidity, and air circulation necessary for proper drying. Most lumber drying kilns are designed for batch processes in which the kiln is completely loaded, or charged, in one operation, and lumber remains stationary during the entire drying cycle. At the elevated temperatures characteristic of lumber kilns, water evaporates quickly, but at the same time organic compounds inherent in the wood are volatilized.

In commercial applications, lumber is dried according to a kiln schedule, that is, a combination of temperature, humidity and time that allows rapid drying while still maintaining acceptable lumber quality (minimum warpage, surface cracks, etc.). Lumber produced from different tree species require different kiln schedules. Softwoods (e.g., southern pine species) can often be dried in less than 24 hours at temperatures of 180° to 260°F without previously undergoing air drying (Culpepper, 1990). On the other hand, hardwoods (e.g., oak, poplar and maple) are usually air-dried for roughly six weeks or pre-dried at about 80°F for at least two weeks before they are kiln-dried for approximately three weeks at temperatures between 95° and 180°F (Stevens and Pratt, 1969). The longer drying time for hardwoods is necessary to minimize formation of surface and structural defects which would compromise the boards' aesthetic and structural quality. In addition to differences in wood chemical composition, differences in kiln temperature and length of drying cause differences in VOC emission rates.

Because exhaust gas flow rates vary with time and because of the large number of emission points in commercial kilns, it is difficult or impossible to gather emission data by collecting measurements at existing commercial kilns. Most VOC emission data reported in the literature are from laboratory or pilot-scale kiln drying operations (Ingram *et al.*, 1995; Granstrom, 2003; Lavery and Milota, 2000).

In the literature, a common notation is to express the mass of VOCs emitted (in grams of

milligrams) per mass of oven dried wood (in kilograms) to derive a total emission factor of grams VOC per kilogram of oven dried wood ($\text{g/kg}_{\text{OD wood}}$). This notation is used to designate total VOC emission during the drying cycle without regard for specific compounds emitted or the period during the drying cycle when emitted. Such calculations are usually based on measurements of aggregate parameters either using a total hydrocarbon analyzer (THA) calibrated using methane or propane or by gravimetric measurement of condensable compounds.

Ingram *et al.* (1995b) reported emissions of $2.75 \text{ g/kg}_{\text{OD wood}}$ by sampling the exhaust stream of laboratory kiln charges of southern pine (*Pinus taeda*) dried at 82°C (180°F) and 118°C (245°F), with a flame ionization detector (FID). In contrast, NCASI (1996) reported $1.53 \text{ g/kg}_{\text{OD wood}}$ of emissions for southern pine, indicating that there can be considerable variability among sources, even for the same species and measurement method. NCASI (1996) reported emissions for several western softwood species, including inland Douglas-fir (*Pseudotsuga menziesii*) sapwood at $0.15 \text{ g/kg}_{\text{OD wood}}$, heartwood at $0.99 \text{ g/kg}_{\text{OD wood}}$, and coastal Douglas-fir at $0.35 \text{ g/kg}_{\text{OD wood}}$. Granstrom (2003) reported $0.083\text{--}0.39 \text{ g/kg}_{\text{OD wood}}$ of VOCs emissions depending on the temperature of the drying medium entering the drying tower and on the final moisture content of the sawdust from drying Norway spruce sawdust. By condensing the water and volatiles from a kiln exhaust, McDonald and Wastney (1995) measured emissions of 0.23 to $0.32 \text{ g/kg}_{\text{OD wood}}$ for Monterrey pine (*Pinus radiata*). Using EPA method 25D, Dallons *et al.*, (1994) determined that approximately $1.1 \text{ g/kg}_{\text{OD wood}}$ of emissions was released from southern pine as it was dried. Lavery and Milota (2000) used US EPA method 25A to test Douglas-fir in both a commercial and a laboratory kiln. The commercial kiln emitted an averaged $0.87 \text{ g/kg}_{\text{OD wood}}$ while the laboratory kiln averaged $0.79 \text{ g/kg}_{\text{OD wood}}$. This evidence suggests that an FID may indicate emission rates higher than those determined by condensing, possibly because of more

complete detection with the FID.

While the composition of VOCs in off-gases is important for determining impacts on air quality, most previous studies have quantified only the total mass of VOCs emitted without consideration for the specific composition of the gases. While it is expected that some treatment systems (e.g., biofiltration) require knowledge of changes in off-gas VOC composition and concentration over time during the drying schedule, most previous studies have reported only total masses in the effluent, not a time profile.

Results reported by Wu and Milota (1999) suggest that simple changes in kiln drying schedules (e.g., changing the dry and wet bulb temperatures) can result in decreased VOC emissions from Douglas-fir (a common softwood) kiln drying operations. Because the drying schedule was shown to affect emissions, manufacturers could minimize emissions by altering operating conditions. Wu and Milota (1999) also report that the VOC emission rate (measured as total hydrocarbons) changed by more than one order of magnitude during the kiln-drying schedule. During the initial five hours of drying, the emission rate was much higher than the rest of the drying cycle. After the initial spike in effluent VOC concentration, there was a gradual decrease in VOC emissions during the remaining 67 hours of drying.

2.1.2 Drying Strands in Oriented Strand Board Manufacture

As the initial step in the production of oriented strand board (OSB), logs are debarked and fed into a machine with rotating blades, a strander, which slices the logs along the grain into strands 25-30 thousands of an inch thick, 1/2 inch wide and between 4 and 6 inches long. The green strands are then conveyed to wet storage bins (OSB and the environment, Technical bulletin, SBA, 1999).

Rotary-drum drying, a common method used in the OSB industry, employs a high

operating temperature, normally up to 740 °F and drying time less than one minute at the inlet (Wang *et al.*, 2005). Other drying methods such as oven-drying, air-drying, freeze-drying and microwave-drying are also used by some mills. As strands are discharged from the wet bins, they enter one of three types of hot air dryers; the triple pass or the single pass rotary dryer or a single pass conveyor dryer. The operation of the rotary dryer tumbles the strands at the same time as they are being carried forward. In the triple pass dryer, the strands make three trips the length of the dryer before discharging versus one trip for the single pass and conveyor unit. The environmental advantages of the conveyor dryer are higher recovery and much lower drying temperatures. Humidity is controlled by metering the air entering the kiln to maintain the desired wet bulb temperature. The strand/air mix out feeds from the dryers through a series of cyclones to drop out usable strands, precipitators to remove fine particles, and finally, a device to reduce or eliminate VOCs before the hot gases are discharged into the atmosphere. After drying, the strands are screened to eliminate a percentage of fines and then enter a blending bin. The hot air used for drying is most often generated by a separate energy system which uses screened fines, saw waste, and sander dust as fuel (OSB and the environment, Technical bulletin, SBA, 1999).

2.1.3 Production of OSB and Plywood

Oriented strand board (OSB) is an engineered, mat-formed panel product made of strands, flakes or wafers sliced from wood logs and bonded with an exterior-type binder under heat and pressure. OSB panels consist of layered mats. Exterior or surface layers are composed of strands aligned in the long panel direction; inner layers consist of cross or randomly aligned strands. These large mats are then subjected to intense heat and pressure to become a OSB panel and then are cut to size. OSB manufacture contains several procedures including log hauling and sorting, jackladder, debarking, stranding, wet bins, drying, blending, forming line, pressing and

finishing line (OSB Performance by Design TM Oriented Strand Board in Wood Frame Construction U.S. Edition 2005).

Plywood is an assembly of layers of wood (veneer) joined together by means of an adhesive (glue). Veneers are cut to thicknesses ranging from 1/40 to 3/8 inch, and then conveyed to dryers. The veneers are usually dried to a moisture content of less than 10 percent. The next step is gluing. Protein and urea-formaldehyde are chiefly interior glues and phenol-formaldehyde is exterior glue. Glue is applied to the veneer by means of a spreader. After that, the layers of veneer are subject to pressure to insure proper alignment and an intimate contact between the wood layers (veneers) and the glue. Depending upon the operation and the product desired, any number of a series of finishing steps may be taken after the pressing operation (Plywood Manufacture, Washington State Air Toxic Sources and Emission Estimation Methods).

For both OSB and plywood manufacturing processes, the drying operation produces the highest environmental impact from the mill. The hot gas discharge going to the dryer stack contains a mixture of CO, NO_x, VOCs and water vapor, and like construction plywood, OSB panels are bonded under heat and pressure with phenol formaldehyde or isocyanate binders that become durable, insoluble heat-resistant polymers that resist age, moisture and chemical degradation. During the pressing operation, hot gases often including free formaldehyde are driven off and collected in a venting system. Depending on the permit requirements, the collected gases either go to the energy system as part of the underfire air supply, are incinerated in a regenerative thermal oxidizer (RTO) or treated with a biofilter. Like the forming and blending area, maintenance is undertaken wearing a self-contained breathing apparatus (OSB and the environment, Technical bulletin, SBA, 1999).

2.2 Terpenes Emission from Wood Industry

2.2.1 Emission of Terpenes from Wood Industry

A wood-drying process is a source of VOC emissions. The basic emission mechanisms are direct evaporation (i.e. vapor pressure of pure components increases as the temperature increases), steam distillation and thermal degradation (Wastney, 1994). VOC emissions from wood drying are principally strong smelling terpenes, of which monoterpenes such as α - and β -pinenes are the major components (Cronn *et al.*, 1983; Wastney, 1994; Bridgewater *et al.*, 1995; Lavery and Milota, 2001; Danielsson and Rasmuson, 2002).

VOC emissions from softwood and hardwood drying are reported to differ from each other both qualitatively and quantitatively, with softwood drying releasing higher quantities of VOCs than hardwood drying (Otwell *et al.*, 2000; Banerjee *et al.*, 1998). VOCs from hardwood drying are mainly degradation products from the thermal degradation of wood, whereas most VOCs from softwood drying are terpenes (Otwell *et al.*, 2000; Banerjee *et al.*, 1998). There are differences between terpene concentrations in different parts of one wood species, and these differences influence wood drying emissions (Setzman *et al.*, 1993). In spruce, for example, the terpene concentration in wood is 1-2 kg terpenes / ton dry solids, while fresh knots of spruce contain 10-15 kg terpenes / ton dry solid (Setzman *et al.*, 1993). It is also noticed from lumber drying that much greater amounts of terpenes are found in heartwood than in sapwood (Ingram *et al.*, 2000).

An emission value of 75 % of total terpene content for chipped forest wood fuels (Nordic pine and spruce) is reported for both direct flue gas dryers and indirect dryers (i.e. steam dryers) (Setzman, 1993). Manninen *et al.* (2002) studied VOC emissions between air-dried and heat-heated scots pine wood; 41 individual volatile compounds were identified in the collected air

samples on the basis of mass spectra, but only 14 of them were found in the VOC emission of both air-dried and heat-treated wood blocks. Terpenes were found as the main group of compounds, consisting of about 71% of total VOCs. The other main group is aldehydes, consisting of 25% of the total VOC emissions. However, in the emission of heated dried, the main group of the emission is aldehydes which account for 35% of total VOC, and the relative proportion of terpenes emitted decreased.

Terpenes, which have the general formula of $(C_5H_8)_n$ may be further classified as monoterpenes $(C_5H_8)_2$, sesquiterpenes $(C_5H_8)_3$, diterpenes $(C_5H_8)_4$, triterpenes $(C_5H_8)_6$, tetraterpenes $(C_5H_8)_8$, and polyterpenes (when $n \geq 10$). The boiling points of monoterpenes are in the range of 150-180 °C. According to Granstrom (2003), predominantly monoterpenes were found in the ice trap, account for more than 50 percent of the total VOCs.

2.2.2 Emission of Monoterpenes from Wood Industry

Monoterpene compounds such as α -pinene, β -pinene and 3-carene originate from softwoods and products thereof can be considered as the most important volatile compounds (Roffael, 2006). According to Granstrom (2003), monoterpenes $(C_5H_8)_2$ are dominant in exhaust fumes. This class of compounds was identified as the major chemical component and had been quantified as 13 to 250 mg/kg_{OD wood} from drying sawdust in a spouted bed in VOCs emissions. Danielsson and Rasmuson (2002) also pointed out that monoterpenes constitute the main part of all the components released; and α -terpene and 3-carene dominate when pine is dried, and α -terpene and β -terpene dominate when spruce is dried. Studies also showed the vapor-fraction consists primarily of monoterpenes (Stromvall and Petersson, 1993). Lavery and Milota (2000) studied VOC emissions from Douglas-fir and found that α -pinene, β -pinene, myrcene, P-cymene, and limonene were the chief monoterpenes emitted from drying. Granstrom (2003) reported the

concentration of VOCs in the drying medium, and the amount of emitted monoterpenes increased with drying temperature.

Danielsson and Rasmuson (2002) found that monoterpenes constitute the main part of all the components released under convective drying of wood chips. Lavery and Milota (2000) studied VOC emissions from commercial and laboratory kilns and reported that monoterpenes were detected about 210 mg/kg_{OD wood} consisting about 21% of the emissions, and which α -pinene about 170 mg/kg_{OD wood} is the dominant monoterpene followed by β -pinene. Fritz *et al.* (2004) reported that α -pinene is the most prevalent VOC emitted by Douglas-fir.

2.2.3 Emission of Sesquiterpenes from Wood Industry

Granstrom (2009) studied sesquiterpenes from spruce sawdust during drying reported sesquiterpene emissions amounted to about 20% of the monoterpene emissions and drying at 200°C caused markedly larger sesquiterpene emissions than did drying at 140 or 170 °C. The sesquiterpene emissions increased considerably at low wood moisture contents. According to Stromvall and Petersson (1993a), the sesquiterpenes have been reported as 10% in a kraft mill digester blow tank; and as 5% at a thermo mechanical pulp mill pretreatment of chips, and as 5% at a sulfite mill seasoning silo (1993b).

Some sesquiterpenes such as isolongifolene, alfa-gurjunene, alfa-longipinene, alfa-copaene and longifolene were detected by condensing the exhaust streams and measured with GC-MS by Granstrom (2009), the sesquiterpene was identified as a group from their mass spectrum, and the individual sesquiterpenes were quantified using an average response factor for sesquiterpenes compiled from the response factors of four available sesquiterpenes. Compare to natural emissions, the resin of Norway spruce consists to 25–30% of monoterpenes and a few percent sesquiterpenes (Stromvall and Petersson, 2010).

Granstrom (2010) also studied the emission of sesquiterpenes from processed wood warrants attention in the work environments. He pointed out that workers are exposed to significant amounts of sesquiterpenes at wood processing plants, and the sum of monoterpenes and sesquiterpenes may exceed the occupational exposure limit. It has long been known that monoterpenes are emitted during the processing of wood, while sesquiterpenes are of considerable importance too.

2.3 Biofiltration of Terpenes from Wood Drying and Processing

Biofiltration involves the passage of a polluted airstream through a bed containing microorganisms growing within biofilms attached to bed packing material without producing second pollutants. It is reported that at least 60 of the 189 HAPs have been successfully remediated to 65 to 99 percent efficiency by bench-to pilot-scale biofiltration, including, but not limited to, the aromatics hexane (Morgenroth *et al.*, 1996), BTEX (benzene, toluene, ethylbenzene, and xylene) (Corsi and Seed, 1995; Atoche and Moe, 2004) and styrene (Tonga and Singh, 1994), methyl ethyl ketone (MEK), and methyl isobutyl ketone (MIBK) (Deshusses and Dunn, 1996), and the alcohols ethanol (Hodge and Devlin, 1995) and methanol (Dhamwichukorn *et al.*, 2001).

The monoterpenes, such as α -pinene and β -pinene, have also been successfully treated in lab-scale biofilters. Diehl *et al.* (2000) reported that inoculated biofilters were able to reduce total monoterpenes by at least 94 percent. Hejazi *et al.* (2009) used a silicone oil-coated perlite biofilter to treat with α -pinene-contaminated air and found that the silicone oil-coated biofilter performed better at an inlet gas flow rate of 2.5 L/min with a maximum elimination capacity of 20 g m⁻³ h⁻¹) in comparison with 15 g m⁻³ h⁻¹) for the biofilter without reporting silicone oil. Kleinheinz *et al.* (1999) used biofiltration unit in degrading high levels of α -pinene, that

complete degradation of α -pinene was achieved in 36 h with a maximum rate of degradation of $3.9 \text{ mg L}^{-1} \text{ h}^{-1}$. Kong *et al.* (2001) investigated the potential to biologically treat methanol and α -pinene at thermophilic conditions from 40°C to 70°C using biotrickling filters, it is reported that α -pinene removal was achieved at temperatures up to 60°C with optimal treatment occurring at 55°C at a removal rate up to $60 \text{ g m}^{-3}\text{h}^{-1}$. The microbial communities determined by DNA fingerprinting analysis found that the high-temperature communities treating methanol or pinene were more similar to each other than the mesophilic communities (i.e., 40°C).

Currently, even though full-scale biofiltration has been successfully used at wood products facilities in United States already, application of biofiltration in forest products operations is still limited (Diehl *et al*, 2000). There are few, if any, biofilters on wood dryers, but some are used on the exhaust from hot presses (Milota, 2000).

2.3.1 Pollutant Loading Rates of Biofilters Treating Gas Phase Terpenes

Van Groenestijn and Liu (2002) studied removal of α -pinene from gases using biofilters containing fungi using different packing materials with a loading rate between 24 and $38 \text{ g } \alpha\text{-pinene m}^{-3}\text{h}^{-1}$, the removal efficiencies of more than 90% were observed, but mostly ranged from 50% to 90% due to overloading. Dhamwichukorn *et al.* (2001) reported thermophilic biofiltration of methanol and α -pinene using bench-scale biofiltration systems with volume of 1085 cm^3 and 1824 cm^3 at influent concentrations of 110 ppm_v methanol and 15 ppm_v α -pinene at a flow rate of 100 mL/min , corresponding to loading rates of $0.796 \text{ g methanol m}^{-3} \text{ h}^{-1}$ and $0.461 \text{ g } \alpha\text{-pinene m}^{-3} \text{ h}^{-1}$, respectively. The removal efficiency of methanol varied from 95-98%, and the removal efficiency of α -pinene varied from 23-95%. Langolf and Kleinheinz (2006) used lava rock-based laboratory biofiltration systems to remove α -pinene at an influent concentration of 150 ppm_v at low flowrate and high flowrate conditions, make a corresponding loading rate

30.4-106.4 g α -pinene $\text{m}^{-3} \text{h}^{-1}$. The elimination capacities were as high as 100 g $\text{m}^{-3} \text{h}^{-1}$; the removal efficiencies averaged 99%. Table 2.1 summarized previous studies of off-gases treatment from wood drying and processing.

Table 2.1 Previous studies of off-gases treatment from wood drying and processing.

References	Pollutant	Biofilter	Loading rate	Removal Efficiency
Van Groenestijn and Liu (2002)	α -pinene	Fungi	24 - 38 g α -pinene $\text{m}^{-3} \text{h}^{-1}$	50% to 90%
Dhamwichukorn et al. (2001)	Methanol and α -pinene	Thermophilic biofiltration	0.796 g methanol $\text{m}^{-3} \text{h}^{-1}$ and 0.461 g α -pinene $\text{m}^{-3} \text{h}^{-1}$	95-98% for methanol and 23-95% for α -pinene
Langolf and Kleinheinz (2006)	α -pinene	Lava rock-based Laboratory biofiltration	30.4-106.4 g α -pinene $\text{m}^{-3} \text{h}^{-1}$	99%
Jin et al. (2006)	α -pinene	Fungi	1.5-100 g α -pinene $\text{m}^{-3} \text{h}^{-1}$	40-98%
Rene et al. (2009)	Hydrogen sulphide, methanol and α -pinene	Two stage gas phase bioreactor	2.1 and 93.5 g $\text{m}^{-3} \text{h}^{-1}$ for H_2S , 55.3 and 1260.2 g $\text{m}^{-3} \text{h}^{-1}$ for methanol, and 2.8 and 161.1 g $\text{m}^{-3} \text{h}^{-1}$ for α -pinene	Elimination capacities were 894.4 g $\text{m}^{-3} \text{h}^{-1}$ for methanol, 45.1 g $\text{m}^{-3} \text{h}^{-1}$ for H_2S and 138.1 g $\text{m}^{-3} \text{h}^{-1}$ for α -pinene

Jin *et al.* (2006) studied the performance optimization of the fungal biodegradation of α -pinene in gas-phase biofilter with a loading rate of 1.5-100 g α -pinene $\text{m}^{-3} \text{h}^{-1}$. α -Pinene removal efficiency of the biofilter varied from 40-98%. Rene *et al.* (2009) studied two stage gas phase bioreactor of the combined removal of hydrogen sulfide, methanol and α -pinene. The first stage was a biotrickling filter packed with pall rings, and the second one was a perlite plus pall ring mixed biofilter operated in series. It has been reported that α -pinene was removed predominantly by the fungus *Ophjostoma tenoceras* in the second stage. The maximum elimination capacities

reached by the two stage bioreactor for individual pollutants were $894.4 \text{ g m}^{-3} \text{ h}^{-1}$ for methanol, $45.1 \text{ g m}^{-3} \text{ h}^{-1}$ for H_2S , and $138.1 \text{ g m}^{-3} \text{ h}^{-1}$ for α -pinene.

2.3.2 Temperature Effects on Biofilter Operation

The common temperature of biofiltration systems using ambient temperature microorganisms to biodegrade contaminated gases. However, Kong et al. (2001) studied that the high-temperature communities treating methanol or pinene were more similar to each other than the mesophilic communities. Dhamwichukorn *et al.* (2001) reported that biofiltration of methanol and α -pinene at a thermophilic temperature (50°C) was achievable. Biofiltration at high temperatures opens up a range of possibilities for applying biofiltration to hot gas streams.

2.3.3 Impact of β -Caryophyllene to Environment.

The mechanism for ozone formation involves VOCs that react with either hydroxyl radicals (HO), ozone (O_3), or nitrate radicals (NO_3) (Papiez *et al.*, 2009). The true impact of VOC emissions depends not so much on the total amount of VOC but on the reactivity of the VOC species with respect to the OH radical, Terpenes are especially reactive and have a large impact relative to their ambient concentration (Sillman, 1999). Shu and Atkinson (1995) studied atmospheric lifetimes and fates of a series of sesquiterpenes and found that the sesquiterpenes such as α -cedrene, α -copaene, β -caryophyllene, α -humulene, and longifolene are all reactive, with calculated overall lifetimes of a few hours or less. In particular, β -caryophyllene and α -humulene are highly reactive toward O_3 and NO_3 radicals, with calculated lifetimes due to these reactions of 1–2 min. The sesquiterpenes are more reactive in the atmosphere and are more rapidly converted from the gas phase to the liquid phase in the form of polar aerosols, due to their higher molecular weight (Stromvall and Petersson, 1991). Fuentes *et al.* (2000) reported that when the emission rates for β -caryophyllene and d-limonene from orange tree branches were

measured with an ozone scrubber in the sampling train, the emission rate of β -caryophyllene was a little higher than d-limonene. When the ozone scrubber was not used, d-limonene was unaffected, but β -caryophyllene was dramatically reduced due to reaction with ambient O_3 . Jaoui *et al.* (2003) pointed out that part of the uncertainty in emission rates for some sesquiterpenes is due to their very fast reaction rates with ambient ozone concentrations.

In mixed southern pines of the United States, β -caryophyllene appears to be the dominant sesquiterpene (Stromvall and Petersson, 2000). Helming *et al.* (2007) studied sesquiterpene emissions from pine trees, they found that thirteen sesquiterpene compounds were detected and identified in emissions from seven (out of eight) pine species. The most abundant ones were β -caryophyllene, alpha-bergamotene, beta-farnesene, and alpha-farnesene, with emission rates increasing exponentially with temperature.

Some physical/chemical properties of β -caryophyllene are presented in Table 2.2. And the structure of β -caryophyllene was shown in the appendix A.

Table 2.2 Physical/chemical properties of β -caryophyllene

Parameter	Value	Data Source
Molecular Formula	$C_{15}H_{24}$	EPI
CAS #	87-44-5	EPI
Molecular Weight (g/mole)	204.36	EPI
Density at 20 °C (g/mL)	0.9052	EPI
Boiling point (°C)	262-264	EPI
Water Solubility (mg/L)	0.05011	EPI
Vapor Pressure (Pa)	1.1	Hoskovec <i>et al.</i> (2005)
Log K_{ow}	6.30	EPI
Log P	6.38	Hansch <i>et al.</i> (1995)
Henry's LC (atm-m ³ /mole)	1.674E-001	EPI

Zhao *et al.* (2010) studied the mechanism for O_3 -initiated atmospheric oxidation reaction of β -caryophyllene found that the main products of O_3 -initiated β -caryophyllene oxidation are β -

caryophyllonic acid, β -caryophyllene aldehyde and formaldehyde, which are low vapor pressure compounds and are inclined to form secondary organic aerosols. Li *et al.* (2011) studied the production of secondary organic aerosol (SOA) by dark ozonolysis of gas-phase β -caryophyllene and found that the second-generation products contribute substantially to the particle-phase organic material.

2.3.4 Biodegradation of β -Caryophyllene and Other Terpenes

Microorganisms used for biodegrading VOCs including β -caryophyllene and other terpenes has been successfully studied by people. Kleinheinz *et al.* (1999) isolated monoterpene-degrading bacteria and identified them using the Biolog system as *Pseudomonas fluorescens* and *Alcaligenes xylosoxidans*. Pichinoty *et al.* (1990) isolated eleven strains of coryneform bacteria from soil samples by enrichment culture in a mineral medium containing β -caryophyllene as the sole energy and carbon source. Ten of the isolates could also metabolize longifolene. Asselineau *et al.* (1990) studied chemotaxonomy of gram-positive bacteria metabolizing β -caryophyllene and found that strains identified from coryneform bacteria metabolizing β -caryophyllene appeared to be more closely related to the genus *Rhodococcus* than to the genus *Nocardia* since the phospholipids such as cardiolipids, phosphatidylethanolamine, phosphatidylinositol and mannosides of phosphatidylinositol were identified as the main components of the bacterial extracts. In characterization of monoperpene biotransformation, *Pseudomonas rhodesiae* and *Pseudomonas fluorescens* from water organic solvent systems using terpene substrates were studied by Bicas *et al.* (2008). It was reported that *Pseudomonas rhodesiae* was the most suitable biocatalyst for the production of isonovalal from α -pinene oxide. Enzymatic isomerization of β to α pinene was described for the first time to both strains. α terpineol production by *P. fluorescens* was very efficient and appeared promising. Kim *et al.* (2003) studied

Rhodococcus sp. T104 in the presence of monoterpenes, it has been shown to induce the degradation pathway by utilizing limonenes, cymenes, carvones, and pinenes as sole carbon sources. Javidnia *et al.* (2009) studied microbial biotransformation of some monoterpene hydrocarbons such as alpha-pinene beta-pinene, myrcene and p-cymene by seven strain bacteria and two strains of fungi. It was reported that some microorganisms transformed monoterpenes to oxygenated monoterpenes in good yield, especially *Staphylococcus epidermidis*.

CHAPTER 3 MATERIALS AND METHODS FOR BIOREACTOR EXPERIMENTS

3.1 Introduction

As the initial step in preparing to test the ability of a biofilter to treat gas-phase β -caryophyllene, experiments were conducted aimed at development of an enrichment culture able to biodegrade β -caryophyllene. This chapter describes the materials and methods employed for the enrichment culture experiments as well as the results from tests aimed at assessing the cultures' abilities to biodegrade β -caryophyllene.

3.2 Materials and Methods

3.2.1 Chemicals

Unless specified otherwise, β -caryophyllene (purity >90%, GC) purchased from TCI America (Portland, OR, catalog No. C0796) was used as the model pollutant in studies described herein. For select experiments, higher purity β -caryophyllene (purity >98.5%, GC) purchased from Sigma-Aldrich Inc. (Allentown, PA, catalog No. 22075) was employed. Table 2.2 in section 2.3.3 summarized the physical/chemical properties of β -caryophyllene.

3.2.2 Experimental Apparatus

Experiments aimed at developing an enrichment culture able to biodegrade β -caryophyllene employed two 4.0 L glass kettle reactors (Pyrex, Acton, MA), each of which was configured as shown in Figure 3.1. One of the bioreactors (hereafter referred to as the “low temperature bioreactor”) was maintained at ambient laboratory temperature. The other bioreactor (hereafter referred to as the “high temperature bioreactor”) was heated using an electrical heating tape affixed to the exterior surface of the glass to maintain the liquid temperature at a target level 50°C. Compressed air from a laboratory air tap flowed through a pressure regulator and then

separated to two air lines. Each of the air flows passed through a glass tube equipped with a septum-filled injection port. A KD Scientific model 1000 syringe pump (Boston, MA, USA) delivered β -caryophyllene from a glass gas-tight syringe (Hamilton, Reno, NV, USA) through a needle that pierced the septum into the injection port and into each of the two airstreams. The β -caryophyllene contaminated air then passed through an aeration stone submerged in the reactor. Flow meters measured and regulated the air flow rate. The gas exiting the reactors was released to a fume hood. This sparged-gas bioreactor configuration is similar to that employed successfully in previous experiments aimed at development of enrichment cultures able to biodegrade a variety of volatile organic compounds including acetone, ethylbenzene, methyl ethyl ketone, toluene, and *p*-xylene (Lee *et al.*, 2002; Atoche and Moe, 2004; Moe and Qi, 2005; Qi and Moe, 2006).

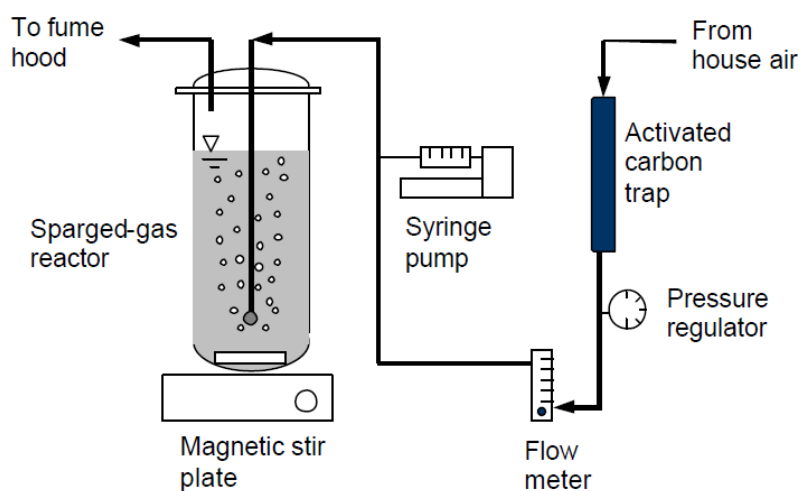


Figure 3.1 Schematic diagram of the gas-sparged bioreactors used for cultivating β -caryophyllene degrading microbial populations.

3.2.3 Bioreactor Start-up and Operation

The reactor was filled with 2.5 L of nutrient solution containing the following constituents added to tap water (Qi and Moe, 2006): NH_4NO_3 1.25g/L, KH_2PO_4 1.0 g/L,

MgSO₄·7H₂O 0.5 g/L, CaCl₂·2H₂O 0.02 g/L, CuCl₂·2H₂O 0.17 mg/L, CoCl₂·6H₂O 0.24 mg/L, ZnSO₄·7H₂O 0.58 mg/L, MnSO₄·H₂O 1.01 mg/L, Na₂MoO₄·2H₂O 0.24 mg/L, NiCl₂·6H₂O 0.10 mg/L and FeSO₄·7H₂O 1.36 mg/L. The pH was not adjusted.

The microbial consortium used to inoculated the sparged gas reactors was derived from commercially available potting soil (Showscape Potting Soil, Phillips Bark, MS, USA) comprised of ground and composted organic forest material, mason's sand, and perlite or other aggregate. A 150 g mass of potting soil (wet basis) was added to 1.5 L nutrient solution (composition as above), and then the slurry was manually stirred for one minute. After passing through a sieve to remove coarse materials, the slurry was allowed to quiescently settle for five minutes to separate sand which visibly accumulated on the bottom of the flask. A 0.5 L volume of the supernatant was then added to each bioreactor which already contained 2.5 L nutrient solution, resulting in a total of 3.0 L liquid volume in each reactor. Immediately thereafter, syringe pumps and gas flow were turned on to deliver β-caryophyllene-contaminated air to each reactor. The start of β-caryophyllene-contaminated air was designated as time zero. (Time zero = 2:45 p.m. on Oct. 18, 2010). The air flow rate was 1.0 L/min.

During the initial two days of operation, β-caryophyllene was delivered to the influent air supplies via glass gas tight syringes (5.0 mL capacity) at a flow rate of 0.06 mL/hr. After two days, it was observed that liquid β-caryophyllene had accumulated in the bottom of the glass injection ports, indicating that the rate of evaporation was lower than the rate of injection. Thereafter, continuous injection by syringe pumps was discontinued and aliquots of β-caryophyllene were manually injected into the septum-filled injection ports when it was visually observed that the previous injection had mostly evaporated (approximately 3-day intervals).

To compensate for evaporative losses of water in the sparged gas reactors, deionized (DI)

water was added to each bioreactor on a daily basis to maintain a liquid volume of 3.0 L. After adding DI water to reach a total volume of 3.0 L in each reactor, 100 mL of the mixed liquid was removed from each reactor, and 100 mL of nutrient solution was added while the reactors remained mixed. This resulted in a solids residence time (SRT) and hydraulic residence time (HRT) of 30 days. Liquid temperature, total suspended solids (TSS) concentration, and pH were measured in both reactors on a regular basis.

3.2.4 β -Caryophyllene Biodegradation Test

In an effort to further assess the capacity of the microbial populations in the two reactors to biodegrade β -caryophyllene, experiments were conducted using 160 mL glass serum bottles configured as shown in Figure 3.2.

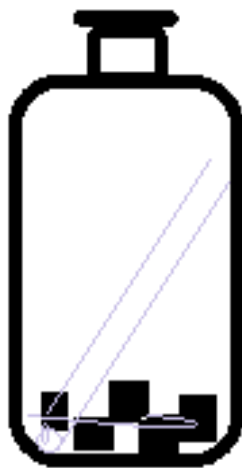


Figure 3.2 Serum bottles used for β -caryophyllene biodegradation test.

Each serum bottle contained five cubes of polyurethane foam approximately 1 cm per side (Honeywell-PAI, Lakewood, CO), a small glass tube, 4.0 mL nutrient solution (composition as used in the sparged gas reactor), and 1.0 mL of inoculum.

The inoculum for six serum bottles was comprised of an aliquot of the aqueous-phase

removed from the low temperature sparged gas reactor. Of these, two of the bottles received 0.1 mL of high purity β -caryophyllene, two of the bottles received 0.1 mL of low purity β -caryophyllene, and two of the bottles received no β -caryophyllene (negative control). The β -caryophyllene was dispensed into the upright glass tubes inside the serum bottles prior to sealing the bottles with butyl rubber stoppers and aluminum crimp caps. Headspace gas was comprised of air. Six additional serum bottles were likewise prepared, but with inoculum comprised of an aliquot of the aqueous-phase removed from the high temperature sparged gas reactor. At the time of inoculation of the serum bottles on day 42 of operation of the sparged gas reactors (Nov. 29, 2010), the TSS concentrations in the aqueous phases of the low temperature and high temperature sparged gas reactors were 116 mg/L and 38.7 mg/L, respectively.

Table 3.1 Summary of the serum bottle tests. Each treatment was conducted in duplicate.

Treatment ID	Inoculum source	β -caryophyllene purity ¹	Incubation temperature ²
A	Low temperature bioreactor, aqueous-phase	Low	Ambient
B	Low temperature bioreactor, aqueous-phase	High	Ambient
C	Low temperature bioreactor, aqueous-phase	-	Ambient
D	Low temperature bioreactor, lid	Low	Ambient
E	Low temperature bioreactor, lid	High	Ambient
F	Low temperature bioreactor, lid	-	Ambient
G	High temperature bioreactor, aqueous-phase	Low	30°C
H	High temperature bioreactor, aqueous-phase	High	30°C
I	High temperature bioreactor, aqueous-phase	-	30°C
J	High temperature bioreactor, lid	Low	30°C
K	High temperature bioreactor, lid	High	30°C
L	High temperature bioreactor, lid	-	30°C

¹ “Low” = purity >90% (TCI America, Portland, OR, catalog no. C0796); “High”= purity >98.5% (Sigma-Aldrich Inc., Allentown, PA, catalog no. 22075); “-” indicates that no β -caryophyllene was added (negative control).

² “Ambient” = ambient laboratory temperature (23±2°C)

Additional serum bottles were prepared as described above but with inoculum comprised of biomass scraped from the sides of the high temperature reactor and low temperature reactor above the water line. Biomass scraped from the lids (visually estimated to be approximately 50 μ L) using sterile loops was suspended in 100 mL of nutrient solution prior to use in inoculating serum bottles. Table 3.1 summarizes the treatments, each of which was conducted in duplicate.

Serum bottles inoculated with biomass originating from the low temperature bioreactor were incubated at ambient laboratory temperature following inoculation. Serum bottles inoculated with biomass originating from the high temperature bioreactor were incubated at 30°C. Gas samples (100 μ L) withdrawn from the serum bottles via glass, gas-tight syringes (Hamilton, Reno, NV) were analyzed for carbon dioxide concentration at regular time intervals.

3.3 Analytical Procedures

Total suspended solids (TSS) concentration in each reactor was measured in triplicate using Standard Method 2540D (Clesceri *et al.*, 1998). pH was measured using a model 290A pH meter from Orion Research Inc. (Boston, MA, USA). Temperature was measured using an electronic temperature monitor from Oakton Temp Lab (China) by submerging the probe directly into the liquid in the reactors.

The carbon dioxide concentration in gas-phase samples removed from serum bottles was measured using a gas chromatograph (SRI) equipped with a 6' packed column (80/100 Chromosorb 102, Supelco, Bellefonte, PA) and a thermal conductivity detector (TCD). 100 μ L samples were introduced via direct injection. A calibration curve was prepared using various dilutions of certified calibration standards (BOC, Port Allen, LA). Images of polyurethane foam cubes from serum bottles inoculated with biomass from sparged gas bioreactor were taken using a 3032 series preconfigured microscope from Accu-Scope® Inc (Commack, NY).

3.4 Results

3.4.1 Temperature

The temperature measured in the aqueous phase of each bioreactor as a function of time following startup was relatively stable (Figure 3.3). For the high temperature bioreactor, the temperature ranged from 45 °C to 50 °C, averaging 49.6 °C, close to the target temperature of 50 °C. For the low temperature bioreactor, the temperature ranged from 18 °C to 19 °C, averaging 18.9 °C.

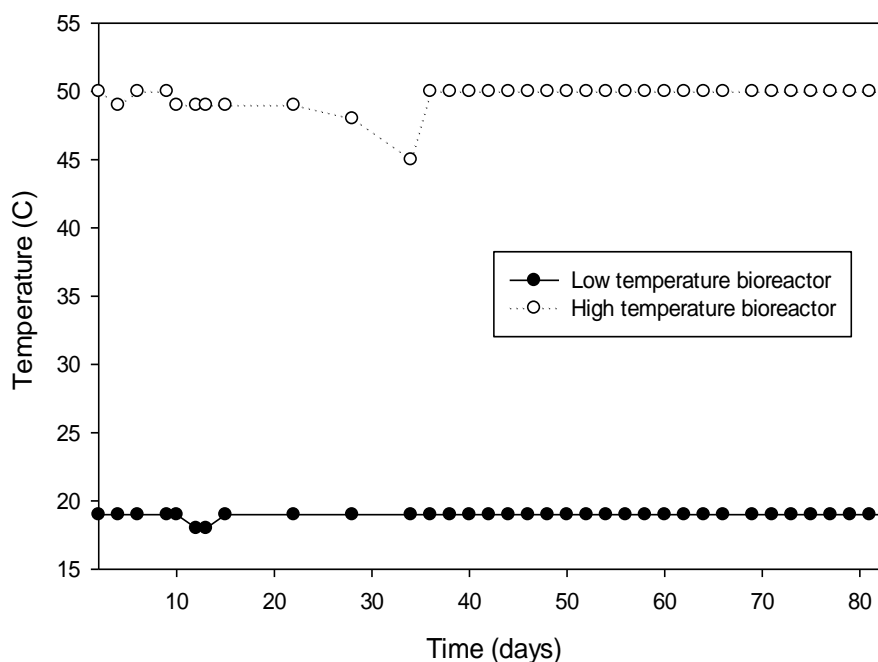


Figure 3.3 Temperature measured in the aqueous phases of the sparged-gas bioreactors.

The temperature measured on the lid surface of each bioreactor is shown in Figure 3.4. As shown, the temperature on each lid of the low temperature sparged gas bioreactors was relatively stable, averaging 19°C, essentially identical to the aqueous-phase temperature of the reactor. For the high temperature bioreactor, the temperature measured on the upper lid surface

ranged from 32 to 35°C and averaged 34°C, considerably lower than the temperature measured in the aqueous phase. It should be noted that the electrical heating tape did not extend above the liquid level in the high temperature bioreactor (see Figure 3.7). The relatively low thermal conductivity of the glass reactor combined with cooler surrounding laboratory temperature was apparently sufficient to result in an average lid surface temperature 15.6°C cooler than the average aqueous-phase temperature in the reactor.

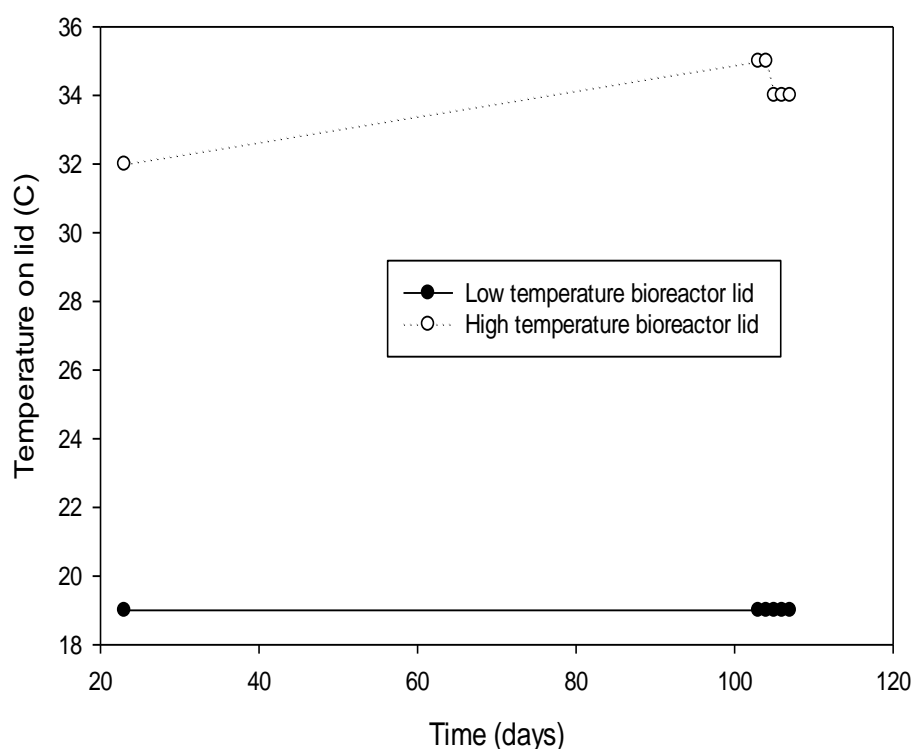


Figure 3.4 Temperature measured on the lid of the sparged-gas-bioreactors.

3.4.2. pH

Figure 3.5 depicts the pH measured in the aqueous phase of both bioreactors. As shown, the pH of both bioreactors decreased during the 30 days after bioreactor startup. The pH of the low temperature bioreactor was consistently higher than that of the high temperature bioreactor, however the differences were less than 0.5 pH units. The pH value of both bioreactors stayed

between 5.8 and 6.8, and the total pH value change of both bioreactors were less than 1.

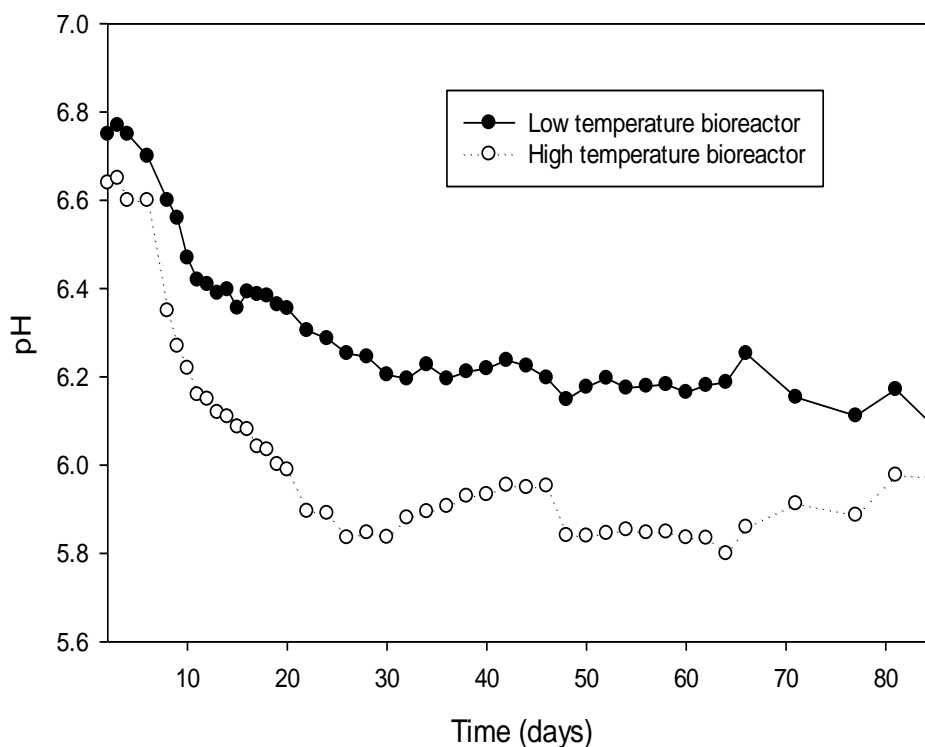


Figure 3.5 pH measured in the aqueous phases of the two sparged-gas bioreactors.

3.4.3. Total Suspended Solids (TSS)

TSS concentrations in the aqueous phase of the two sparged gas bioreactors are shown in Figure 3.6. Each data point represents the average of triplicate measurements. As shown, the TSS concentration in the aqueous-phase of the high temperature bioreactor was less than the TSS concentration in the aqueous-phase of low temperature bioreactor for most of the operation Period. The maximum TSS concentration observed in the aqueous-phase of the high temperature bioreactor was 74.7 mg/L at a time 73 days after startup. The maximum TSS concentration of the low temperature bioreactor was 170.7 mg/L at a time 36 days after startup.

Beginning about 7 days after startup, orange-colored biomass was visually observed to be growing on the inside walls and lid above the water level of the high temperature bioreactor. At

the same time, some white-colored biomass was visually observed to grow on the inside walls and lid above the water level of the low temperature bioreactor.

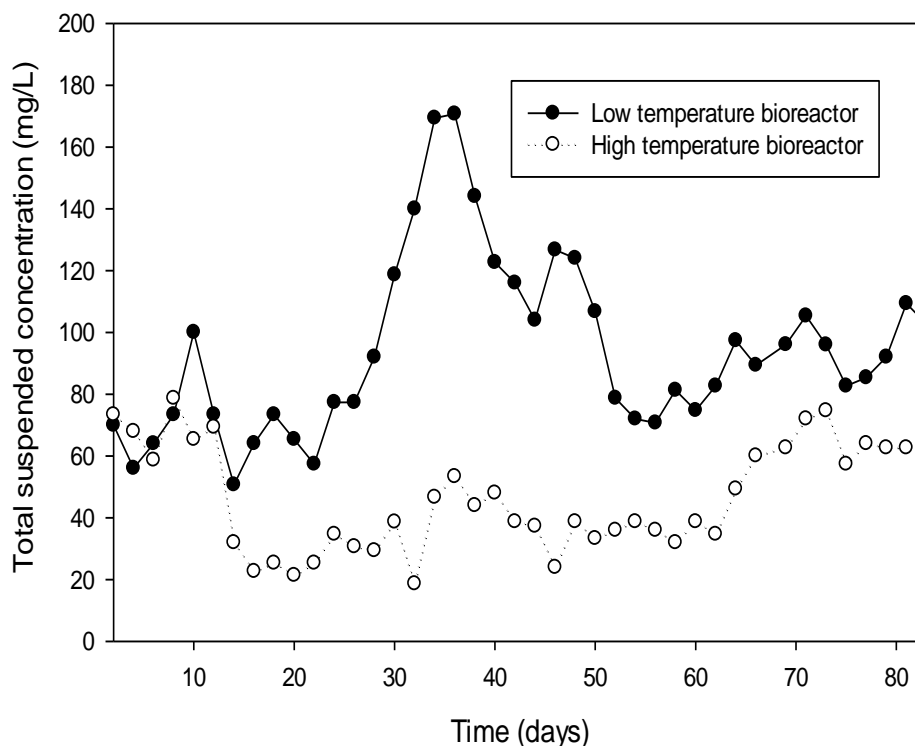


Figure 3.6 TSS concentrations measured in the aqueous phase of the low and high temperature sparged-gas bioreactors.

The quantity of biomass was visually observed to increase over time, particularly in the high temperature bioreactor. Figure 3.7 (top) shows photographs of the biomass on day 22 of bioreactor operation. As also visible in Figure 3.7 (top left), foaming was visually observed in the low temperature bioreactor starting about 20 days after startup.

The quantity of foaming in the low temperature bioreactor (top left) increased over the following weeks, as evident in Figure 3.7 (bottom left). Comparison of the two photographs revealed that the quantity of biomass growing above the water line increased over time, particularly in the high temperature bioreactor.

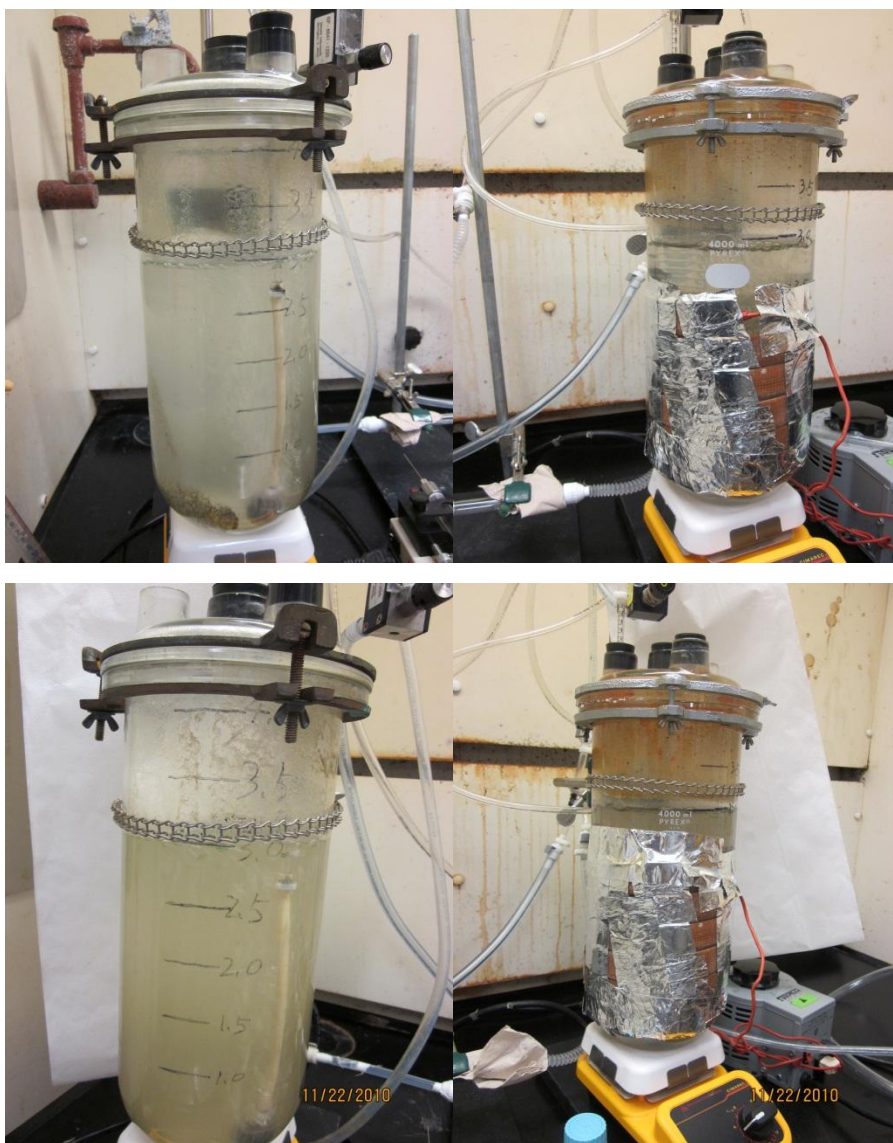


Figure 3.7 Low temperature bioreactor (left) and high temperature bioreactor (right) on day 22 (top) and 34 (bottom) following startup.

3.4.4 Serum Bottle Tests

Carbon dioxide concentrations measured in the gas headspace of serum bottles inoculated with biomass from the low temperature sparged gas bioreactor are shown in Figure 3.8. As shown in the figure 3.8, CO₂ concentrations in serum bottles amended with both high purity β -caryophyllene and low purity β -caryophyllene increased over time. The CO₂ concentration also increased over time in the negative control bottles (inoculated with biomass but not provided

with β -caryophyllene), but to a much lower degree. Aside from the initial 4 days following inoculation, the CO_2 concentrations observed in bottles supplied with high purity β -caryophyllene were consistently higher than CO_2 concentrations bottles containing low purity β -caryophyllene. The CO_2 concentrations observed in serum bottles inoculated with biomass removed from the lid (Figure 3.8, left) were somewhat higher than for serum bottles inoculated with suspended biomass from the aqueous-phase of the sparged gas bioreactor (Figure 3.8, right).

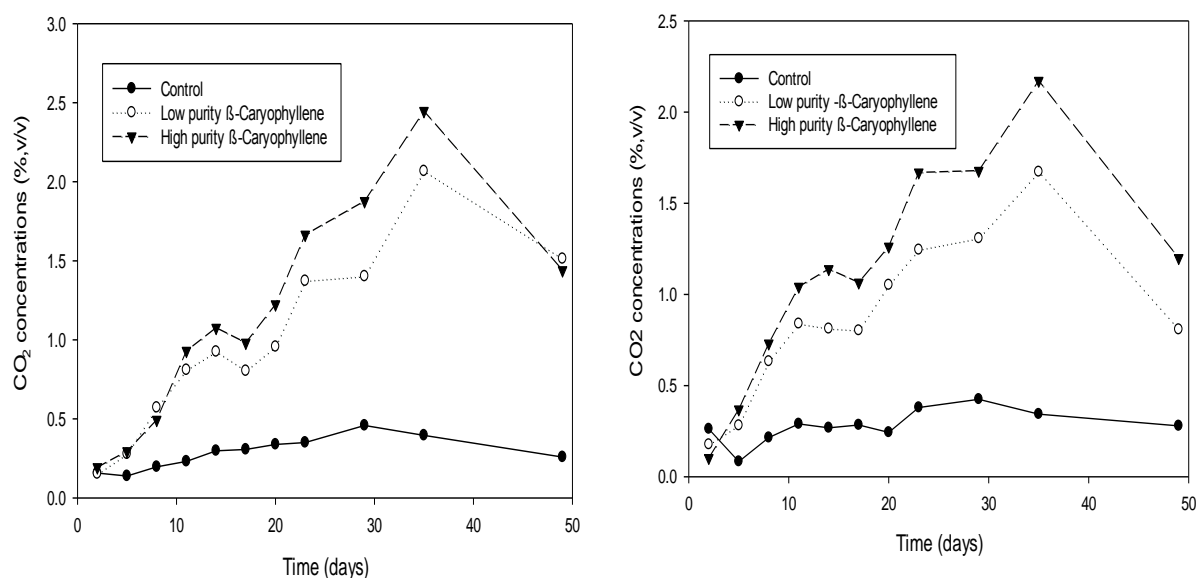


Figure 3.8 CO_2 concentrations measured in serum bottles inoculated with biomass from the lid (left) and aqueous-phase (right) of the low temperature sparged gas bioreactor.

Carbon dioxide concentrations measured in the gas headspace of serum bottles inoculated with biomass from the high temperature sparged gas bioreactor are shown in Figure 3.9. The CO_2 concentrations in serum bottles amended with both high purity β -caryophyllene and low purity β -caryophyllene increased over time to levels appreciably higher than was observed in negative control bottles inoculated with biomass but not provided with β -caryophyllene. The CO_2 concentrations observed in serum bottles inoculated with biomass removed from the lid (Figure.

3.9, left) were roughly the same as for serum bottles inoculated with suspended biomass from the aqueous-phase of the sparged gas bioreactor (Figure 3.9, right). As was observed with serum bottles inoculated with biomass from the low temperature sparged gas bioreactor, CO₂ concentrations observed in bottles supplied with high purity β -caryophyllene were consistently higher than CO₂ concentrations bottles containing low purity β -caryophyllene by a small amount.

The CO₂ concentrations increased faster in serum bottles inoculated with biomass from the high temperature sparged gas bioreactor than in serum bottles inoculated with biomass from the low temperature sparged gas bioreactor and reached higher maximum concentrations.

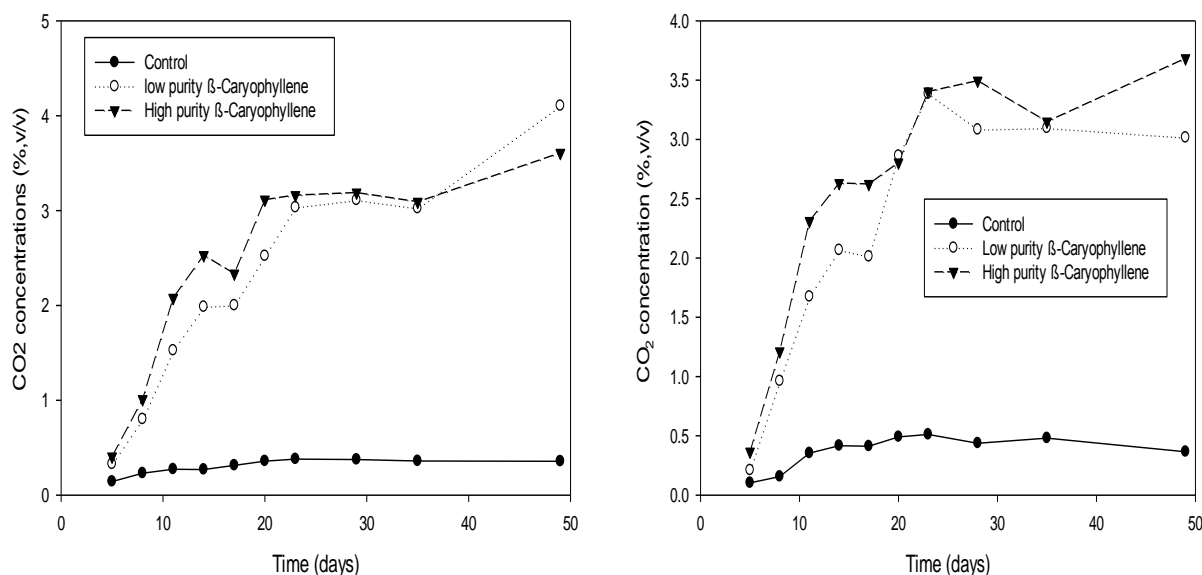


Figure 3.9 CO₂ concentrations measured in serum bottles inoculated with biomass from the lid (left) and aqueous-phase (right) of the high temperature sparged gas bioreactor.

As shown in Figure 3.10, the CO₂ increase in bottles supplied with β -caryophyllene (calculated by equation A-3 as the CO₂ concentration in bottles supplied with β -caryophyllene minus the CO₂ concentration in inoculated bottles not receiving any β -caryophyllene, see Appendix B) was obvious. This is consistent with the notion that β -caryophyllene was

biodegraded by the microbial culture. Because there was no abiotic control in which β -caryophyllene was placed in a sealed serum bottle lacking inoculum, however, a definitive conclusion that the CO_2 production resulted from biodegradation is not possible based on this data alone. The maximum CO_2 concentration observed in the serum bottles supplied with β -caryophyllene was also much smaller than the maximum amount of CO_2 calculated to be possible under the assumption that O_2 would stoichiometrically limit the extent of β -caryophyllene (see Appendix B). Because pH was not measured at the end of the serum bottle tests, a complete mass balance on carbon mineralization (i.e., accounting for aqueous-phase carbonate species) is not possible based on the data collected.

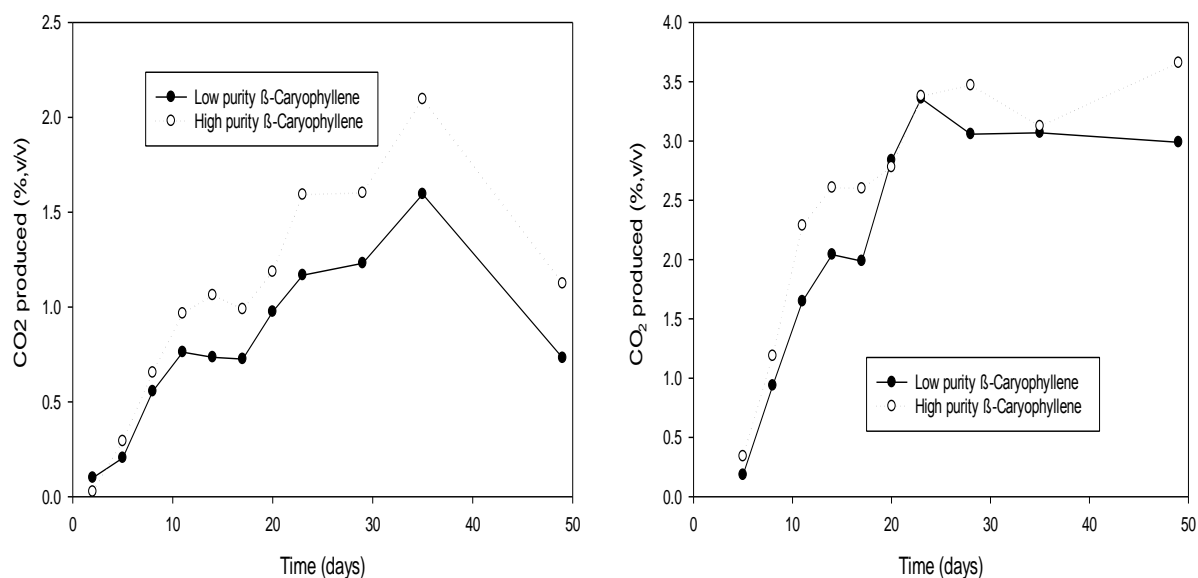


Figure 3.10 CO_2 produced by β -caryophyllene for low temperature aqueous phase bottles (left) and high temperature aqueous phase bottles (right).

At the end of the incubation period, visual observation revealed that the liquid present in serum bottles inoculated with biomass from all four sources (lid and aqueous phases of both low temperature and high temperature sparged gas reactors) and supplied with β -caryophyllene was more turbid than the liquid in negative control bottles lacking β -caryophyllene. Additionally, in

the serum bottles supplied with β -caryophyllene but not in the negative controls, the gas-water interface appeared to have a cloudy film present, biomass was visually observed on the glass side walls, and white-colored biomass growth was visible on the polyurethane foam cubes, particularly in serum bottles originating from the high temperature sparged gas bioreactor.

Images of polyurethane foam cubes from serum bottles inoculated with biomass from the lid of the high temperature sparged gas bioreactor are shown in Figure 3.11. As shown in the left image of figure, there was little biomass on the polyurethane foam cube structure of the foam cube from serum bottles supplied with no β -caryophyllene (left). In contrast, biomass can be readily observed in image of polyurethane foam cube from serum bottles supplied with high purity β -caryophyllene (right).

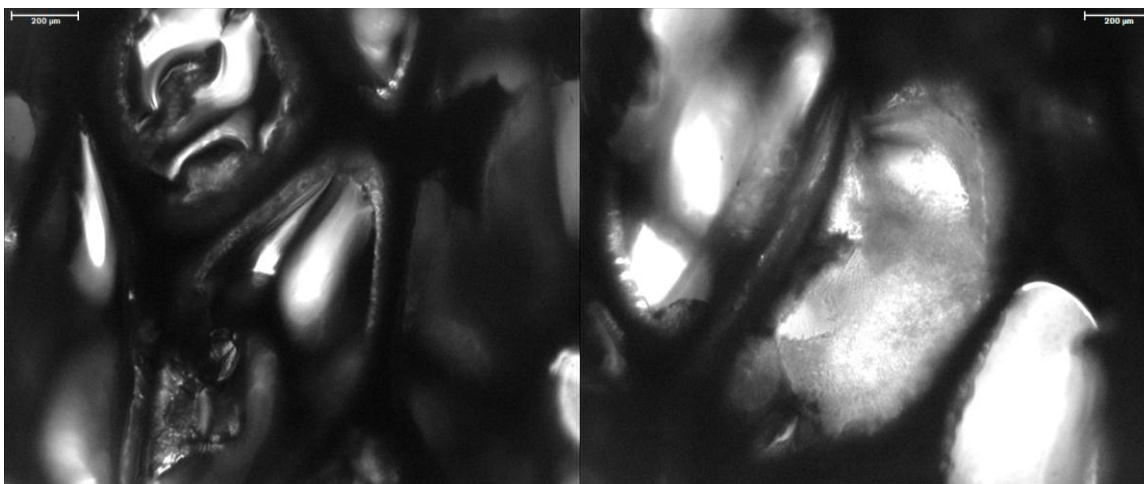


Figure 3.11 Image of a polyurethane foam cube from a serum bottle inoculated with biomass from the lid of the high temperature sparged gas bioreactor and supplied with no β -caryophyllene (left) and high purity β -caryophyllene (right) at the end of the incubation

3.5 Discussions and Conclusions

Collectively, the data presented in this chapter support the notion that β -caryophyllene was biodegradable and that the microbial community that developed in the sparged-gas reactors over time was able to biodegrade this target compound.

CHAPTER 4 BIOFILTER OPERATION AND PERFORMANCE

4.1 Introduction

After development of an enrichment culture able to biodegrading β -caryophyllene as described in Chapter 3, the microbial culture was used to inoculate a laboratory-scale biofilter that was subsequently operated for 244 days. This chapter describes the materials and methods employed for the biofilter experiments as well as the resulting bioreactor performance.

4.2 Materials and Methods

4.2.1 Experimental Apparatus

Laboratory studies employed a glass biofilter column configured as shown in Figure 4.1. The biofilter consisted of a bottom, a top, and five 25-cm sections, each with an inner diameter of 10 cm. perforated stainless steel plates placed at the bottom of the column and between each section supported the packing medium. The packing material consisted of polyurethane foam cubes (Honeywell-PAI, Lakewood, CO). The medium, supplied by the vendor in the form of cubes approximately 5.0 cm per side, was cut into cubes approximately 1.25 cm per side prior to use. The bottom-most biofilter section was filled with packing medium to a packed bed depth of 20 cm, and other sections each contained packed bed depths of 25 cm. The mass of packing medium was 49 g (dry mass basis) in the bottom-most section and 61 g in each of the four upper sections. This provided a total packed bed depth of 1.20 m, total packed bed volume of 9.42 L, and total mass of 293 g packing medium in the biofilter. The column was assembled by placing Viton™ O-rings between the sections and then clamping the assembly together using horseshoe type clamps. Gas sampling ports located in each column section were filled with Thermogreen™ LB-1 half-hole type septa (Supelco, Bellefonte, PA).

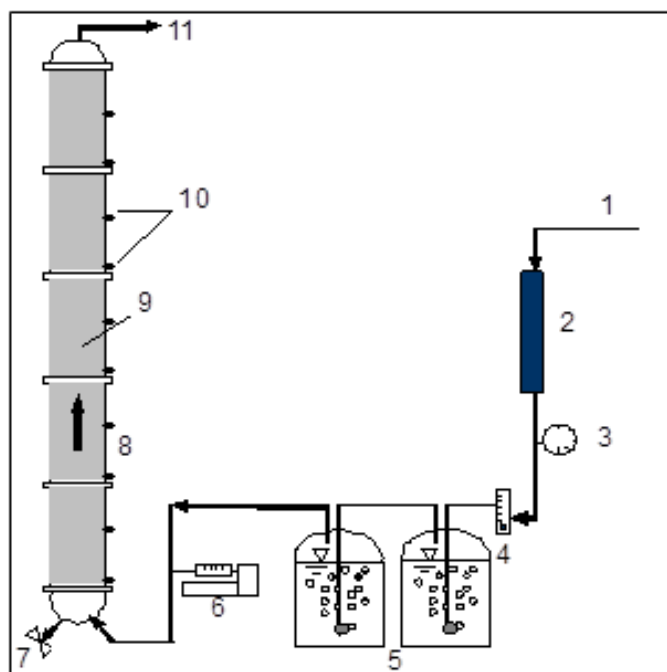


Figure 4.1 Schematic diagrams of the laboratory-scale biofilter apparatus. 1) laboratory air supply, 2) activated carbon filter, 3) pressure regulator, 4) electronic mass flow controller, 5) humidification chambers in series, 6) syringe pump, 7) liquid drain, 8) glass column assembled in sections, 9) foam packing medium, 10) septum-filled monitoring ports, and 11) effluent.

During operation, pollutant-free compressed air was humidified by passage through aeration stones submerged in deionized water in two 20 L glass carboys connected in series that were heated by electrical heating tapes (Cole-Parmer). A syringe pump (KD Scientific model 1000, Boston, MA) delivered β -caryophyllene from a glass, gas-tight syringe (Hamilton Co., Reno, NV) through a needle into a glass injection port where it evaporated into the air stream. Glass marbles were placed in the bottom of the column to evenly distribute air flow. An electronic gas mass flow controller (Aalborg Inc., Orangeburg, NY) measured and regulated air flow rates. The biofilter column was wrapped with electrical heating tapes (Cole-Parmer) attached to a variable controller (Variac) to regulate temperature with a target temperature of 30°C. Gas sampling lines were constructed of Teflon tubing.

During the large majority of operation, the β -caryophyllene supplied to the biofilter was

purity >90% (GC) (TCI America, Portland, OR, Cat No. C0796). During selected, short-term intervals (days 35 - 40, 120 - 125), higher purity β -caryophyllene (purity >98.5% GC, Sigma-Aldrich Allentown, PA, Cat No. 22075-25mL) was supplied to the biofilter.

At daily intervals, water accumulated in the bottom of the biofilter column was drained by briefly (~1 min) opening a valve located at the bottom of the column (see Figure. 4.1).

4.2.2 Abiotic Adsorption Capacity Test

Immediately prior to inoculation and startup of the biofilter, a preliminary test was conducted to determine the abiotic adsorption capacity of the biofilter packing medium. The system operation during the adsorption test was as described below for the biofilter's operation (β -caryophyllene injection rate of $0.03 \text{ m}^{-3} \text{ h}^{-1}$, air supplied continuously at a flow rate of 4.62 L/min) except that the test was conducted at ambient laboratory temperature ($23 \pm 2^\circ\text{C}$). β -caryophyllene (purity >90%) was used during this abiotic adsorption test. Pollutant concentrations exiting the system were measured as a function of time. The loading conditions were maintained for a duration of 8 days, at which time complete pollutant breakthrough had occurred (see Section 4.3.1).

4.2.3 Biofilter Inoculation and Start-up

For inoculation of the biofilter, biomass from the lid of the high temperature sparged-gas reactor (see Section 3.2.2) was mixed with 1 L of freshly prepared nutrient medium and was blended for 1 minute. The resulting suspension was then mixed with 11.0 L of freshly prepared nutrient solution (12.0 L total) and introduced into the bottom of the biofilter via a peristaltic pump (Masterflex) at a flowrate of 200 mL/min. After filling the column, the suspension was recirculated for a duration of 1 hour (withdrawl at top and reintroduction at the bottom, flow rate 200 mL/min), and then drained from the column at a flow rate of 200 mL/min. Time was

measured in days from the start of pollutant loading immediately following this inoculation.

4.2.4 Biofilter Operation

There were seven distinct Periods of operation, arbitrarily designated as Periods 1, 2, 3A, and 3B, 4, 5A, 5B, as summarized in Table 4.1.

Table 4.1 Summary of biofilter operating conditions

Period ID	Time of operation (days)	Gas flow rate (L/min)	Empty bed contact time (seconds)	Nutrient concentration*
1	0-40	4.62	122	1
2	41-60	8.30	68	1
3A	61-90	16.6	34	1
3B	91-138	16.6	34	3-6
4	139-169	28.2	20	6
5A	170-201	56.4	10	6
5B	202-244	56.4	10	6*

Nutrient concentration is expressed relative to the concentration used to develop the biofilter inoculum. 1× concentration refers to nutrient solution composition identical to that described in Section 3.2.3. 3× and 6× concentration refers to nutrient solution with all constituents added at three and six times the concentration described in Section 3.2.3 respectively. 6 concentration stands for nutrient solution with all constituents added at six times the concentration except the ammonium nitrate added at twelve times the concentration as described in Section 3.2.3.

At weekly intervals, nutrients were added to the biofilter by temporarily halting gas flow, filling the column with 10.0 L of freshly prepared nutrient solution, and then draining by gravity before restoring normal operation. For Periods 1, 2, and 3A, the nutrient solution was identical in composition to that used to grow the initial inoculum (see Section 3.2.3). During Period 3B, the nutrient solution was added with all constituent concentrations increased by a factor of three for the first week, and then it was added with six times the initial nutrient concentrations and with pH of 7 (this resulted a nutrient suspension) for the remainder operational Period 3B, Period 4, and Period 5A. During Period 5B, the nutrient suspension was added with all constituent concentrations six times higher the initial nutrient concentrations except the ammonium nitrate added at twelve times the concentration described in section 3.2.3. Although nutrient addition to

full-scale biofilters containing inert packing media is normally accomplished by spraying nutrient solution over the medium and allowing it to trickle through the packed bed, a fill-and-drain method similar to that described here has proven convenient for laboratory-scale systems (Moe and Qi, 2005).

At regular intervals, pollutant removal profiles as a function of biofilter height were determined by measuring pollutant concentrations from gas directed to the on-line analyzer from the lower-most sampling port within each of the four sections of the biofilter in addition to the influent and effluent. During profile studies, sampling commenced at the outlet end of the biofilter, and monitoring of the concentration at each port was conducted for a duration of one hour.

4.2.5 Analytical Procedures

The pH was measured daily from the drainage of the biofilter using a model 290A (Orion Research, Boston, MA, USA). Head loss across the biofilter packed bed depth was measured using a water manometer. Pollutant concentrations were measured using a model 600 HFID hydrocarbon analyzer (California Analytical, Orange, CA) in terms of carbon concentration. Calibration was performed daily. Influent and effluent temperature were measured using an electronic temperature monitor (Oakton Temp Lab, China) by wrapping the probe with the inlet pipe and inserting the probe directly into top section of the biofilter respectively.

4.3 Results

4.3.1 Abiotic Adsorption Test

As described in Section 4.2.2, after the biofilter column was initially assembled but prior to inoculation, β -caryophyllene was supplied to the system to assess the abiotic adsorption

capacity of the polyurethane foam packing medium. The experimentally measured breakthrough curve during β -caryophyllene loading to the abiotic column (prior to inoculation) is depicted in Figure 4.2. As shown, 5% pollutant breakthrough occurred within one day, and 95% pollutant breakthrough occurred after five days of continuous loading. Complete breakthrough was achieved after 5.83 days of operation (effluent concentrations varied $<5\%$). Mass balance calculations indicate that the pollutant mass entering and exiting the biofilter column differed by 0.939 g C. Assuming that all of the pollutants measured as C were comprised of β -caryophyllene and using the empirical formula for β -caryophyllene ($0.882 \text{ g C} / \text{per g } \beta\text{-caryophyllene}$ based on the formula $\text{C}_{15}\text{H}_{24}$), the pollutant mass accumulating in the biofilter column was calculated to be 1.06 g β -caryophyllene. The corresponding mass of β -caryophyllene adsorbed per unit mass of polyurethane foam was calculated to be 3.63 mg/g. Figure 4.2 shows the effluent pollutant concentration throughout the 8-day loading period of the abiotic adsorption test (left) as well as the influent concentration measured during the following 24 hour period of abiotic loading.

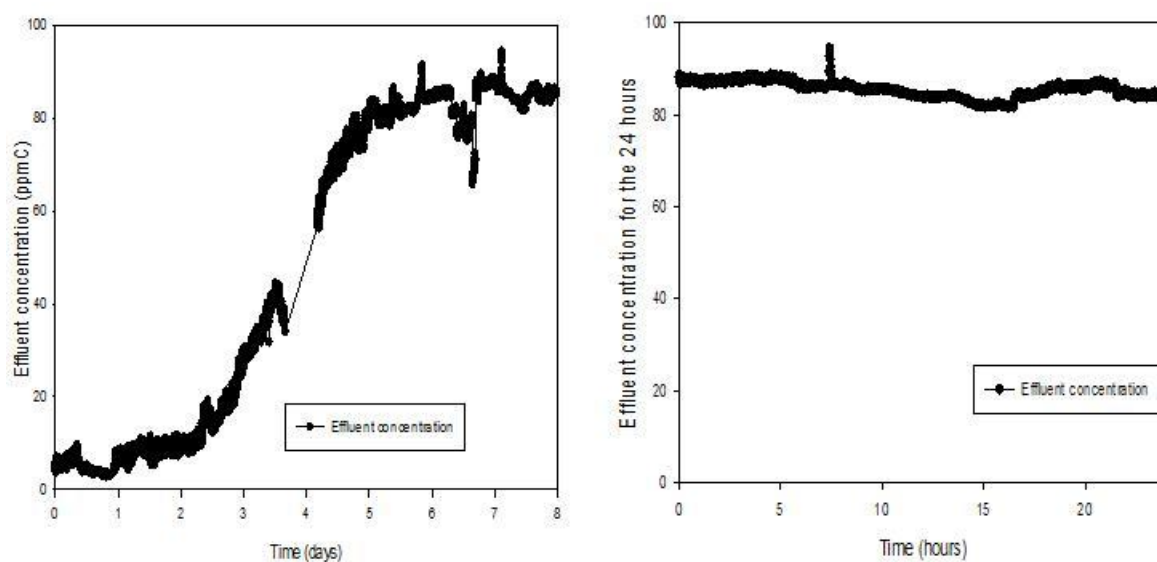


Figure 4.2 The effluent concentration of the adsorption test for a Period of 8 days (left) and the effluent concentration of adsorption test for the last 24 hours(right).

4.3.2 Inoculation, Startup, and Summary of Overall Performance

The suspended solids concentrations measured in the inoculum suspension before and after filling the column to inoculate at time zero were 142 mg/L and 54 mg/L, respectively, indicating that roughly one gram of the inoculum biomass was retained in the system at the time of startup. The influent gas temperature was 31°C. Table 4.2 summarizes biofilter loading conditions for the seven periods of operation.

Table 4.2 Summary of the biofilter loading conditions during each Period.

Period ID	Influent concentration (ppm-C) (mean±standard deviation)	Influent concentration (ppm _v as β-caryophyllene) ^a (mean±standard deviation)	Mean loading rate (g-C m ⁻³ hr. ⁻¹) ^b	Mean loading rate (g-β C m ⁻³ hr. ⁻¹)
1	84.8±6.12	5.62±0.41	1.20±0.04	1.36±0.05
2	103.58±5.18	6.90±0.35	2.64±0.06	2.99±0.07
3A	99.28±20.52	6.62±1.39	5.18±0.12	5.87±0.14
3B	93.75±12.76	6.25±0.85	4.77±0.15	5.40±0.17
4	98.09±20.80	6.54±1.39	8.49±0.39	9.62±0.44
5A	89.30±17.71	5.95±1.18	15.47±2.28	17.52±2.58
5B	91.99±20.12	6.13±1.34	15.80±2.38	17.90±2.70

^a Calculated assuming all VOCs measured by the HFID were β-caryophyllene and the ratio of 1.133 g β-caryophyllene per g C (based on the chemical formula of C₁₅H₂₄).

As shown in Table 4.2, during Period 1 (days 0-40) operation, the influent pollutant concentration was 84.8±6.12 ppm C (mean±standard deviation, parts per million by volume as carbon), corresponding to an average loading rate of 1.36±0.05g β-caryophyllene m⁻³·h⁻¹ (grams β-caryophyllene per m³ packed bed volume per hour). During Period 2 (days 41-60), the influent pollutant concentration was 103.58±5.18 ppm C, corresponding to an average loading rate of 2.99±0.07 g- β-caryophyllene·m⁻³·h⁻¹. During Period 3A (days 61-90), the influent pollutant concentration was 99.28±20.52 ppm C, corresponding to a mean loading rate of 5.87±0.14 g- β-caryophyllene m⁻³ h⁻¹.

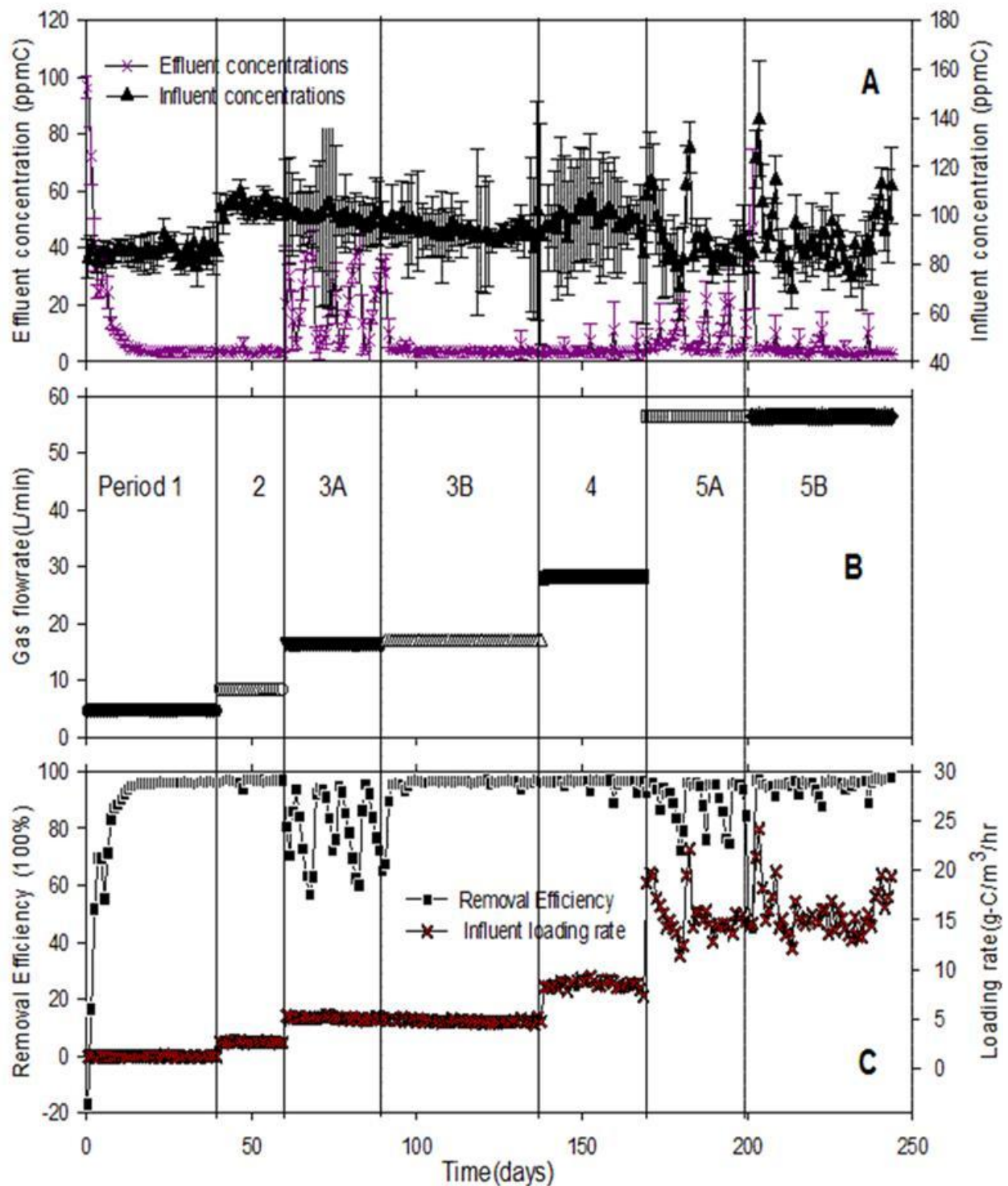
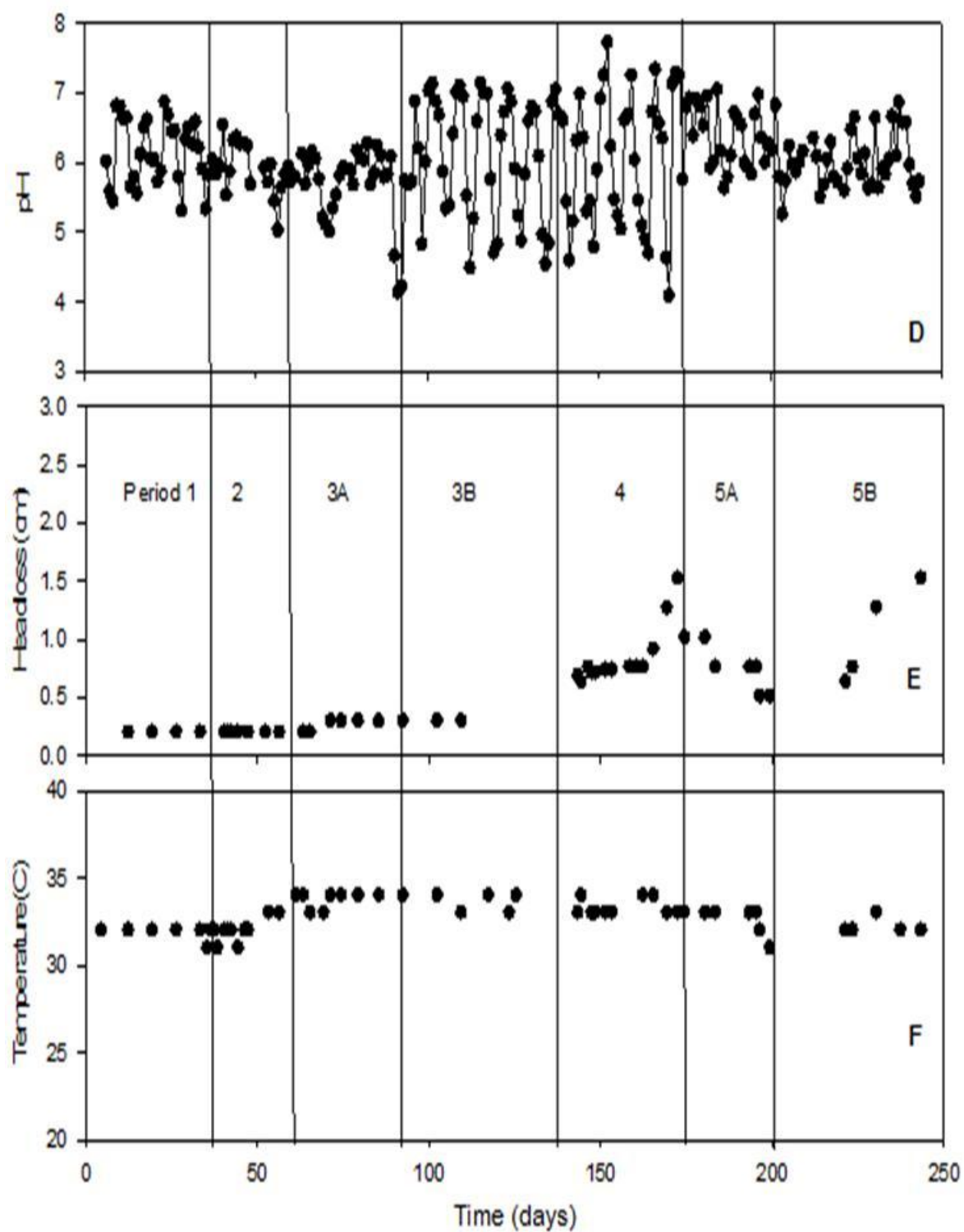


Figure 4.3 (A) Influent and effluent pollutant concentrations; (B) Influent gas flow rate (C) Influent loading rate and overall elimination capacity; (D) pH of leachate collected at the bottom of the biofilter (E) Headloss across the packed bed; (F) Gas temperature exiting the biofilter (In continued).



During Period 3B (days 91-138), the influent concentration was 93.75 ± 12.76 ppm C, corresponding to a loading rate of 5.40 ± 0.17 g β -caryophyllene $\text{m}^{-3} \text{h}^{-1}$. During Period 4 (days

139-169), the influent concentration was 98.09 ± 20.80 ppm C, corresponding to a loading rate of 9.62 ± 0.44 g β -caryophyllene $\text{m}^{-3} \text{h}^{-1}$. During Period 5A (days 170-201), the influent concentration was 89.30 ± 17.71 ppm C, corresponding to a loading rate of 17.52 ± 2.58 g β -caryophyllene $\text{m}^{-3} \text{h}^{-1}$. And during Period 5B (days 202- 244), the influent concentration was 91.99 ± 20.12 ppm C, corresponding to a loading rate of 17.90 ± 2.70 g β -caryophyllene $\text{m}^{-3} \text{h}^{-1}$.

Data regarding the overall performance of the biofilter is presented in Figure 4.3, and a more detailed presentation and discussion of results from each Period of operation appears in subsequent sections. Data points depicted in Figure 4.3A are the average of concentrations measured at one minute intervals $> 12 \text{ hr. day}^{-1}$ (influent) and 1 hr. day^{-1} (effluent). Error bars represent one standard deviation. Figure 4.3B depicted the mass flowrate of the four Periods. Data points in Figure 4.3C depicted the pollutant loading rate and removal efficiency. Figure 4.3D, E, and F depicted the pH of the drainage, headloss across the bed, and effluent gas temperature, respectively.

4.3.3 Biofilter Performance during Period 1 Operation

During Period 1, the biofilter received pollutant loading with gas flow rate of 4.62 L/min for a duration of 40 days (corresponding EBCT of 122 seconds). Influent and effluent concentration data points depicted in Figure 4.4 represent the average of concentrations measured at one minute intervals, and error bars represent standard deviation. Time zero in the figure denotes the time immediately after the biofilter was inoculated.

As shown in Figure 4.4, the effluent concentration consistently decreased over the first four days of operation. The effluent concentration reached a local minimum of 24.74 ± 2.48 ppm C on day four, and then it subsequently increased to 37.92 ± 1.95 ppm C on day 6. Following the nutrient addition on day 7 (denoted by red arrow in Figure 4.4), the effluent pollutant

concentration further decreased, reaching 10.26 ± 0.53 ppm C on day 10 and 3.64 ± 0.17 ppm C on day 17. Thereafter, the effluent pollutant concentration remained stable at a level between three and four ppm C for the remainder of Period 1 operation.

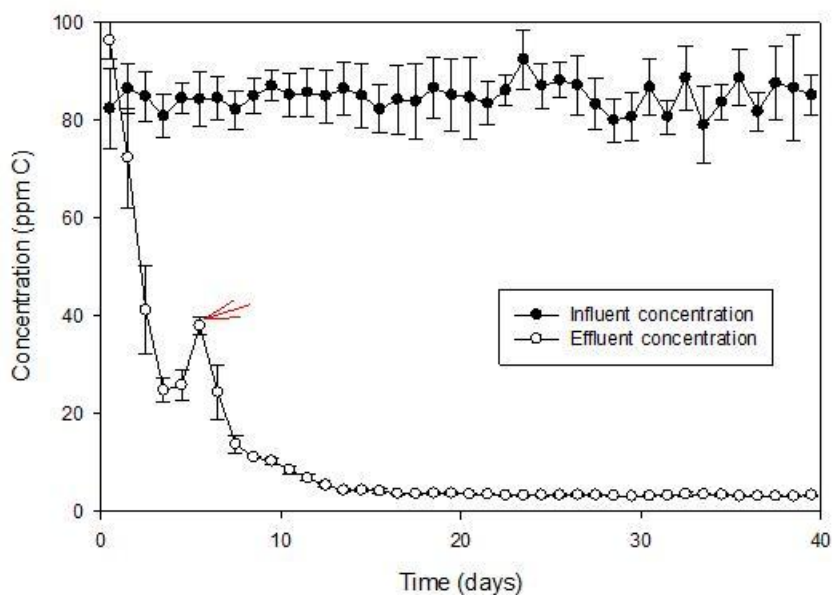


Figure 4.4 Experimentally measured influent and effluent gas-phase pollutant concentrations during Period 1.

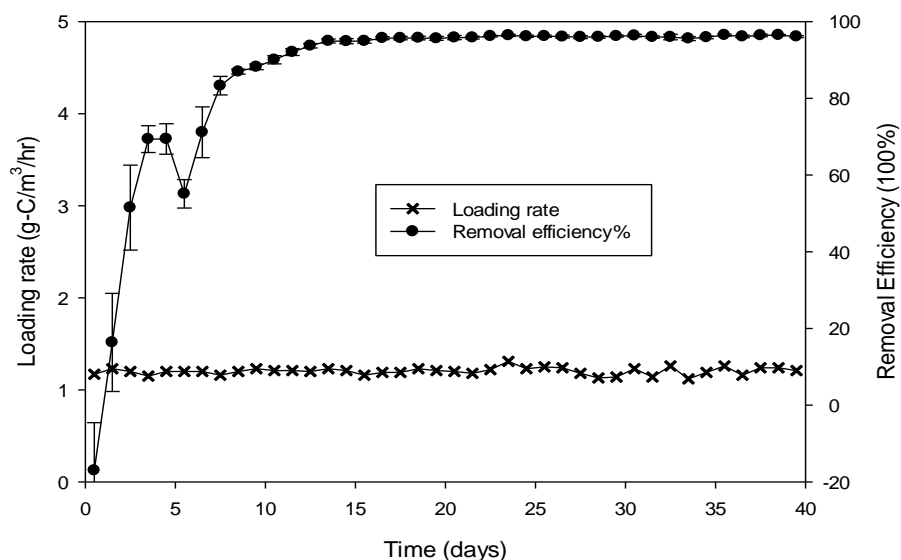


Figure 4.5 Loading rates and removal efficiency for Period 1.

Figure 4.5 depicts the average loading rates and pollutant removal efficiencies during Period 1. As shown in the figure, over 90% of the pollutant was removed after 11 days operation. After day 16, the mean average daily removal efficiency remained greater than $96.04 \pm 0.27\%$ throughout the remainder of Period 1.

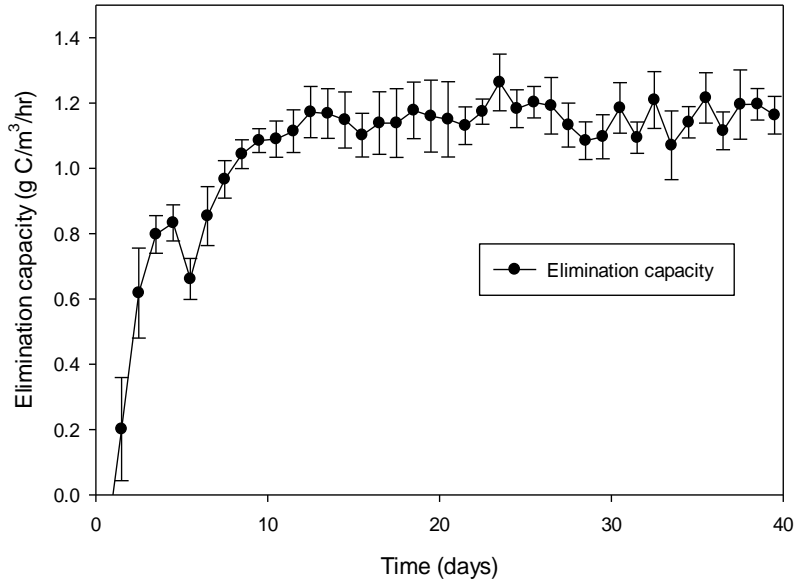


Figure 4.6 Elimination capacities for Period 1.

Figure 4.6 depicts the elimination capacity of Period 1, as shown in the figure, the elimination capacity increased over time for the first 16 days. After that, the elimination capacity was relatively stable at a level of $1.16 \pm 0.05 \text{ g C m}^{-3} \text{ hr}^{-1}$, corresponding to an elimination capacity of $1.31 \pm 0.05 \text{ g } \beta\text{-caryophyllene m}^{-3} \text{ hr}^{-1}$. The overall elimination capacity of this operation period excluding the first day was $1.07 \pm 0.20 \text{ g C m}^{-3} \text{ hr}^{-1}$, corresponding to an elimination capacity of $1.21 \pm 0.23 \text{ g } \beta\text{-caryophyllene m}^{-3} \text{ hr}^{-1}$.

Pollutant concentration profiles were measured along the height of the biofilter at different times to determine the spatial distribution of pollutant removal (Figure 4.7). The pollutant removal profile on day 4 was roughly linear with pollutant removal throughout the

entire column height. Over time, however, the pollutant removal profile shifted, with more rapid pollutant removal in the first section of the column followed by slower pollutant elimination up to the outlet height. On days 18 and 36, pollutant removal was mostly completed within the first 73 cm bed depth.

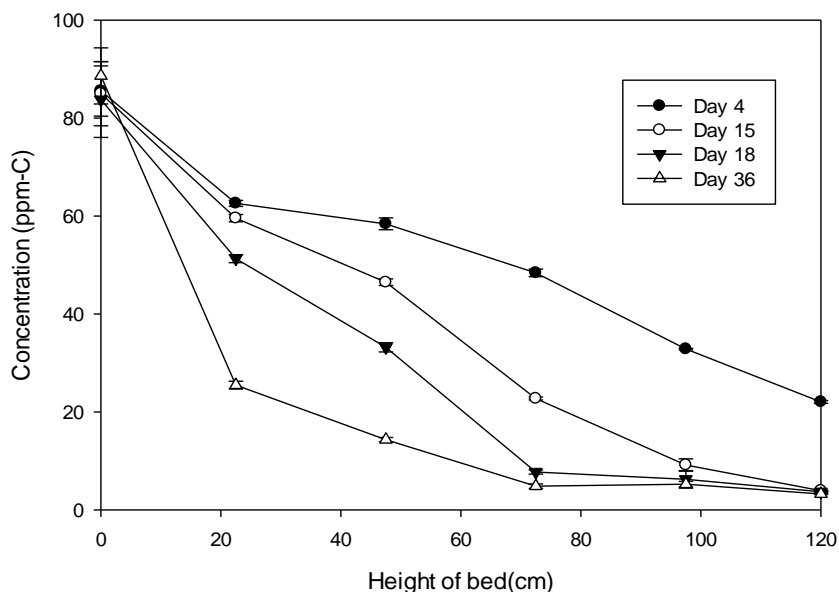


Figure 4.7 VOC concentration profiles measured on days 4, 15, 18, and 36.

During the last five days of Period 1 (days 35-40), higher purity β -caryophyllene (>98.5% purity as opposed to >90% purity) was supplied to the biofilter (see Section 4.2.1). Figure 4.8 depicts the influent and effluent concentrations for five days (days 30-35) low purity β -caryophyllene (>90% purity) supplied to the biofilter following five days higher purity β -caryophyllene (>98.5% purity) was applied. As shown in the figure, the mean influent concentration for the higher purity β -caryophyllene duration was 85.89 ± 2.67 ppm C, it did not differ from the low purity β -caryophyllene duration of 83.7 ± 4.0 ppm C. The effluent concentration was quite stable throughout the ten days at the value of 3.3 ± 0.2 ppm C.

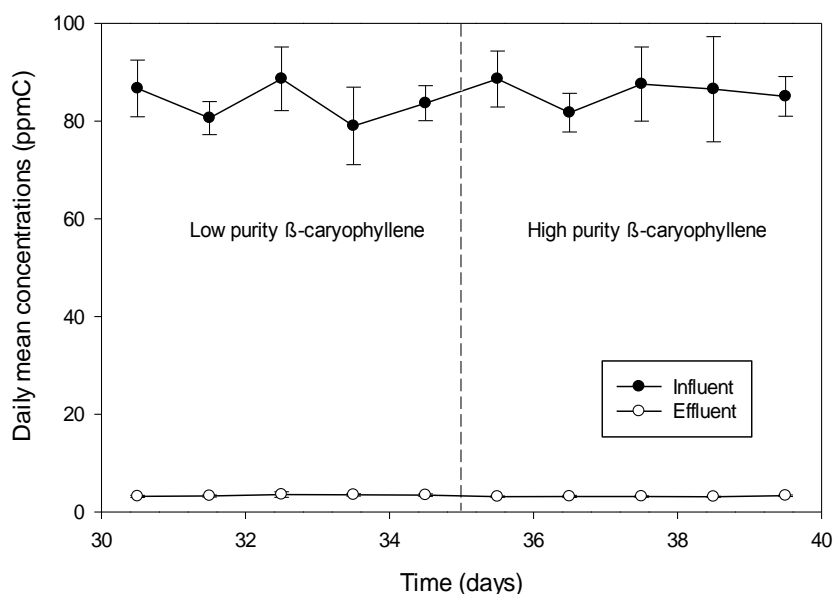


Figure 4.8 Influent and effluent concentrations from high purity β -caryophyllene experiment at the end of Period 1.

4.3.4 Biofilter Performance during Period 2 Operation

At the start of Period 2 on day 41, the influent gas flow rate was increased from 4.62 to 8.30 L/min, decreasing the EBCT from 122 to 68 seconds. As shown in Figure 4.9, the biofilter quickly adapted to the new loading condition. The influent concentration increased from 84.8 ± 6.12 ppm C in Period 1 to 103.06 ± 5.82 ppm C on day 41, and it maintained at a mean influent concentration of 103.6 ± 2.5 ppm C in Period 2. The mean effluent concentration was at a level of 3.54 ± 0.8 ppm C during Period 2, and it did not vary much from mean effluent concentration of Period 1.

Both the influent and effluent concentration were quite stable for the entire Period 2, even during the interval immediately following the doubling of polluted gas flow rate. The pollutant loading rates and the pollutant removal efficiency are shown in Figure 4.10. As shown in the figure, it had a mean pollutant removal efficiency of $96.58 \pm 0.74\%$ throughout the Period 2.

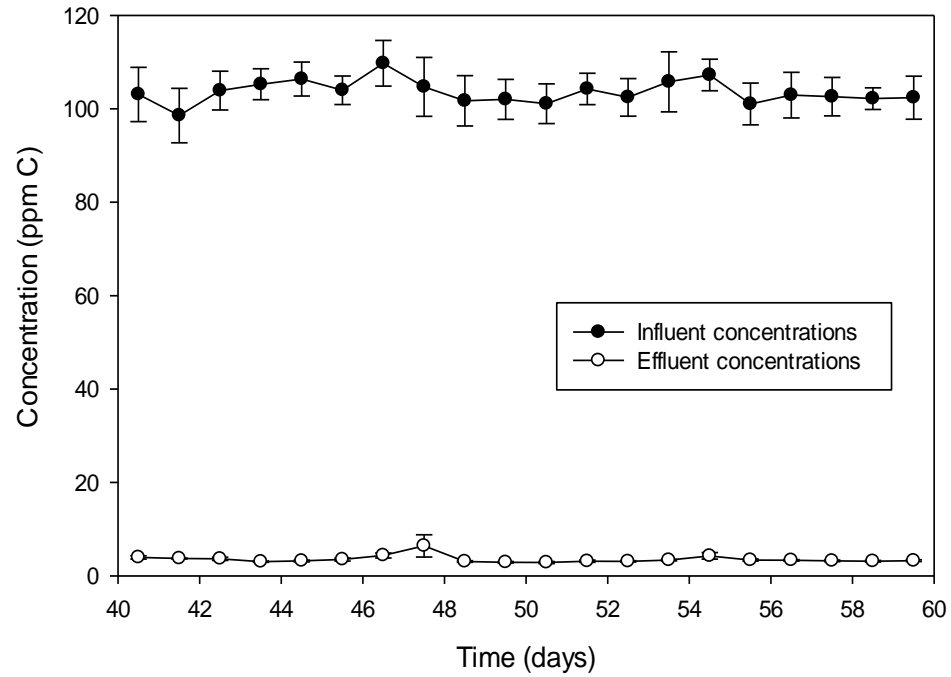


Figure 4.9 Influent and effluent concentration of Period 2.

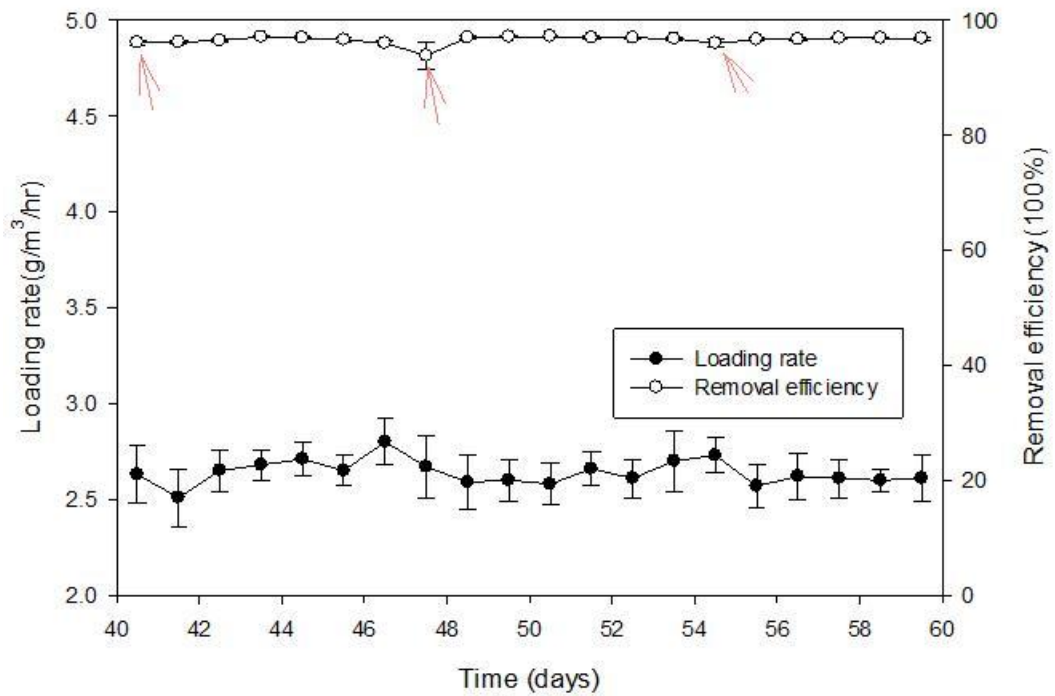


Figure 4.10 Loading rates and removal efficiency for Period 2.

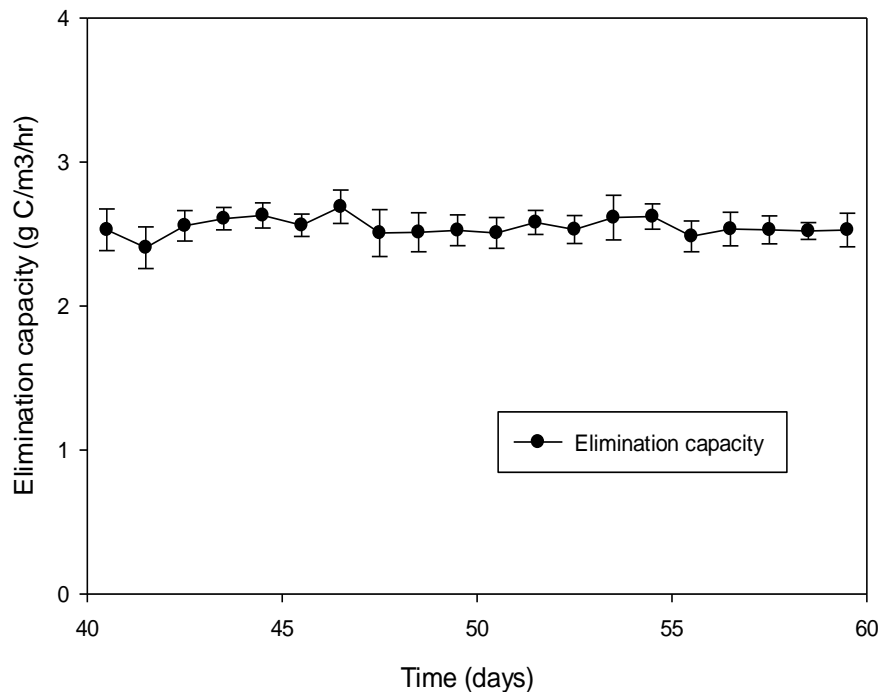


Figure 4.11 Elimination capacities for Period 2.

As shown in Figure 4.11, the elimination capacity of this Period was $2.55 \pm 0.06 \text{ g C m}^{-3} \text{ h}^{-1}$, corresponding to an elimination capacity of $2.89 \pm 0.07 \text{ g } \beta\text{-caryophyllene m}^{-3} \text{ h}^{-1}$.

Figure 4.12 depicts the pollutant concentration profiles measured along the height of the biofilter at different times in Period 2. Figure 4.12 (top) depicts the pollutant concentration profile data collected two days after the nutrient addition, and Figure 4.12 (bottom) depicts the pollutant concentration profile data collected five days after the nutrient addition.

As shown in the figure (top), pollutant removal was mostly completed within the first 73 cm bed depth two days after the nutrient addition. However, the pollutant removal was mostly completed within the first 100 cm bed depth two days before the nutrient addition (bottom), and the profile data collected on depth 22.5 cm and 47.5 cm were higher than the profile data collected two days after nutrient addition.

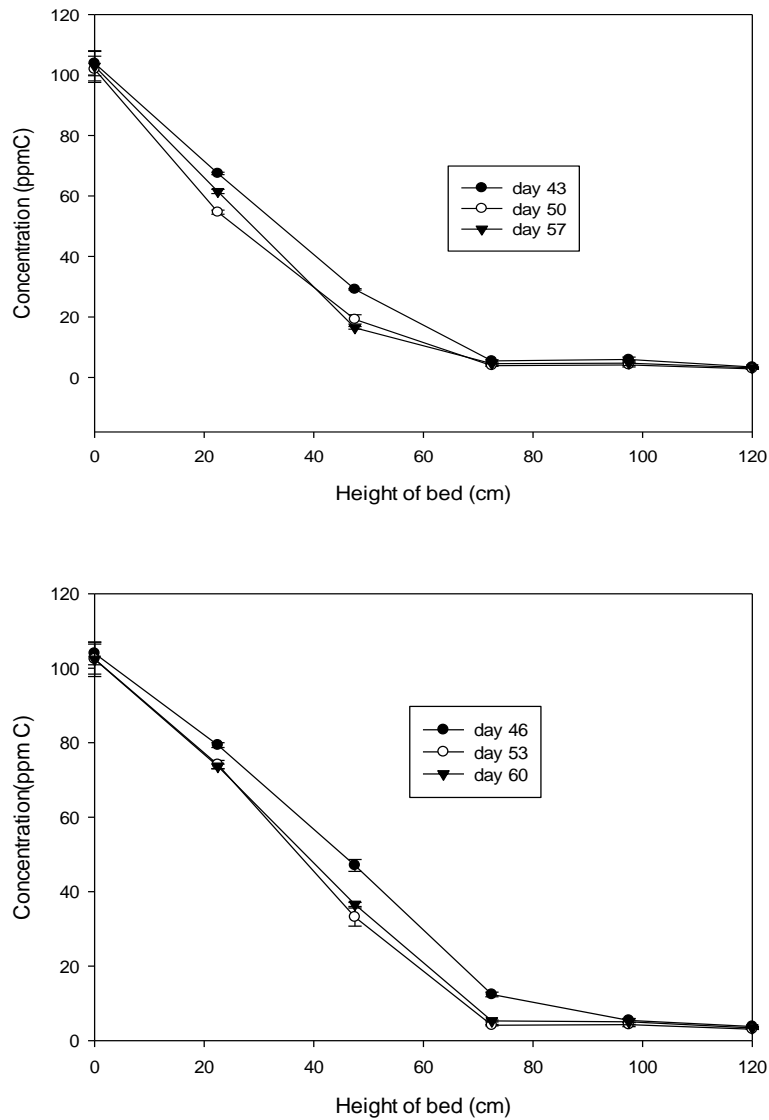


Figure 4.12 VOC concentration profiles measured two days after the nutrient addition on days 43, 50, 57 (top) and five days after nutrient addition on day 46, 53, 60 (bottom) during Period 2.

4.3.5 Biofilter Performance during Period 3A Operation

At the start of Period 3A on day 61, the influent gas flow rate was doubled again from 8.30 to 16.6 L/min, decreasing the EBCT from 68 to 34 seconds. As shown in Figure 4.13, the average influent concentration was relatively stable at a level of 99.28 ± 20.52 ppm C throughout

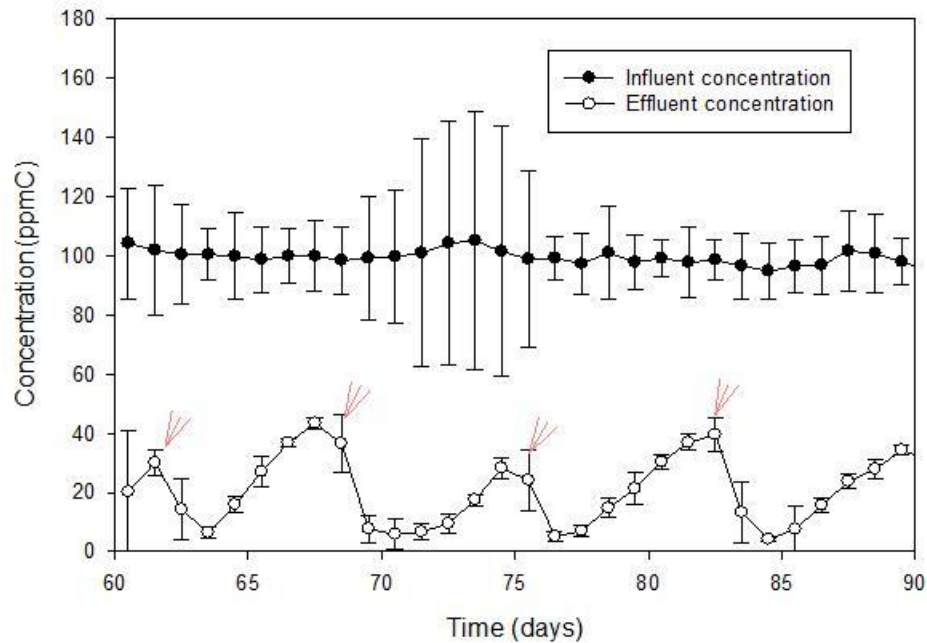


Figure 4.13 Influent and effluent concentration of Period 3A. Arrows denote the days when nutrients were added.

However, a higher standard deviation in daily measurements was observed in the middle of the Period.3A As shown in the Fig. 4.13, the effluent pollutant concentration exhibited a consistent pattern on a weekly basis. After the weekly nutrient addition (denoted by red arrows in Figure 4.13), the effluent concentration decreased, and reached a local minimum within 3 days. Then the effluent concentration subsequently increased, reaching a local maximum on the subsequent nutrient day.

The effluent concentration versus time since nutrient addition is plotted in Figure 4.14, with data shown for separate weeks (top) and as averages for all weeks (bottom). As shown in the figure, the effluent concentration rapidly decreased immediately after nutrient was added, and it reached the lowest concentration on day 2. After that the effluent concentration slowly increased until the next nutrient addition day. As shown in Figure 4.14 (bottom), the mean effluent concentration of the four weeks reached the breakthrough of 4.62 ± 0.81 ppm C on day 2

after the nutrient was added. As the nutrient consumed over time by the microorganisms in the biofilter, the effluent concentration showed a roughly linear increase for the remainder days.

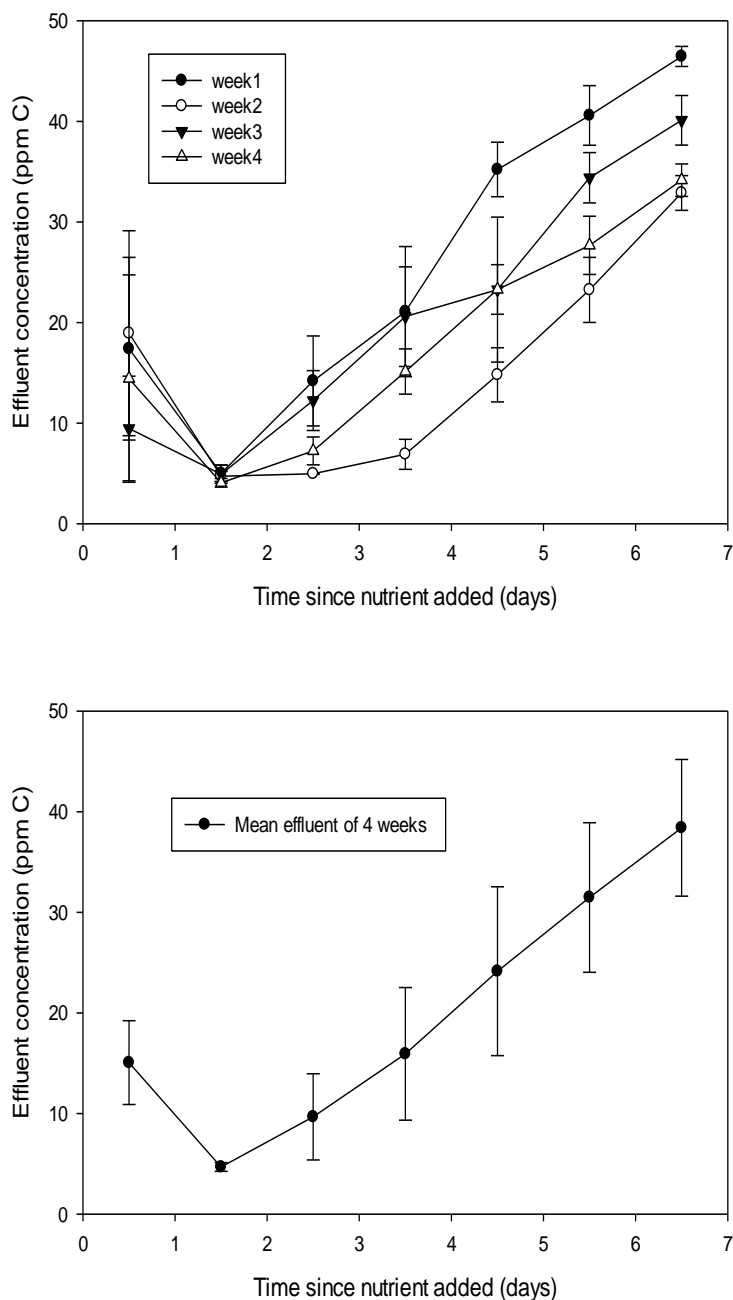


Figure 4.14 Effluent concentrations as a function of time since nutrient addition in Period 3A with data plotted separately for each week (top); Effluent concentration as a function of time since nutrient addition with data plotted as average of all four full weeks of operation during Period 3A (bottom).

Figure 4.15 depicts the mean daily loading rates and removal efficiency (top) and elimination capacities (bottom) for Period 3A. As shown in the figure, the removal efficiency was fluctuant weekly.

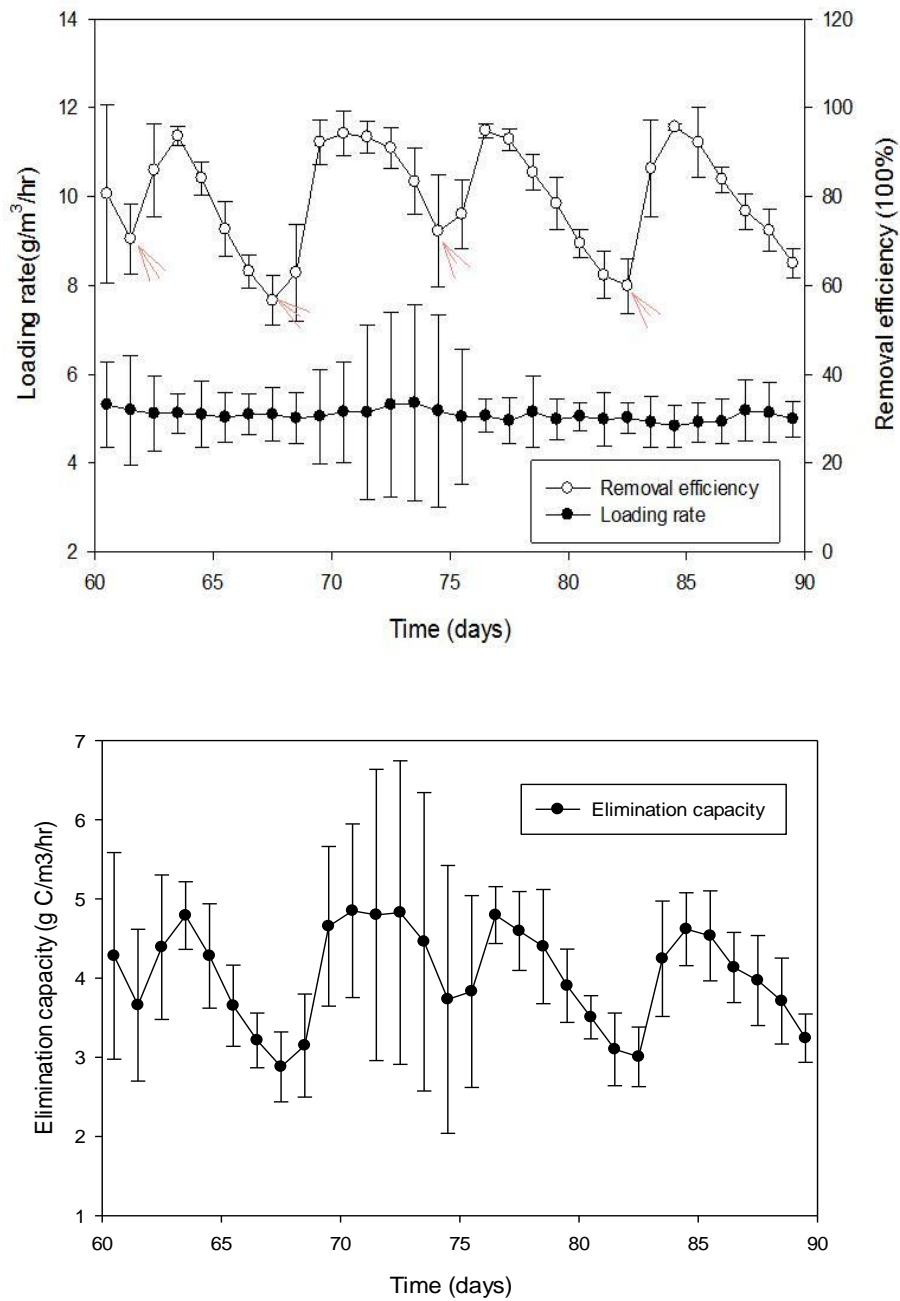


Figure 4.15 Loading rates and removal efficiency (top) and elimination capacities (bottom) for Period 3A.

It's overall removal efficiency for period 3A was $79.55 \pm 12.07\%$ (mean \pm standard deviation), and the highest removal efficiency was $95.60 \pm 0.70\%$ on day 85. The mean loading rate was $5.18 \pm 0.12 \text{ g C m}^{-3} \text{ h}^{-1}$, corresponding to a mean loading rate of $5.87 \pm 0.14 \text{ g } \beta\text{-caryophyllene m}^{-3} \text{ h}^{-1}$. The mean elimination capacity of this period was $4.04 \pm 0.62 \text{ g C m}^{-3} \text{ h}^{-1}$, corresponding to an elimination capacity of $4.58 \pm 0.70 \text{ g } \beta\text{-caryophyllene m}^{-3} \text{ h}^{-1}$ in this Period.

4.3.6 Biofilter Performance during Period 3B Operation

During Period 3B, the influent gas flow rate was the same as in Period 3A (16.6 L/min, EBCT 34 seconds). The difference was that during Period 3B, higher concentration of the nutrient solutions were supplied to the biofilter on a weekly basis. For the first week (i.e., the nutrient addition on day 91), the concentration of the nutrient solution supplied was three times the initial, and for the remaining 6 weeks (i.e., the nutrient additions on days 97, 104, 111, 118, 125, and 132), six times concentration was employed relative to the baseline concentration supplied during Periods 1-3A.

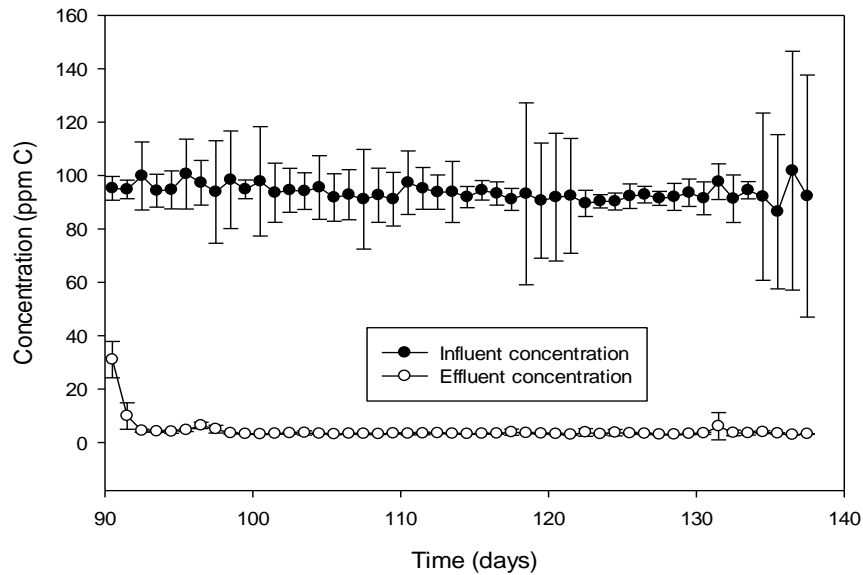


Figure 4.16 Experimentally measured influent and effluent gas-phase pollutant concentrations during Period 3B.

Figure 4.16 depicts the influent and effluent gas-phase pollutant concentrations measured for Period 3B. As shown in the figure, the effluent concentration decreased dramatically immediately after three times nutrient solution was applied to the biofilter on day 91. The effluent concentration reached a local minimum of 4.1 ± 0.6 on day 95, three days after the first addition of the higher concentration nutrient solution, but slightly increased to 6.4 ± 1.2 on day 97, seven days after the initial application of increased nutrient concentration. This suggested that a nutrient limitation still occurred under three times higher nutrient solution was applied to the biofilter. On day 97, six times higher concentration nutrient solution (relative to baseline) was employed, and the effluent concentration decreased again to a local minimal of 3.47 ± 0.29 ppm C on day 99. From day 99, the effluent concentration stayed quite stable for the remainder of Period 3B at a level of 3.3 ± 0.2 ppm C.

Loading rates and pollutant removal efficiencies during Period 3B are depicted in Figure 4.17. As shown in the figure, $95.44 \pm 4.30\%$ of the pollutant was removed during all 48 days of Period 3B operation. Considering the interval only after changing to six-times the baseline nutrient concentration on day 91 the removal efficiency was $96.24 \pm 0.72\%$. The elimination capacity was 4.57 ± 0.25 g C $m^{-3}h^{-1}$, corresponding to an elimination capacity of 5.17 ± 0.28 g β -caryophyllene $m^{-3}h^{-1}$.

On day 120, higher purity β -caryophyllene ($>98.5\%$ versus $>90\%$) was supplied to the biofilter for a duration of 4.85 days. Figure 4.18 depicts influent and effluent pollutant concentrations during this short Period of time. As shown, the influent concentration was 90.9 ± 1.2 ppm C, essentially the same as the previous influent concentration measurement, and the effluent concentration was 3.34 ± 0.37 ppm C which is quite similar to the effluent mean of 3.3 ± 0.2 ppm C in Period 3B.

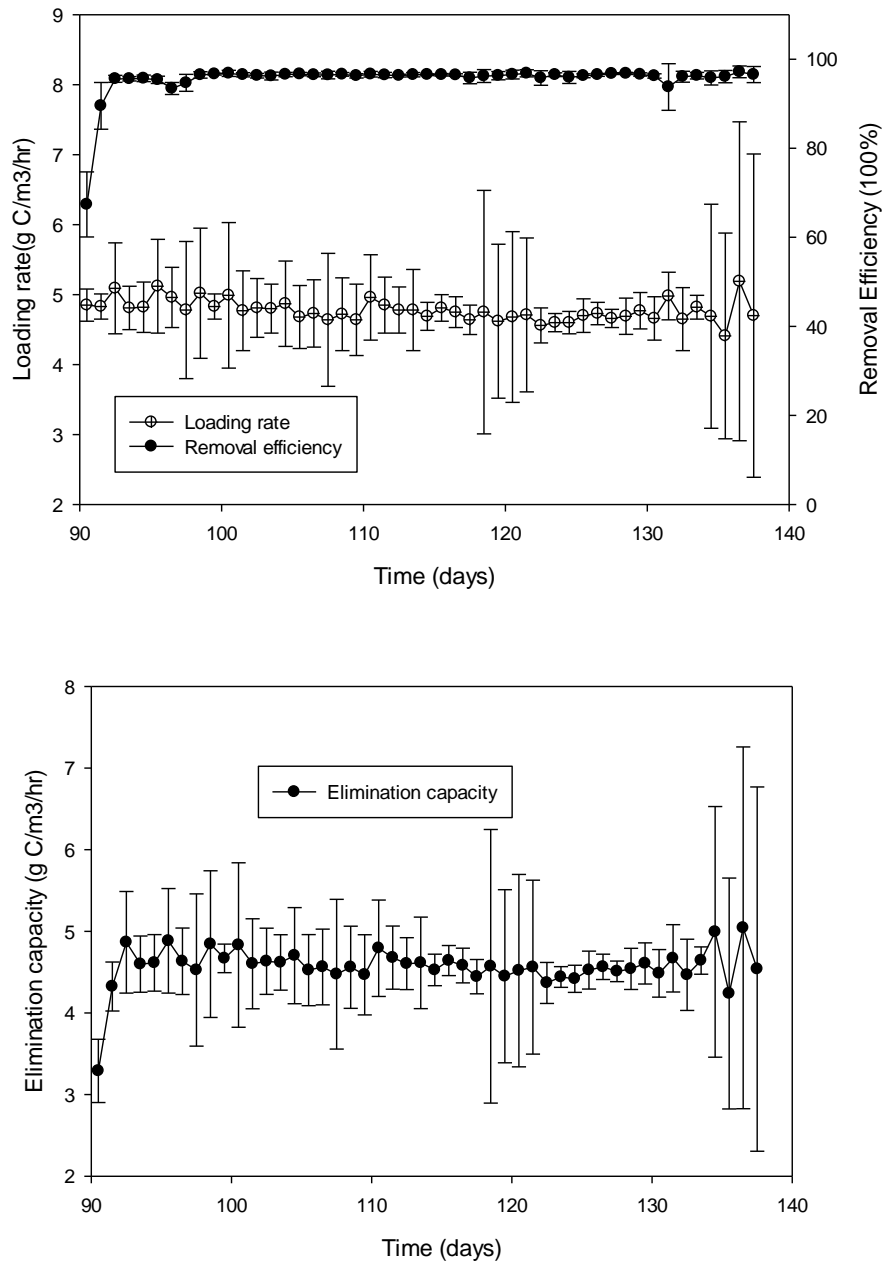


Figure 4.17 Loading rate and removal efficiency (top) and elimination capacities (bottom) of Period 3B.

Pollutant concentration profiles measured along the height of the biofilter during intervals when different nutrient solution concentrations were supplied are depicted in Figure 4.19. All three profiles were measured during intervals when the same pollutant loading rate was supplied

to the biofilter, and all were determined two days after the preceding nutrient addition.

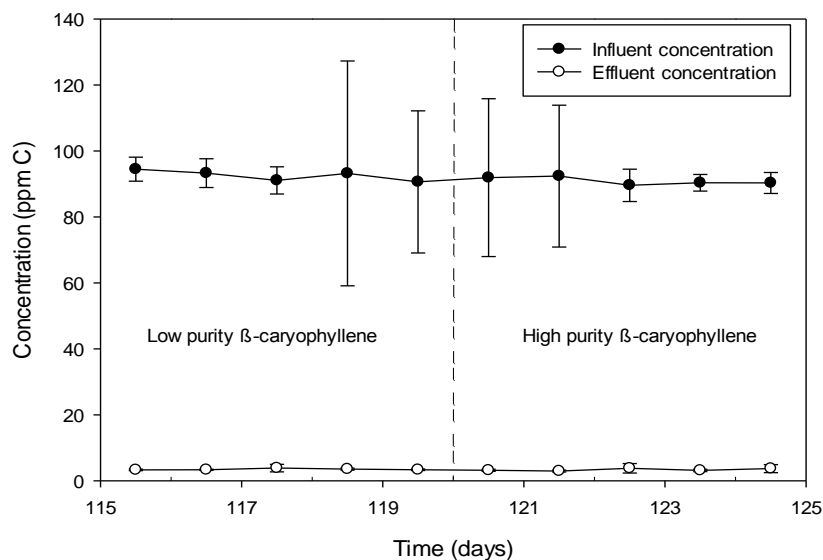


Figure 4.18 Influent and effluent concentrations measured during high purity β -caryophyllene test in Period 3B

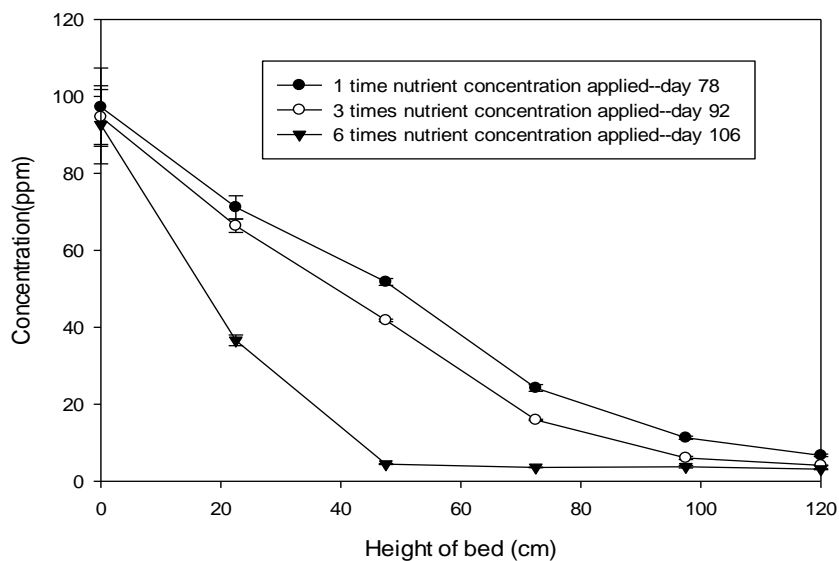


Figure 4.19 VOC concentration profiles measured on days 78 (Period 3A) and 92 and 106 (Period 3B) following addition of three different nutrition solution concentrations (one, three, and six times the baseline nutrient concentrations, respectively).

As shown in Figure 4.19, the pollutant removal profile observed following addition of the

original nutrient solution on day 78 was roughly linear, with pollutant removal occurring throughout the entire column height.

The pollutant removal profile observed after six times higher nutrient solution demonstrated that the zone of pollutant removal shifted toward the inlet section with more rapid pollutant removal, and the pollutant was almost completely removed in the first two sections.

4.3.7 Biofilter Performance during Period 4 Operation

At the start of Period 4 on day 139, the gas flow rate was doubled from 16.6 L/min to 28.2 L/min, decreasing the EBCT from 34 to 20 seconds. To accommodate the higher gas flow rate, the influent pollutant-free compressed air was split evenly into two parallel sets each comprised of two carboys in series (four carboys total) for humidification prior to contaminant injection.

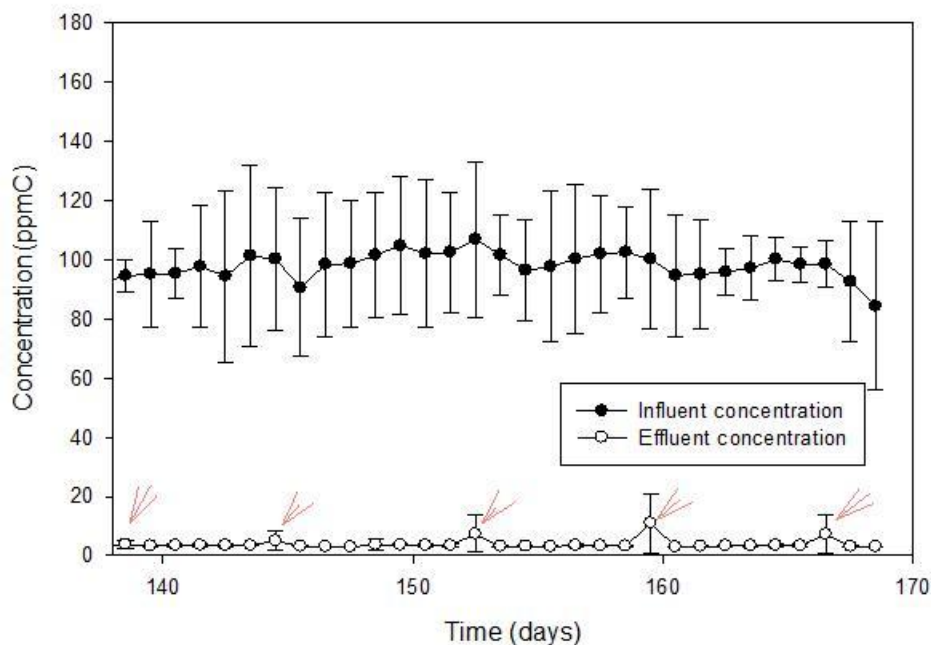


Figure 4.20 Influent and effluent concentration of Period 4. Arrows denote the days when nutrients were added.

As shown in Figure 4.20, the average influent concentration was 98.09 ± 20.80 ppm C, and the effluent concentration was maintained at stable low concentration of 3.84 ± 2.74 ppm C. The effluent pollutant concentration exhibited a consistent pattern on a weekly basis, the same as in Period 3A except it had a much smaller fluctuation.

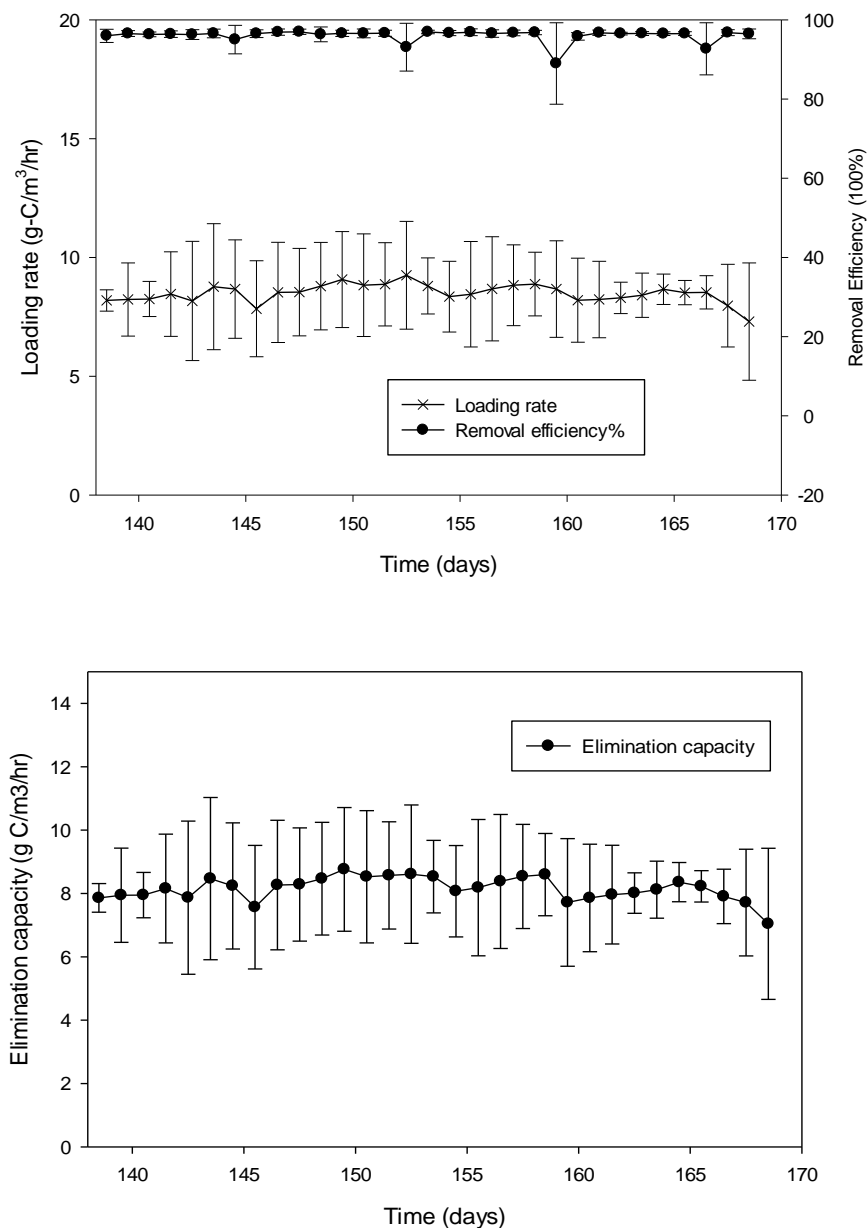


Figure 4.21 Loading rate and removal efficiency (top) and elimination capacities (bottom) of Period 4.

After the nutrient addition (denoted by red arrows in Figure 4.20), the effluent concentration decreased to a local minimum immediately the following day. The effluent concentration stayed quite stable at the bottom level. The highest peak concentration was 11.0 ppm C on day 160.

Loading rates and pollutant removal efficiencies during Period 4 are depicted in Figure 4.21. As shown in the figure, $96.02 \pm 1.63\%$ of the pollutant was removed during all 30 days of Period 4 operation. The elimination capacity was $8.15 \pm 0.37 \text{ g C m}^{-3}\text{h}^{-1}$, corresponding to an elimination capacity of $9.24 \pm 0.42 \text{ g } \beta\text{-caryophyllene m}^{-3}\text{h}^{-1}$.

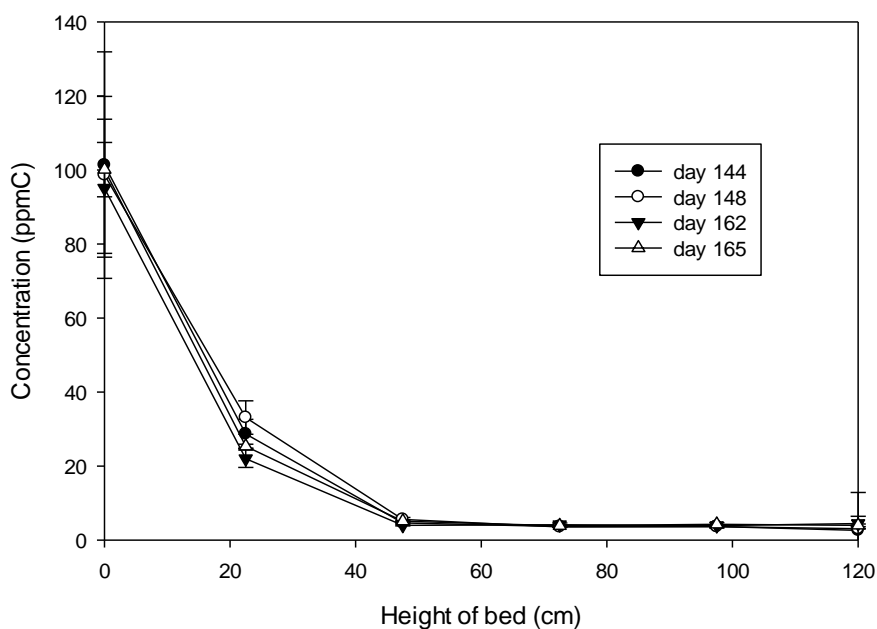


Figure 4.22 VOC concentration profiles measured on days 144, 148, 162, and 165 during Period 4.

Pollutant concentration profiles measured along the height of the biofilter during Period 4 are depicted in Figure 4.22. As shown in the figure, the pollutant was almost completely removed in the first 47.5 cm bed depth of the biofilter through the entire Period 4.

4.3.8 Biofilter Performance during Period 5A Operation

During Period 5A, the biofilter received pollutant loading with a gas flow rate of 56.4 L/min for a duration of 31 days (corresponding EBCT of 10 seconds). Figure 4.23 depicts influent and effluent pollutant concentrations during Period 5A. As shown, the average influent concentration was 89.30 ± 17.71 ppm C; it fluctuated and had a large standard deviation. The average effluent concentration was 9.9 ± 8.6 ppm C. The effluent concentration exhibited a similar pattern as previous in Period 3A. The effluent concentration rapidly decreased after nutrient was added and it reached a local minimum concentration on the third day. After that, the effluent concentration slowly increased until the subsequent nutrient addition day. The highest peak pollutant concentration was 45.03 ± 9.76 ppm C on day 201.

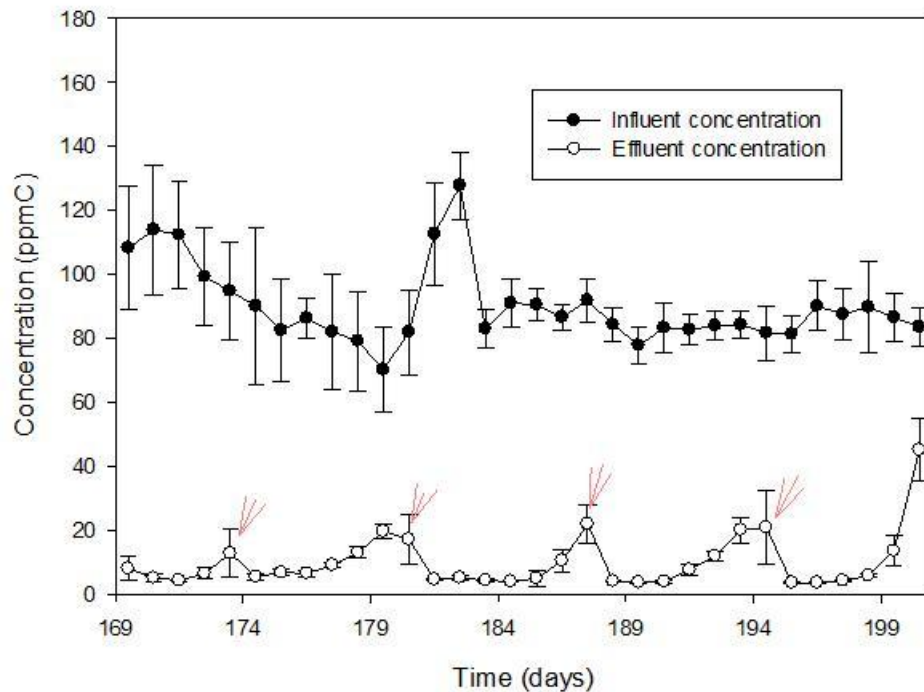


Figure 4.23 Influent and effluent concentration of Period 5A. Arrows denote the days when nutrients were added.

Figure 4.24 depicts the first day following the start of Period 5A. The biofilter quickly

adapted to the new loading condition again. As shown in the figure, within 10 minutes after increasing the loading rate at the start of Period 5A, the effluent pollutant concentration rapidly increased to 26 ppm C and then it decreased to 6 ppm C within the first 3 hours.

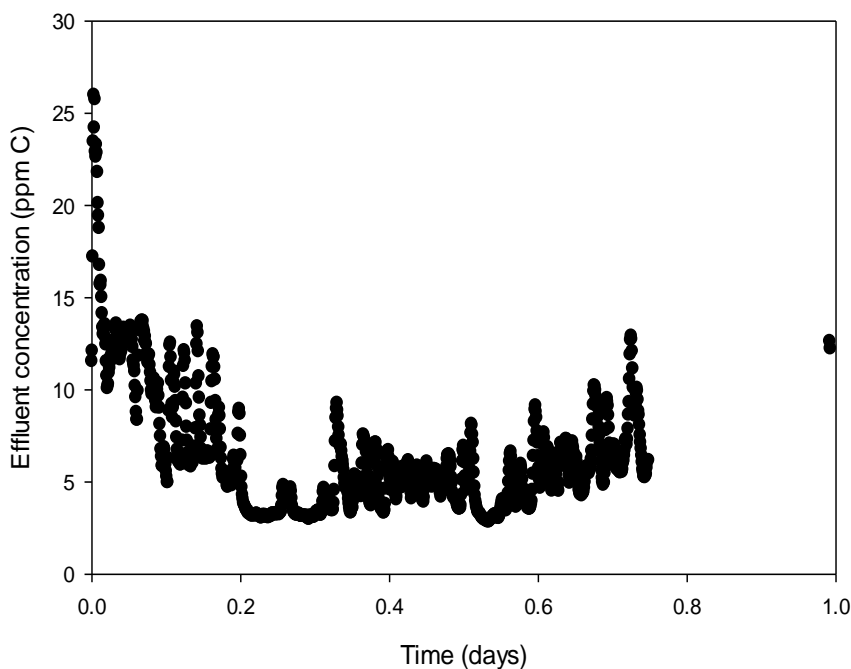


Figure 4.24 Effluent concentration of the first day after the start of Period 5A.

Figure 4.25 depicts the mean daily loading rates, pollutant removal efficiencies, and pollutant elimination capacities during Period 5A. As shown in the figure, the removal efficiency fluctuated on a weekly basis. The overall removal efficiency was $88.50 \pm 10.60\%$. The average loading rate was $15.47 \pm 2.28 \text{ g C m}^{-3}\text{h}^{-1}$, corresponding to $17.52 \pm 2.58 \text{ g } \beta\text{-caryophyllene m}^{-3}\text{h}^{-1}$. The pollutant elimination capacity was $13.78 \pm 2.70 \text{ g C m}^{-3}\text{h}^{-1}$, corresponding to an elimination capacity of $15.61 \pm 3.44 \text{ g } \beta\text{-caryophyllene m}^{-3}\text{h}^{-1}$.

Figure 4.26 depicts the pollutant concentration profiles measured along the height of the biofilter during Period 5A. As shown in the figure, the pollutant removal profile observed two days after the nutrient addition (red solid line) was somewhat more rapid than the pollutant

removal profile observed two days before the next nutrient addition (black solid line).

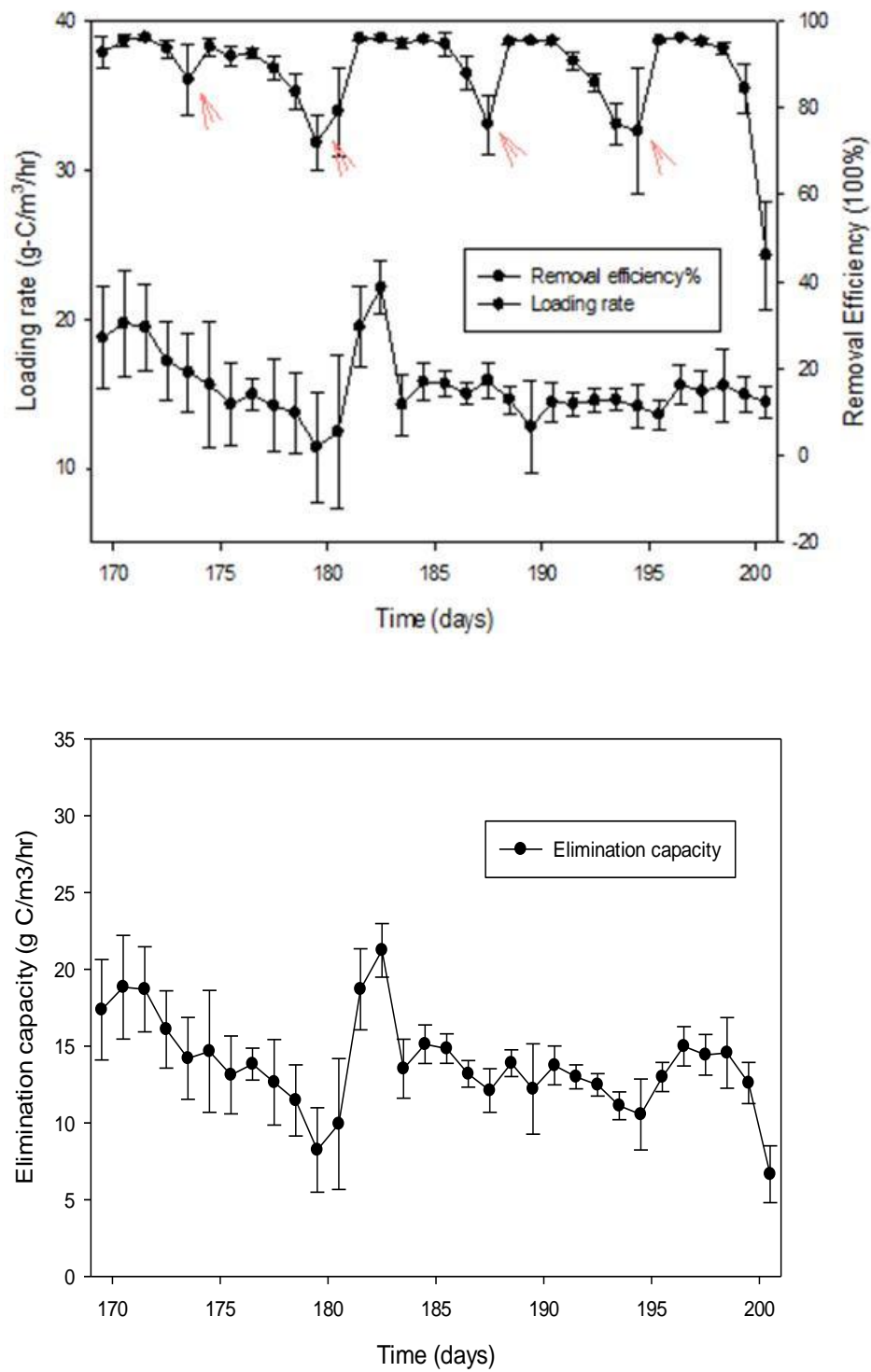


Figure 4.25 Loading rate and removal efficiency (top) and elimination capacities (bottom) of Period 5A.

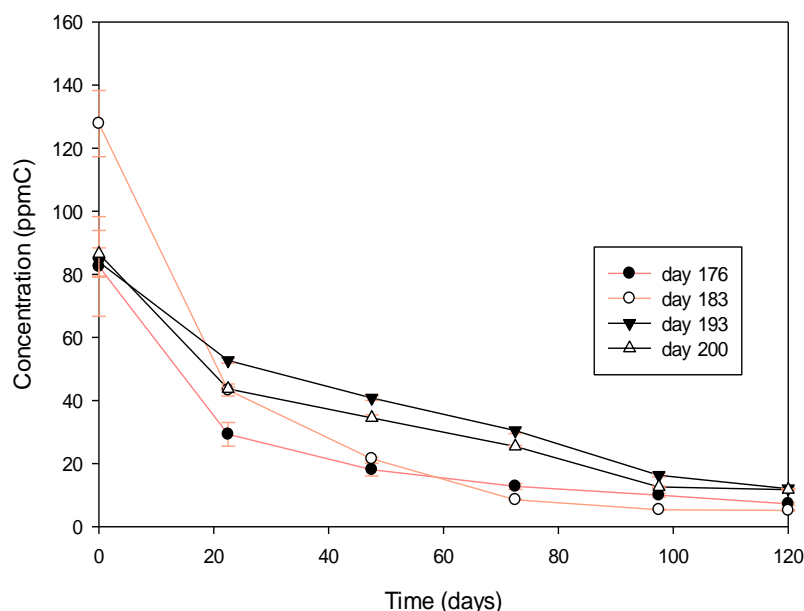


Figure 4.26 VOC concentration profiles measured two days after nutrient addition day (days 176, and 183), and five days after nutrient addition day (days 193 and 200) during Period 5A.

4.3.9 Biofilter Performance during Period 5B Operation

During Period 5B, the influent gas flow rate was the same as in Period 5A (56.4 L/min, EBCT 10 seconds). However, the ammonia nitrate concentration in Period 5B was twice that of the nutrient recipe supplied in Period 5A. Figure 4.27 depicts the influent and effluent pollutant concentrations measured for Period 5B. As shown in the figure, the effluent concentration sharply decreased immediately after the nutrient suspension was applied to the biofilter on day 202. The effluent concentration reached a local minimum of 3.76 ppm C the following day on day 203, and maintained at a stable low level until the next nutrient day. The overall average influent pollutant concentration of this Period was 91.99 ± 20.12 ppm C. Small temporary increases in effluent pollutant concentration occurred on the nutrient days on a weekly basis. The overall average effluent pollutant concentration was 5.3 ± 7.0 ppm C.

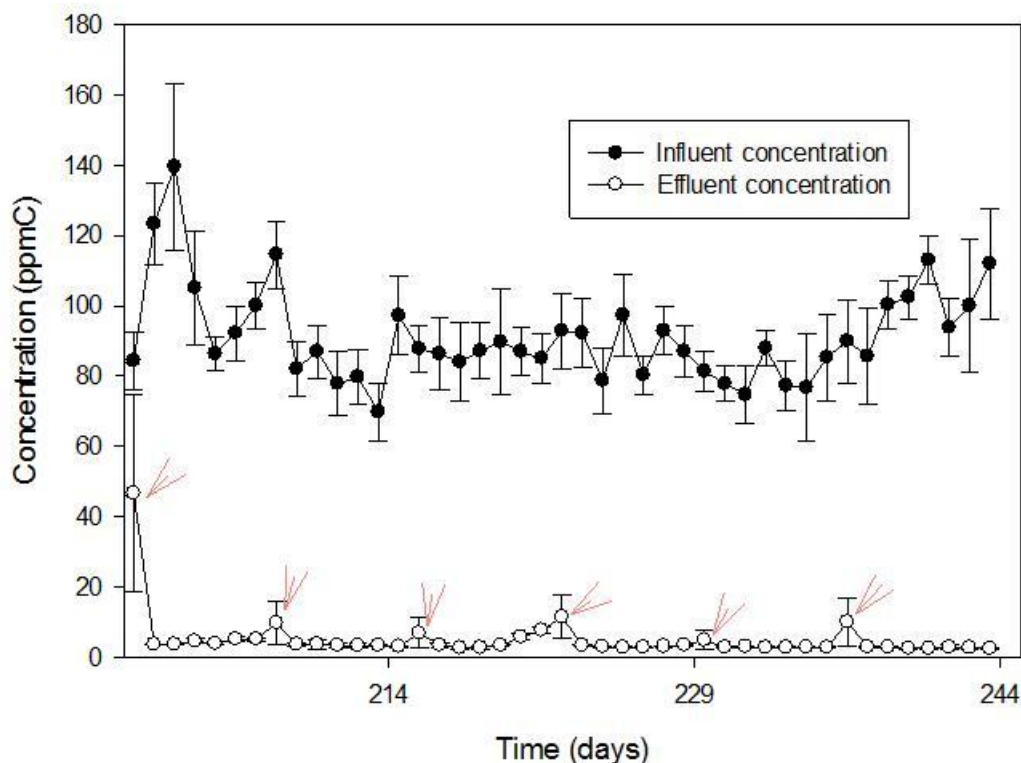


Figure 4.27 Influent and effluent concentration of Period 5B. Arrows denote the days when nutrients were added.

Loading rates, pollutant removal efficiencies, and pollutant elimination capacities during Period 5B are depicted in Figure 4.28. As shown in the figure, the pollutant removal efficiency reached $96.95 \pm 0.33\%$ the following day after the nutrient addition on day 203.

The overall average pollutant removal efficiency was $94.20 \pm 8.05\%$ during Period 5B operation. Considering the interval of nutrient change, the average pollutant removal efficiency excluding the first day was $95.38 \pm 2.25\%$.

The overall average loading rate of Period 5B was $17.90 \pm 2.70 \text{ g } \beta\text{-caryophyllene m}^{-3}\text{h}^{-1}$. The elimination capacity was $14.92 \pm 2.70 \text{ g C m}^{-3}\text{h}^{-1}$ in Period 5B, corresponding to an elimination capacity of $16.90 \pm 3.05 \text{ g } \beta\text{-caryophyllene m}^{-3}\text{h}^{-1}$.

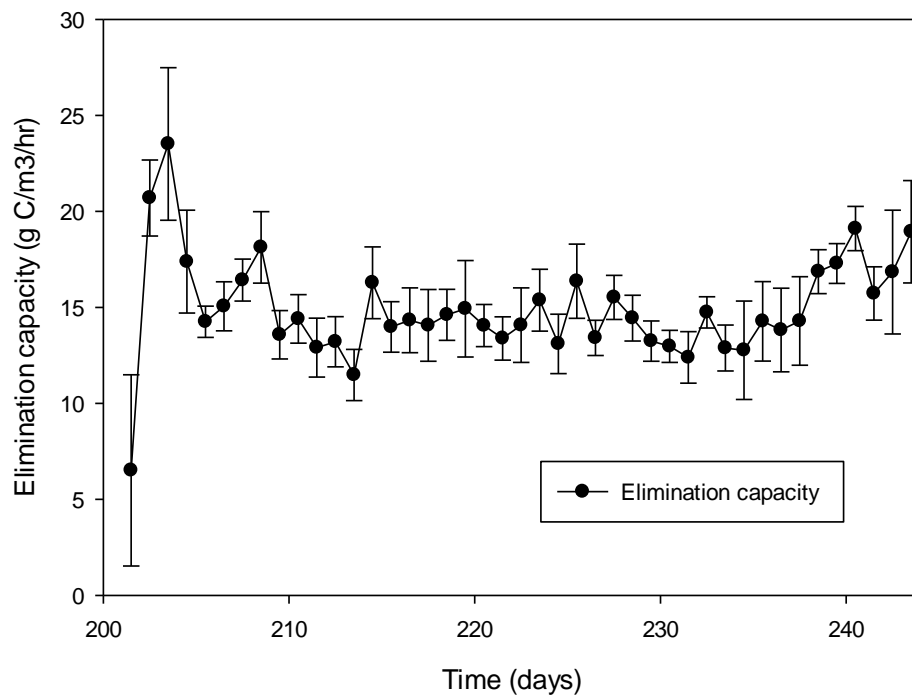
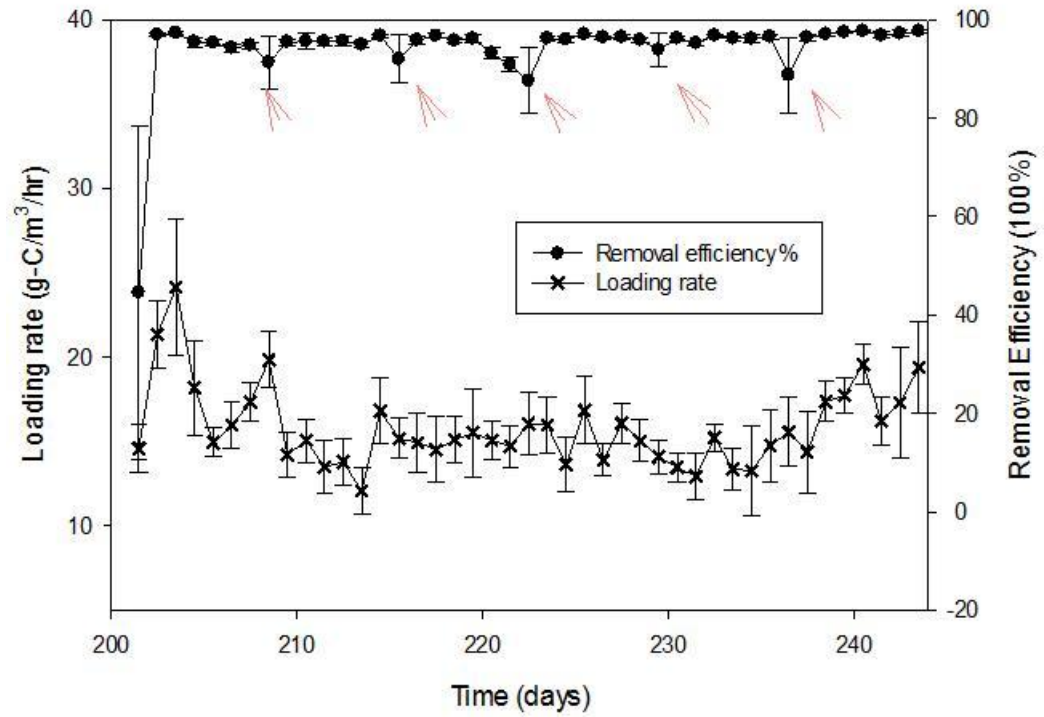


Figure 4.28 Loading rate and removal efficiency (top) and elimination capacities (bottom) of Period 5B.

Figure 4.29 depicts the pollutant concentration profiles measured along the height of the biofilter in Period 5B. As shown in the figure, the pollutant removal profiles remained roughly constant throughout the period the inlet concentration data. The pollutant was rapidly removed in the first section of the column followed by slower pollutant elimination up to the outlet height. The pollutant removal was mostly completed with the first 97.5 cm bed depth.

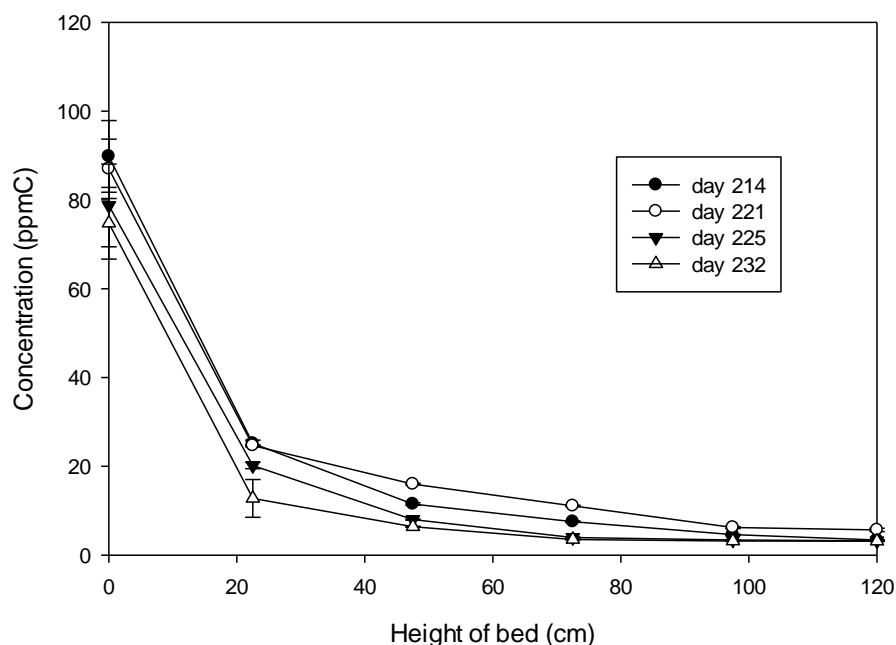


Figure 4.29 VOC concentration profiles measured two days after nutrient day on days 214, 221, 225, and 232 during Period 5B.

4.3.10 pH, Headloss and Temperature

pH, head loss and effluent gas temperature for all periods' operations are depicted in Figure 4.30. As shown in Figure 4.30 D, the pH in Period 1, 2, 3A were between 5 and 7, and the fluctuations were small. The pH in Period 3B and Period 4 had larger fluctuations within the range of 4 to 7. The pH in Period 5A and Period 5B was between 5.5 and 6.8. As shown in Figure 4.30 E, the head loss in Period 5A and Period 5B was bigger than the head loss of Periods 1, 2, 3A, 3B and Period 4. The head loss observed during the entire operation interval, however,

was less than 2 cm water. According to Figure 4.30 F, the effluent gas temperature was stable at 31 °C even it varies within 3 °C for the entire operation periods.

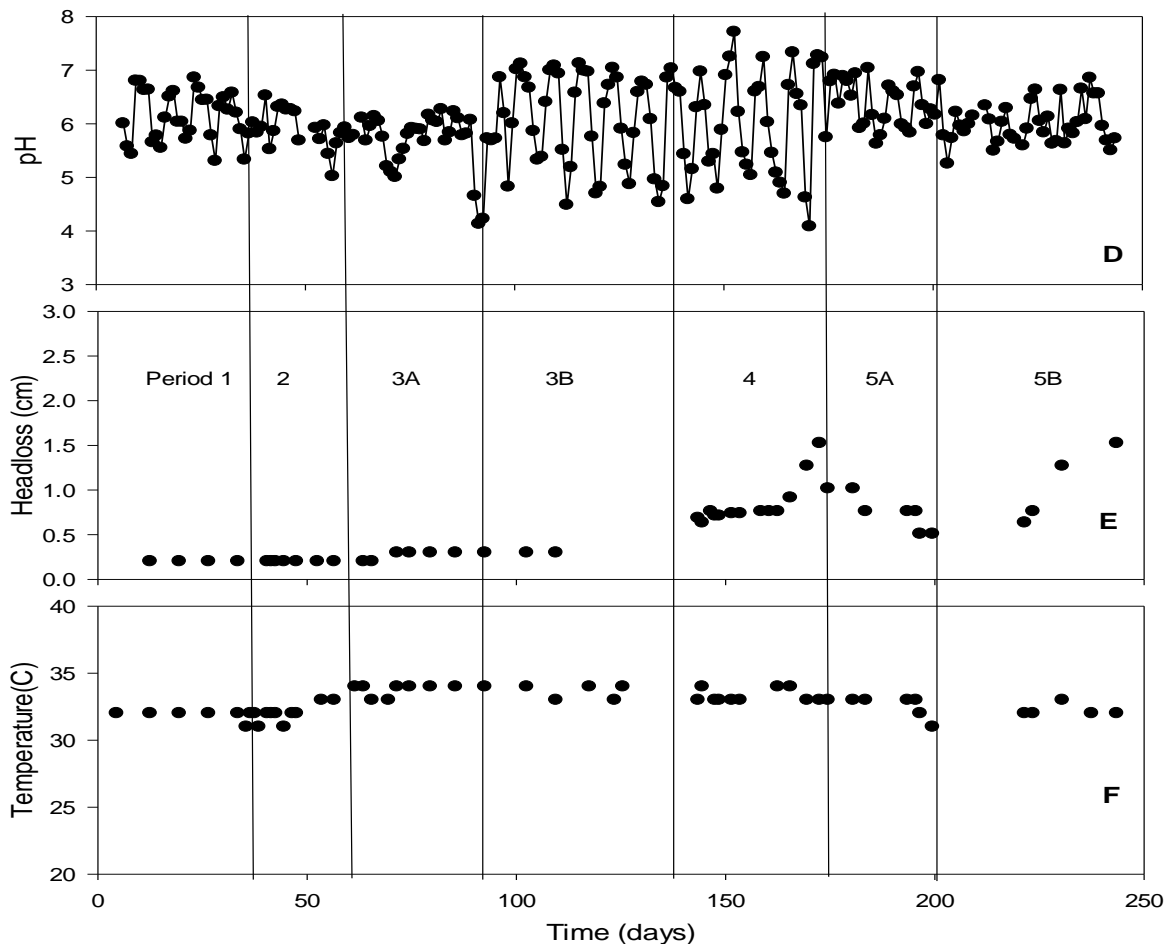


Figure 4.30 pH of the drainage (D), head loss across the bed (E), and effluent gas temperature (F).

4.4 Discussion and Conclusions

The performance of a laboratory-scale biofilter was tested to handle β -caryophyllene vapors at loading rates varying between 1.36 ± 0.05 and $17.90 \pm 2.70 \text{ g m}^{-3} \text{ h}^{-1}$ for an efficient long-term operation of 262 days, β -caryophyllene was successfully removed with removal efficiencies between 80% and 97% while subjected to different nutrient supply rates. β -caryophyllene removal efficiency higher than 95% was achieved with an EBCT of 10 seconds under the loading

rate of $17.90 \pm 2.70 \text{ g m}^{-3} \text{ h}^{-1}$. Collectively, the data presented in this chapter demonstrate that β -caryophyllene can be successfully treated in biofilter systems. This expands the range of pollutants successfully treated in biofilters to include sesquiterpenes.

Potential explanations for the observation of progressively worse pollutant removal as a function of time following the weekly nutrient additions during Period 3A, 5A (see Figures 4.13 and 4.23) are that (A) inhibitory degradation products may have accumulated over time, (B) the system may have become nutrient limited (Moe and Irvine, 2001), or (C) the system may have dried out due to insufficient humidification of the inlet air (Sakuma *et al.*, 2009). These processes have been observed to cause diminished biofilter performance in previous studies. The fact that performance stabilized following the increase in nutrient concentrations (Period 3B, 5B) when the humidification regime and potential washout of inhibitory products presumably would have remained the same, however, strongly implicates local nutrient limitations as the cause of the diminished treatment performance during Period 3A, 5A.

As reported by Deshusses and Johnson (2000), the pollutants with high Henry's Law coefficients are generally difficult to elimination in a biofilter. The reason is that these pollutants have an unfavorable gas-liquid partition, and the pollutant concentration in the biofilm is too low to sustain a high biodegradation rate. Hexane has a high Henry's law coefficient, similar to β -caryophyllene, it was reported has a critical loading and elimination capacity of $1 \text{ g m}^{-3} \text{ h}^{-1}$ and $3-8 \text{ g m}^{-3} \text{ h}^{-1}$, respectively. In the present study, β -caryophyllene could reach an elimination capacity of $16.9 \text{ g m}^{-3} \text{ h}^{-1}$.

According to Deshusses and Johnson (2000), pollutants with high octanol/water partition coefficients are generally not well removed by biofilters. A possible explanation put forth for this observation is that the diffusion limitation of oxygen in the biofilm. However, hexane has a

smaller octanol/water partition coefficient than β -caryophyllene, the reported maximum elimination capacity for hexane was $3\text{--}8\text{ g m}^{-3}\text{ h}^{-1}$. Compared to the maximum elimination capacity of $16.90\text{ g m}^{-3}\text{ h}^{-1}$ of β -caryophyllene observed in the present study, it is not consistent with the trend. As mentioned by Rajagopal (1996), a reversed trend was expected, since the growth of *Pseudomonas* sp. was found to be slowed in the presence of solvents with $\log K_{ow}$ lower than 2.5–3.0, hexane and β -caryophyllene both has a $\log K_{ow}$ value larger than 3.0 followed this trend. However, it is difficult to separate the effect of the toxicity of the VOCs to the process culture and the effect of physicochemical parameters represented by $\log K_{ow}$ values, further research is needed.

CHAPTER 5 BIOFILTER PERFORMANCE UNDER SHUT DOWN/RE-START OPERATIONS

5.1 Introduction

Biofilters are generally expected to handle both steady- and transient-state pollutant loads effectively. Events such as biofilter shutdown for mechanical repairs, maintenance or shut down for a few days (during weekends or holiday breaks), and sometimes for a prolonged duration generally cannot be avoided.

During such temporary intervals of no contaminant loading, the microorganisms in the biofilter are subjected to starvation. When biofilter operation is resumed and the carbon source (pollutant) is again fed to the reactor, the response of the starved microorganisms and the performance of the biofilter during re-start depends on several factors such as microbial population and activity, duration of the starvation period, current state of the packing material and the attached biomass, and the characteristics and composition of the polluted air (Maestre, *et al.*, 2007; Moe and Qi, 2004; Jang, *et al.* 2006). This chapter describes experimental testing of biofilter response to an interruption in β -caryophyllene loading.

5.2 Materials and Methods

On day 244, after the biofilter received a nutrient addition, the biofilter was temporarily shut down for a period of 14 days. During this time, no β -caryophyllene was supplied to the biofilter. To prevent anaerobic conditions of the microbial system, a gas flow rate of 1.0 L/min was maintained to the biofilter with a corresponding EBCT of 9.42 min. On day 258, after receiving another nutrient supply, the biofilter was restarted with the same operation of Period 5B, which had a β -caryophyllene injection rate of 0.4 mL/h, a gas flow rate of 56.4 L/min, and a corresponding EBCT of 10 seconds. Influent and effluent pollutant concentrations were

measured using a model 600 HFID hydrocarbon analyzer (California Analytical, Orange, CA) as described previously.

5.3 Results

The experimentally measured breakthrough curve after β -caryophyllene loading to the biofilter column resumed following the 14-day interval of no loading is depicted in Figure 5.1. As shown in the figure, within the first 2.15 hours, the effluent concentration was as low as 2.3 ppm C. After that, the effluent concentration went up quickly.

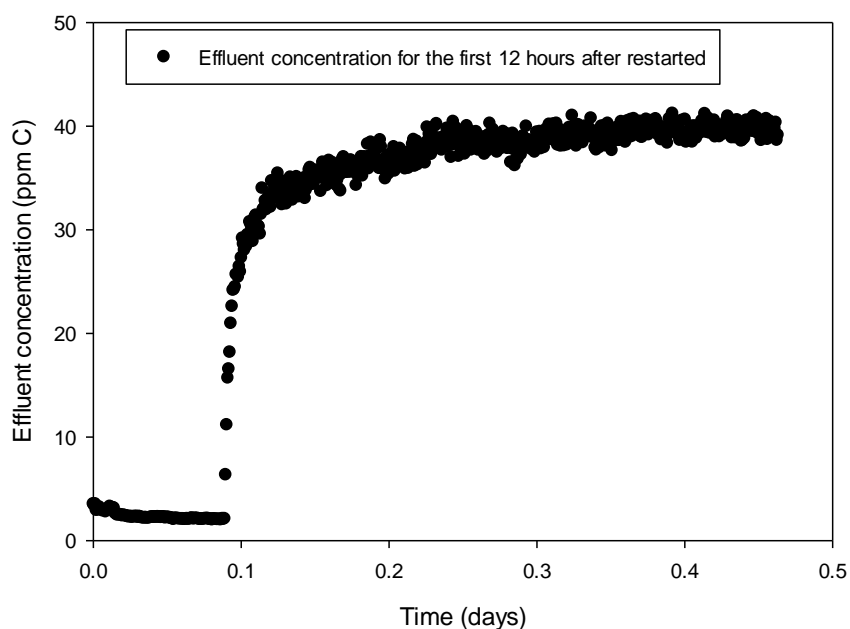


Figure 5.1 The effluent concentration for the first 12 hours following resumption of β -caryophyllene following the 14-day interval of no pollutant loading.

After restarted of the biofilter with the same operation of Period 5B (56.4 L/min, EBCT 10 seconds), the biofilter experienced an adsorption interval to reach the pollutant breakthrough. Figure 5.2 depicts the mean daily influent and effluent concentration of the biofilter for a Period of five days from the biofilter restart.

As shown in the figure, the average influent concentration for these five days was

78.67±5.05 ppm C, and the average effluent concentration was 8.24±10.37 ppm C.

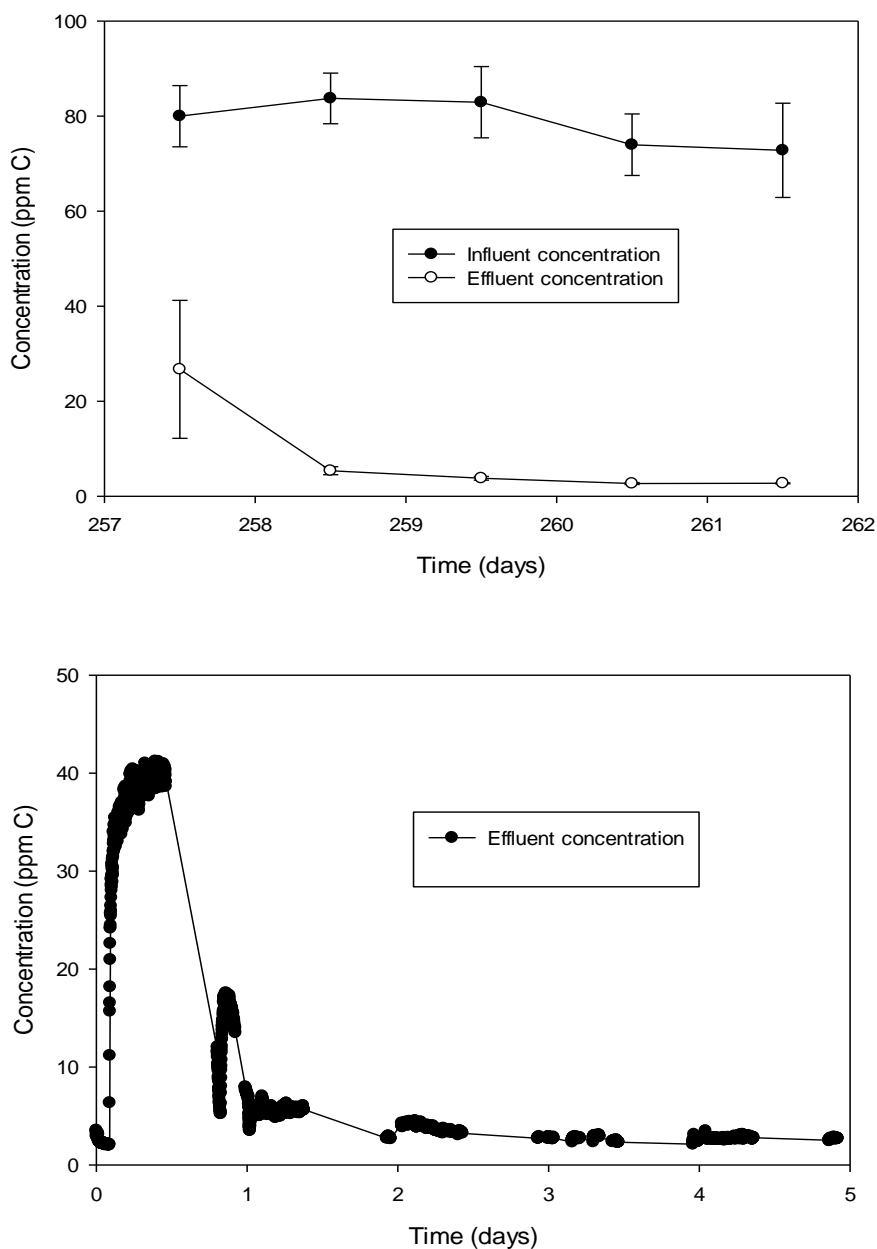


Figure 5.2 Experimentally measured mean daily influent and effluent gas-phase pollutant concentrations after restart (top) and raw effluent concentration data for this Period (bottom).

The effluent concentration was low as 2.33 ± 0.4 ppm C for the first two hours immediately following resumption of β -caryophyllene restarted, then it increased quickly to

reach a peak concentration of 40 ppm C within the next 9 hours. The daily average effluent concentration for the first day was 26.7 ppm C, and then it decreased to mean daily concentration of 5.4 ppm C the following day. After that, the effluent concentration continued to decrease until it stayed relatively stable at round 3.05 ± 0.6 ppm C.

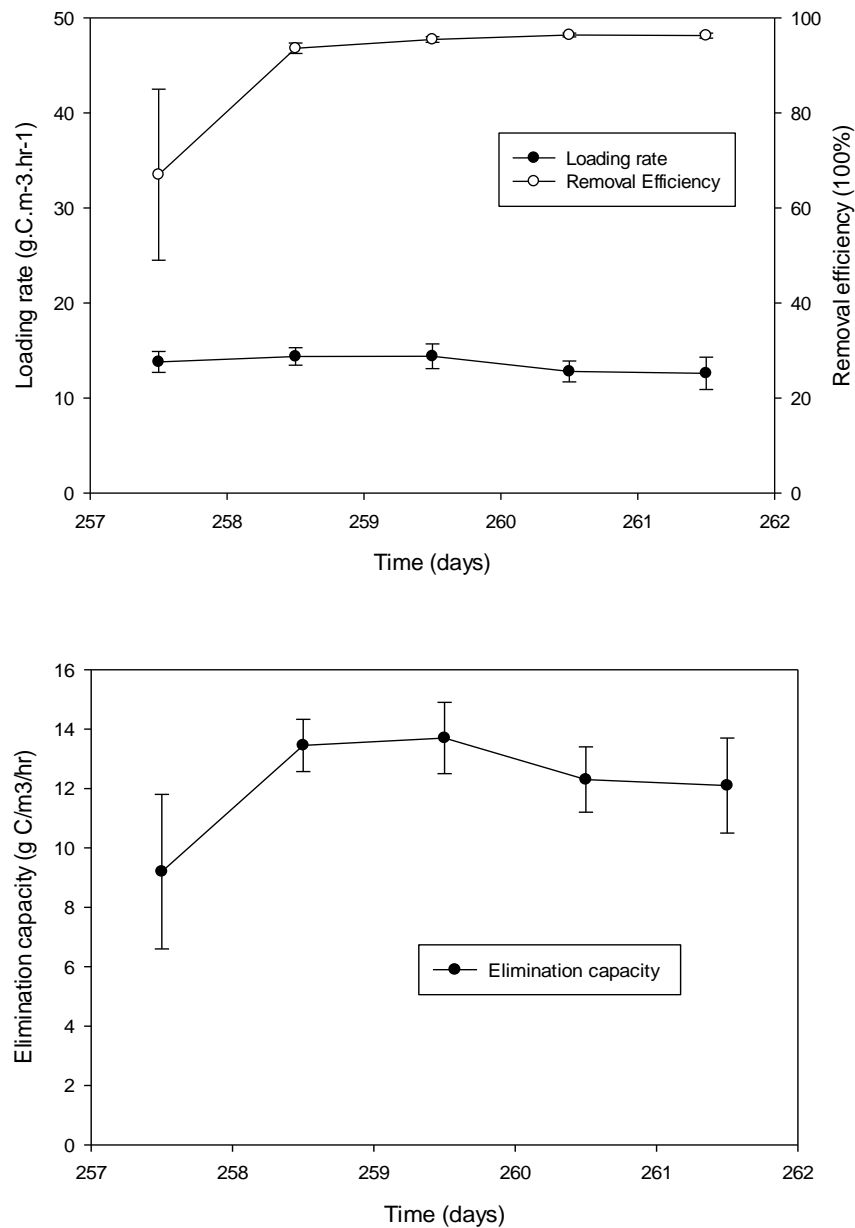


Figure 5.3 Loading rates and removal efficiency (top) and elimination capacities (bottom) for five days after restart.

Loading rates, pollutant removal efficiencies, and elimination capacities for the first five days after restart are depicted in Figure 5.3. As shown in the figure, the average loading rate was $13.6 \pm 0.85 \text{ g} \cdot \text{C m}^{-3} \text{h}^{-1}$, corresponding to $15.4 \pm 0.96 \text{ } \beta\text{-caryophyllene m}^{-3} \text{h}^{-1}$. 93.6 \pm 0.6% of the pollutant was removed after two days following restart, and over 95% of the pollutant was removed after 3 days operation. The mean removal efficiency of these five days operation was 89.7 \pm 12%. The elimination capacity on the first day was $9.2 \pm 2.6 \text{ g C m}^{-3} \text{h}^{-1}$, corresponding to an elimination capacity of $10.42 \pm 2.94 \text{ g } \beta\text{-caryophyllene m}^{-3} \text{h}^{-1}$, and it increased the following day. The mean elimination capacity for the five days was $12.15 \pm 1.79 \text{ g C m}^{-3} \text{h}^{-1}$, corresponding to an elimination capacity of $13.76 \pm 3.33 \text{ g } \beta\text{-caryophyllene m}^{-3} \text{h}^{-1}$.

5.4 Discussion and Conclusions

During short term shutdown and restart conditions, an rapid restoration of biological activity after 14 days of starvation and the quick recovery of the biofilter performance at high loading rate indicated the resilience of the biomass and the stability of the biofilter. The results from this study demonstrated that the biofilter was capable of withstanding relatively long term starvation with rapid recovery to full performance when contaminant loading resumed. Although the removal efficiency was initially lower for few hours after restart. Then, the removal efficiency gradually increased and reached the maximum efficiency after four days. The microorganisms in the biofilter showed good recovery activity.

CHAPTER 6 OVERALL CONCLUSIONS AND RECOMMENDATIONS FOR FUTURE WORK

6.1 Overall Conclusions and Discussions

The performance of a laboratory-scale biofilter was tested to handle β -caryophyllene vapors at loading rates varying between 1.36 ± 0.05 and $17.90 \pm 2.70 \text{ g m}^{-3} \text{ h}^{-1}$ for an efficient long-term operation of 262 days, β -caryophyllene was successfully removed with removal efficiencies between 80% and 97% while subjected to different nutrient supply rates. β -caryophyllene removal efficiency higher than 95% was achieved with an EBCT of 10 seconds under the loading rate of $17.90 \pm 2.70 \text{ g m}^{-3} \text{ h}^{-1}$. Collectively, the data presented in this chapter demonstrate that β -caryophyllene can be successfully treated in biofilter systems. This expands the range of pollutants successfully treated in biofilters to include sesquiterpenes.

During short term shutdown and restart conditions, an rapid restoration of biological activity after 14 days of starvation and the quick recovery of the biofilter performance at high loading rate indicated the resilience of the biomass and the stability of the biofilter. The results from this study demonstrated that the biofilter was capable of withstanding relatively long term starvation with rapid recovery to full performance when contaminant loading resumed. Although the removal efficiency was initially lower for few hours after restart. Then, the removal efficiency gradually increased and reached the maximum efficiency after four days. The microorganisms in the biofilter showed good recovery activity.

As reported by Deshusses and Johnson (2000), the pollutants with high Henry's Law coefficients are difficult to elimination in a biofilter. The reason is that these pollutants have an unfavorable gas-liquid partition, and the pollutant concentration in the biofilm is too low to sustain a high biodegradation rate. Hexane has a high Henry's law coefficient, similar to β -caryophyllene, it was reported has a critical loading and elimination capacity of $1 \text{ g m}^{-3} \text{ h}^{-1}$ and 3-

8 g m⁻³ h⁻¹, respectively. In the present study, β -caryophyllene could reach an elimination capacity of 16.9 g m⁻³ h⁻¹. According to Deshusses and Johnson (2000), pollutants with high octanol/water partition coefficients are generally not well removed by biofilters. A possible explanation put forth for this observation is that the diffusion limitation of oxygen in the biofilm. However, hexane has a smaller octanol/water partition coefficient than β -caryophyllene, the reported maximum elimination capacity for hexane was 3-8 g m⁻³ h⁻¹. Compared to the maximum elimination capacity of 16.90 g m⁻³ h⁻¹ of β -caryophyllene observed in the present study, it is not consistent with the trend. As mentioned by Rajagopal (1996), a reversed trend was expected, since the growth of *Pseudomonas* sp. was found to be slowed in the presence of solvents with log K_{ow} lower than 2.5-3.0, hexane and β -caryophyllene both has a log K_{ow} value larger than 3.0 followed this trend. However, it is difficult to separate the effect of the toxicity of the VOCs to the process culture and the effect of physicochemical parameters represented by log K_{ow} values, Further research is needed.

6.2 Recommendations for Future Research

Some additional experiments could be conducted to obtain information to answer other important questions in biofiltration research. For example, additional profile studies and microbial characterization studies could be conducted to have a better understanding of the way that the contaminants are being biodegraded at different locations in the columns, and also to have a better understanding of the interactions between microbial populations and substrates. Additional studies could also be conducted under thermophilic conditions to obtain more information of the operational capabilities of biofilters treating β -caryophyllene at different temperatures. Finally, pilot-scale testing is recommended to investigate whether there are likely to be scale-up issues in full scale implementation.

REFERENCES CITED

- Aizpuru, A., Malhautier, L., Roux, J. C., Fanlo, J. L. (2001). "Biofiltration of a Mixture of Volatile Organic Emissions." *J. Air & Waste Manage. Assoc.*, 51:1662-1670.
- Atoche, J. C., and Moe, W. M. (2004). Treatment of MEK and toluene mixtures in biofilters: Effect of operating strategy on performance during transient loading. *Biotechnology and Bioengineering* 86(4):468-481.
- Babbitt, C. W., Pacheco, A., and Lindner, A. S. (2009). Methanol removal efficiency and bacterial diversity of an activated carbon biofilter. *Bioresource Technology* 100:6207-6216.
- Bagherpour, M. B., Nikazar, M., Welander U., Bonakdarpour B., and Sanati M. (2005). Effects of irrigation and water content of packings on alpha-pinene vapours biofiltration performance. *Biochemical Engineering Journal* 24:185-193.
- Banerjee, S., Hutten, M., Su, W., Otwell, L., and Newton, L. (1995). Release of water and volatile organics from wood drying. *Environ Sci Technol* 29:1135-1136.
- Baumann, M. G. D., Batterman, S A, and Zhang, G. Z. (1999). Terpene emissions from particle board and medium-density fiber board products. *Forest Prod. J.* 49(1):49-56.
- Baumann, M. G. D., Lorenz, L. F., Batterman, S. A., and Zhang, G. Z. (2000). Aldehyde emissions from particle board and medium density fiber board products. *Forest Prod. J.* 50(9):75-82.
- Beakler, B.W., Blankenhorn, P. R., Brown, N. R., Scholl, M. S., and Stover, L.R. (2007). Quantification of the VOCs released during kiln-drying red oak and white oak lumber. *Forest Prod. J.* 57(11):27-32.
- Bridgewater, A. V., Elliott, D. C., Fagernäs, L., Gifford, K. L. Mackie, and Toft, A. J. (1995). The Nature and Control of Solid, Liquid and Gaseous Emissions from the Thermochemical Processing of Biomass, Biomass. *Bioenerg* 9(1-5):325-341.
- Broege, K., Aehlig, K., and M., Scheithauer (1996). Emissions from sawn wood driers. Rept. From Institut fur Holztechnologie, Dresden, Germany. (In German, English abstract)
- Ciccioli, P., Brancaleoni, E., Frattoni, M., DiPalo, V., Valentini, R., Tirone, G., Seufert, G., Bertin, N., Hansen, U., Csiky, OLenz, R., and Sharma, M. (1999). Emission of reactive terpene compounds from orange orchards and their removal by within –canopy processes. *Journal of Geophysical Research* 104, 8077-8094.
- Corsi, R. L. and Seed, L. (1995). Biofiltration of BTEX: Media, substrate, and loadings effects. *Environmental Progress* 14: 151-158.
- Cronn, D. R., Truitt, S. G., and Campbell, M. J. (1983). Chemical Characterization of Plywood Veneer Dryer Emissions, *Atmos Environ.* 17(2) pp. 201-211.

- Culpepper, L. (1990). High Temperature Drying: Enhancing Kiln Operations.
- Danielsson, S. and Rasmuson, A. (2002). The influence of drying medium, temperature, and time on the release of monoterpenes during convective drying of wood chips. *Drying Technology*, 20(7), 1427-1444.
- Demers, P.A., Teschke, K., Davies, H.W., Kennedy, S.M., and Leung, V. (2000). Exposure to dust, resin acids, and monoterpenes in softwood lumber mills. *Am Ind Hyg Assoc J*; 61: 521–8.
- Deshusses, M. A., Hamer, G., and Dunn, I. J. (1996). Transient-state behavior of a biofilter removing mixtures of vapors of MEK and MIBK from air. *Biotechnology Bioengineering* 49: 587-598.
- Deshusses, M. A. and Johnson, C. (2000). Development and validation of a simple protocol to rapidly determine the performance of biofilters for VOC treatment. *Environmental Science. Technology*, 34: 461-467.
- Dhamwichukorn, S., Kleinheinz, G. T., and Bagley, S. T. (2001). Thermophilic biofiltration of methanol and alpha-pinene. *J. Industrial Microbiol. & Biotechnol.* 26:127-133.
- Diehl, S. V., Saileela, B., Wasson, L. L., and Borazjani, A. (2000). Biofiltration of selected monoterpenes found in southern yellow pine wood emissions. *Forest Prod. J.* 50(1):43-48.
- EPA R.E.D. Fact sheet on Limonene. Sep. 1994.
- Englund, F. and Nussbaum, R. M. (2000). Monoterpenes in Scots pine and Norway spruce and their emission during kiln drying. *Holzforschung*, 54(5), pp. 449-456.
- European commission- European chemicals bureau. Dataset page 48. 19-feb-2000.
- Fuentes, J. D., Lerda, M., Atkinson, R., Baldocchi, D., Bottenheim, J. W., Ciccioli, R., Lamb, B., Geron, C., Gu, L., Guenther, A., Sharkey, T. D., and Stockwell, W. (2000). Biogenic Hydrocarbons in the Atmospheric Boundary Layer: A Review, B. *Amer. Met. Soc.* 81, 1537–1575.
- Fritz, B., Lamb, B., Westberg, H., Folk, R., Knighton, B., Grimsrud, E. (2004). Pilot and full scale measurements of VOC emissions from lumber drying of Inland Northwest species. *Forest Prod. J.* 54(6): 50-56.
- Granstrom, K. M. (2009). Emissions of sesquiterpenes from spruce sawdust during drying. *Eur. J. Wood Prod.* 67:343-350.
- Granstrom, K. M (2010). Emissions of monoterpenes and VOCs during drying of sawdust in a spouted bed. *Forest Prod. J.* 53(10):48-55.

- Granstrom, K. M (2003). Underestimation of terpene exposure in the Nordic wood industry. *Journal of Occupational and Environmental Hygiene*, 7:144-151.
- Granstrom, K.M. and Mansson B. (2008). Volatile organic compounds emitted from hardwood drying as a function of processing parameters. *Int J. Environ. Sci. Tech.*, 5(2):141-148.
- Hansch, C., Leo, A., and Hoekman, D. (1995). Exploring QSAR Hydrophobic, Electronic, and Steric Constants. 2nd Edition.
- Hakola, H., Tarvainen, V., Back, J., Ranta, H., Bonn, B., Rinne, J., Kulmala, M. (2006). Seasonal variation of mono and sesquiterpene emission rate of Scots Pine. *Biogeosciences* 3: 93-101.
- Hodge, D. S. and J. S. Devinny. (1995). Modeling removal of air pollutants by biofiltration. *J. Environmental Engineering* 121:21-32.
- Hoskovec, M., Grygarova D., Cvacka, J., *et al.* (2005). Determining the vapor pressures of plant volatiles from gas chromatographic retention data. *Journal of Chromatography A* 1083:161-172.
- Hejaz, P., Borenberg, F., *et al.* (2010). Treatment of α -pinene-contaminated air using silicone oil-coated perlite biofilter. *Environmental Progress & Sustainable Energy*, 29(3): 313–318.
- Helmig, D., Ortega, J., Guenther, A., Herrick, J. D., and Geron, C. (2006). Sesquiterpene emissions from loblolly pine and their potential contribution to biogenic aerosol formation in the Southeastern US. *Atmospheric Environment* 40, 4150-4157.
- Helmig, D., Ortega, J., Duhl, T., Tanner, D., Guenther, A., Harley, P., Wiedinmyer, C., Milford, J., Sakulyanontvittaya, T. (2007). Sesquiterpene emissions from pine trees-Identifications, emission rates and flux estimates for the contiguous United States. *Environmental science & technology*, 41(5):1545-1553.
- Ingram, L.L., Jr., Taylor, F. W., Punsavon, V., and Templeton, M. C. (1995). Identification of volatile organic compounds emitted during the drying of southern pine in pilot and laboratory experiments. *Forest Prod. Soc., Madison, Wis.*
- Ingram, L. L., Jr., Shmulsky, R., Dalton, A.T., Taylor, F. W., and Templeton, M.C. (2000). The measurement of volatile organic emissions from drying southern pine lumber in a laboratory scale kiln. *Forest Prod. J.* 50(4):91-94.
- International programme on Chemical safety. PIM 335.
- Jang, J. H. *et al.* (2006). Effect of shutdown on styrene removal in a biofilter inoculated with *Pseudomonas* sp. SR-5. *J. Hazard. Material*, B129, 223–227.
- Jaoui, M., Leungsakul, S., and Kamens, R. M. (2003). Gas and particle products distribution from the reaction of β -caryophyllene with ozone. *Journal of Atmospheric Chemistry* 45:261-287.

- Javidnia, K., Aram, F., Solouki, M., Mehdiopour, Ar., Gholami, M., and Miri, R. (2009), Microbial biotransformation of some monoterpene hydrocarbons. *Annals of microbiology*, 59(2):349-351.
- Jin, Y. M., Veiga, M. C., Kennes, C. (2006). Performance optimization of the fungal biodegradation of alpha-pinene in gas-phase biofilter. *Process Biochemistry* 41: 1722-1728.
- Kleinheinz, G. T., Bagley, S. T., John, W. P. St., Rughani, J. R., and McGinnis, G. D. (1999). Characterization of alpha-pinene-degrading Microorganisms and application to a bench-scale biofiltration system for VOC degradation. *Arch. Environ. Contam. Toxicol.* 37: 151-157.
- Kong, Z. D., Farhana, L., Fulthorpe, R. R., Allen, D. G. (2001). Treatment of Volatile organic compounds in a biotrickling filter under thermophilic conditions. *Environ. Sci. Technol.* 35: 4347-4352.
- Langolf, B. M., Kleinheinz, G. T. (2005). A lave rock- based biofilter for the treatment of alpha-pinene. *Bioresource Technology* 97: 1951-1958.
- Lavery, M. and Milota, M. R. (2000). VOC emissions from Douglas-fir: Comparing a commercial and a lab kiln. *Forest Prod.J.* 50(7/8): 39-47.
- Lavery, M. R. and Milota, M. R. (2001). Measurement of VOC Emissions from Ponderosa Pine Lumber Using Commercial and Laboratory Kilns, *Drying Technology- An International Journal* 19 pp. 2151-2173.
- Lee, S., W.M. Moe, K.T. Valsaraj, and J.H. Pardue (2002) Effect of sorption and desorption-resistance on aerobic trichloroethylene biodegradation in soils, *Environmental Toxicology and Chemistry*, 21(8), 1609-1617.
- Li, Y. J., Chen, Q., and Guzman, M. I., *et al.* (2011). Second-generation products contribute substantially to the particle-phase organic material produced by beta-caryophyllene ozonolysis. *Atmospheric Chemistry and Physics* 11(1):121-132.
- Liu, J. W., Liu, J. X., and Lin, L. (2008). Performance of two biofilters with neutral and low pH treating off-gases. *Journal of Environmental Sciences* 20: 1409-1414.
- Maestre, J.P. *et al.* (2007). Fungal biofilters for toluene biofiltration: evaluation of the performance with four packing materials under different operating conditions. *Chemosphere* 67, 684–692.
- Manninen, A.M., Pasanen, P., and Holopainen, J.K. (2002). Comparing the VOC emissions between air-dried and heat-treated scots pine wood. *Atmospheric Environment* 36:1763-1768.

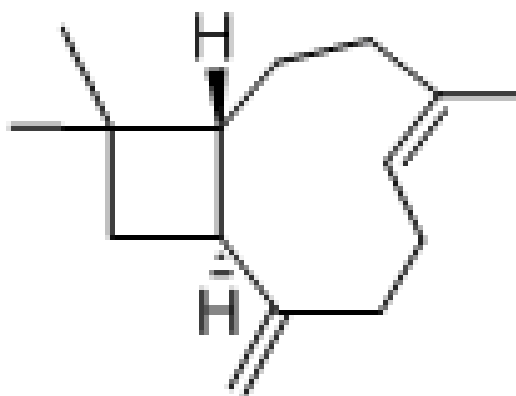
- McDonald, A. G., Gifford, J. S., Steward, D., Dare, P. H, Riley, S., and Simpson, I. (2004). Air emission from timber drying: high temperature drying and re-drying of CCA treated timber. *Holz Roh Werkst* 62:291-302.
- McDonald, A. G. and Wastney, S. (1995). Analysis of volatile emissions from kiln drying of radiate pine. *In: Proc. Of the 8th inter. Symposium on wood and pulping Chemistry*. Vol. 3 Helsinki, Sweden. Pp.431-436.
- Miller, M. J., Allen, D. G. (2004). Transport of hydrophobic pollutants through biofilms in biofilters. *Chemical Engineering Science* 59, 3515-3525.
- Miller, M. J., Allen, D. G. (2005a). Biodegradation of alpha-pinene in model biofilms in biofilters. *Environ. Sci. Technol.* 39: 5856-5863.
- Miller, M. J., Allen, D. G. (2005b). Modelling transport and degradation of hydrophobic pollutants in biofilter biofilms. *Chemical Engineering Journal* 113, 197-204.
- Milota, M. (2000). Emissions from wood drying. The science and issues. *Forest Prod. J.* 50(6):10-20.
- Milota, M. and Mosher, P. (2008). Emissions of hazardous air pollutants from lumber drying. *Forest Prod. J.* 58(7/8): 50-55.
- Milota, M. and Mosher, P. (2008). Emissions from western hemlock lumber during drying. *Forest Prod. J.* 56(5): 66-70.
- Milota, M. R. (2003). HAP and VOC emissions from white fir lumber dried at high and conventional temperatures. *Forest Prod. J.* 53(3): 60-64.
- Misra, G., Pavlostathis, S .G., Perdue, E. M., and raujo, R. A. (1996). Aerobic biodegradation of selected monoterpenes. *Appl. Microbiol. Biotechnol.* 45: 831-838.
- Moe, W. M. and Qi, B. (2005) Biofilter treatment of VOC emissions from reformulated paint: Complex mixtures, intermittent operation, and startup, *Journal of the Air & Waste Management Association*, 55(7), 950-960.
- Moe, W. M. and Qi, B. (2004) Performance of a fungal biofilter treating gas-phase solvent mixtures during intermittent loading. *Water Research*, 38, 2259–2268
- Moe, W. M., Irvine, R. L. (2000). Polyurethane foam medium for biofiltration; Part 2: Operation and performance. *Journal of Environmental Engineering*, 126(9), 826-832.
- Moe, W. M., and Irvine, R. L. (2001), Effect of nitrogen limitation on performance of toluene degrading biofilters. *Water Research*, 35(6):1407-1414.
- Mohseni, M., Allen, D. G. (1999). Biofiltration of mixtures of hydrophilic and hydrophobic volatile organic compounds. *Chemical Engineering Science* 55: 1545-1558.

- Morgenroth, E., Schroeder, E. D., Chang, D. P. Y., and Scow, K. M. (1996). Nutrient limitation in a compost biofilter degrading hexane. *J. Air Waste Management Assoc.* 46:300-309.
- Niemi, B. A., Kleinheinz, G. T., and McGinnis, G. D. (1999). Coupling an online GC with a FIA for multidimensional VOC analysis of industrial air emissions. In *Proc Air Waste Manage. Assoc. Annual Meeting, St. Louis, MO*, Paper No. 597.
- Otwell, L., Hittmeier, M. E., Hooda, U., Yan, H., Su, W. and Banerjee, S. (2000). HAPS Release from Wood Drying, *Environ Sci Technol.* 34(11):2280-2283.
- OSB and the environment. Technical bulletin.SBA
- Papiez, M. R., Potosnak, M. J., Goliff, W. S., Guenther, A. B., Matsunage, S. N. and Stockwell, W. R. (2009). The impacts of reactive terpene emissions from plants on air quality in Las Vegas, Nevada. *Atmospheric Environment* 43: 4109–4123.
- Plywood Manufacture, Washington State Air Toxic Sources and Emission Estimation Methods.
- Prado, O. J., Veiga, M. C., Kennes, C. (2005). Treatment of gas-phase methanol in conventional biofilters packed with lava rock. *Water Research* 39: 2385-2393.
- Qi, B. and W.M. Moe (2006). Performance of low-pH biofilters treating a paint solvent mixture: continuous and intermittent loading, *Journal of Hazardous Materials*, 135(1-3), 303-310.
- Rajagopal, A. N. (1996), Growth of gram-negative bacteria in the presence of organic solvents. *Enzyme Microbial. Technology.* 19: 606-613.
- Rene, E. R.; Jin, Y., Veiga, M.C., Kennes, C. (2009). Two-stage gas-phase bioreactor for the combined removal of hydrogen sulphide, methanol and Alpha-pinene. *Environmental Technology*, 30(12): 1261-1272
- Rupar-Gadd, K., Bagherpour, M. B., Holmstedt, G., *et al.* (2006). Solid phase micro extraction fibers, calibration for use in biofilter applications. *Biochemical Engineering J:* 31: 107-112.
- Roffael, Edmone. (2006). Volatile organic compounds and formaldehyde in nature, wood and wood based panels. *Holz als Roh-und Werkstoff*, 64:144-149.
- Sakuma, T., Hattori, T., and Deshusses, M. A. (2009). The effects of a lower irrigation system on pollutant removal and on the microflora of a biofilter. *Environmental Technology*, 30(6):621-627.
- Srandinger and Roberts. (1996). Moise Ngwa(2010-10-25).
- Sillman, S. (1999). The relation between ozone, NO_x and hydrocarbons in urban and polluted rural environments. *Atmos Environ* 33(12):1821-1854.

- Simpson, W.T. Editor, (1991). *Dry Kiln Operator's Manual*, Reprint of USDA Agricultural Handbook No. 188, *Forest Products Society*, Madison, WI. pp.274.
- Shmulsky, R., Dahlen, J. (2008). Laboratory scale VOC emissions testing of air-dried basswood lumber. *Forest Prod. J.* 58(4):94-96.
- Shu, Y., and Atkinson, R. (1995), Atmospheric lifetimes and fates of a series of sesquiterpenes, *J. Geophys. Res.*, 100(D4): 7275–7281, doi: 10.1029/95JD00368
- Stromvall, A. M. and Petersson, G. (1993a). Monoterpenes emitted to air from industrial barking of Scandinavian conifers. *Environmental Pollution* 79:215-218.
- Stromvall, A. M. and Petersson, G. (1993b). Photooxidant-forming monoterpenes in air plumes from kraft pulp industries. *Environmental Pollution* 79:219-223.
- Stromvall, A. M. and Petersson, G. (2000). Volatile terpenes emitted to air. In *Pitch Control, wood Resin and Deresination*; Back, E.L., Allen, L.H., Eds. 77-79.
- Tonga, A. P. and Singh, M. (1994). Biological vapor-phase treatment using biofilter and biotrickling filter reactors: Practical operating regimes. *Environmental Progress* 13:94-97.
- Thompson, A., Ingram, L., Jr. (2006). Variation of terpenes in sapwood and heartwood of loblolly pine: Impact on VOC emissions from drying lumber samples. *Forest Prod. J.* 56(9):80-83.
- van Groenestijn J. W., Liu, J. X. (2002). Removal of alpha-pinene from gases using biofilters containing fungi. *Atmospheric Environment* 36: 5501-5508.
- Wang, S. Q., Du, G. B., Zhang Y. (2005). Microwave wood strand drying: energy consumption, VOC emission and drying quality. IADC 3th Inter-American drying conference. Page: III -4.
- Wastney, S. C. (1994). Emissions from Wood and Biomass Drying: A Literature Review, New Zealand Forest Research Institute, 68
- Winer, A. M., Arey, J., Atkinson, R., Aschmann, S. M., Long, W. D., Morrison, Clolszyk, D.M. (1992). Emission rates of organics from vegetation in California's Central Valley. *Atmospheric Environment* 26: 2647-2659.
- Wu, J. and Milota, M. R. (1999). Effect of temperature and humidity on the total hydrocarbon emissions from Douglas-fir lumber. *Forest Products* 49(6):52-60.
- Zhao, Y., Zhang, R., Sun, X., *et al.* (2010). Theoretical study on mechanism for O₃-initiated atmospheric oxidation reaction. *Molecular structure: Theochem. J.* 947(1-3):68-75

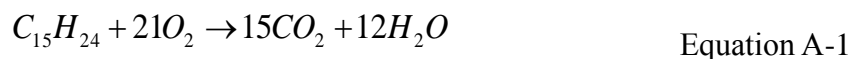
APPENDIX A: STRUCTURE OF β -CARYOPHYLLENE

β -caryophyllene with a formula of $C_{15}H_{24}$, and it's structure is as follows:

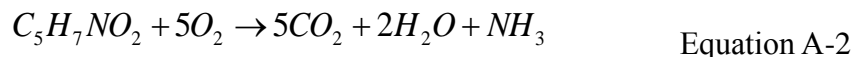


APPENDIX B: CALCULATIONS RELATED TO The β -CARYOPHYLLENE BIODEGRADATION TEST

Design of the serum bottle test was based on the assumption that β -caryophyllene would be oxidized to carbon dioxide and water, with overall stoichiometric equation A-1 neglecting biomass yield:



Assuming that biomass (measured as TSS) present in the inoculum could be represented as $C_5H_7NO_2$, and that all of it will convert to produce CO_2 based on the following stoichiometric equation A-2:



At time zero, the O_2 in each serum bottle was approximately $160\text{mL} \times 21\% = 33.6\text{mL}$, corresponding to an O_2 mass equivalence of 43.8 mg (assuming $T=30^\circ\text{C}$, $P=1\text{atm}$). The initial TSS concentration in the 1 mL aqueous-phase inoculum added to the serum bottles was 116 mg/L for the low temperature bioreactor and 38.7 mg/L for the high temperature bioreactor. The theoretical oxygen demand (ThOD) of biomass calculated by equation A-2 was 164.2 μg and 54.7 μg respectively, accounting for 0.37% and 0.12% of the initial O_2 provided. And the CO_2 concentration produced from mineralization of the biomass inoculum calculated by equation A-2 was 0.077 v/v % for the low temperature aqueous bottles, and 0.0257 v/v % for the high temperature aqueous bottles.

Under the assumption of equation A-1 which neglects biomass yield, to consume all the O_2 in the bottle approximately 0.013 mg β -caryophyllene needed, corresponding to 0.015 mL β -caryophyllene (converted by an assumed density of 0.9052 mg/mL). To guarantee enough carbon sources for biodegradation, 0.1 mL (about seven times as calculated) of β -caryophyllene (both

low purity and high purity) was supplied in the serum bottles. And the maximum amount of CO₂ concentration produced by β-caryophyllene calculated by equation A-1 was 15%.

Combine this with the CO₂ concentration data collected, CO₂ produced by β-caryophyllene biodegradation for the aqueous bottles was calculated as the following equation A-3:

$$C = C_t - C_b \quad \text{Equation A-3}$$

$C \rightarrow$ CO₂ concentration produced by β-caryophyllene biodegradation

$C_t \rightarrow$ CO₂ concentration collected by test

$C_b \rightarrow$ CO₂ concentration produced by biomass conversion

VITA

Weili Hu was born in China. She received her bachelor's degree of science in Agricultural Resources and Environment from Huazhong Agricultural University, Wuhan, in 2007. Hu conducted the project "Mechanisms of Phosphorus Forms in Sediments Influenced by Macrophyte *Potamogeton Crispus*" as her undergraduate research thesis. In 2009, she moved to Louisiana with family and in spring 2010, she entered the graduate school of Louisiana State University in the department of Civil Engineering to obtain a master's degree under the guidance of Dr. William M. Moe. Her research was studying biofiltration for treatment of gases contaminated by β -caryophyllene.